

THESIS

SUPERHYDROPHOBIC TITANIA NANOTUBE ARRAYS FOR REDUCING ADHESION  
OF BACTERIA AND PLATELETS

Submitted by

Kevin Bartlett

Department of Mechanical Engineering

In partial fulfillment of the requirements

For the Degree of Master of Science

Colorado State University

Fort Collins, Colorado

Summer 2017

Master's Committee:

Advisor: Ketul C. Popat

Arun Kota  
Melissa Reynolds

Copyright by Kevin Bartlett 2017

All Right Reserved

## ABSTRACT

### SUPERHYDROPHOBIC TITANIA NANOTUBE ARRAYS FOR REDUCING ADHESION OF BACTERIA AND PLATELETS

Hemocompatibility and bacterial infections cause challenges for medical devices. When any material is implanted into the body bacteria, blood, proteins and platelets will adsorb and attach to its surface. The platelet adsorption leads to thrombosis and clot formation on the surfaces, restricting blood flow and in some cases leading to inflammation and device failure. Bacteria adhesion leads to colony formation and eventually infection if left untreated. Infections can be treated with antibiotics, but growing antibiotic resistance among bacteria has spurred a search for methods that reduce infections without increasing resistance. Proposed methods have included diamond-like carbon surfaces, drug-eluting surfaces, and titania nanotube arrays. These methods have all shown some initial improved, but no approach has proven durable over long periods of time. Superhemophobic surfaces are a new approach to improving performance of medical devices, but the interactions of blood components and bacteria with these surfaces have not been well-documented. In this work, superhemophobic surfaces were developed by modifying the surface topography and surface chemistry of titanium. The surface topography was modified by creating titania nanotube arrays through a well-documented anodization and chemical etching technique. Superhemophobicity was induced by modifying the titania nanotube arrays with different silanes using chemical vapor deposition. The investigations of blood interactions with superhemophobic surfaces showed reduced protein adsorption. The bacteria adhesion studies showed reduced attachment for both gram-positive and gram-negative bacteria. The results indicate these surfaces have potential for enhancing material hemocompatibility and reducing the attachment of bacteria.

## ACKNOWLEDGEMENTS

I have a lot of people to thank for their help in completing this thesis. First, thanks to my advisor Dr. Ketul Popat. He has been incredibly helpful in guiding me through my research and graduate school work.

There are lots of people in the lab to thank as well – Rachael Simon, Yanyi Zhang, Kari Cowden, Stephen Hughes, Bryant Hiraki, and Nick Peters, all of whom have helped me through difficulties in the lab work and are great people.

Thanks to both Dr. Arun Kota and Dr. Melissa Reynolds for serving on my committee even with their other commitments. Thanks to Sanli Movafaghi for teaching me how to silanize the nanotube arrays and measure contact angles. Thanks to Bella Neufeld for showing me how to conduct bacteria studies and helping me through that work.

Thanks to Dr. Pat McCurdy, Dr. Roy Geiss, and Dr. Brian Newell at CSU who were very patient and helpful in teaching me to use SEM and XPS. Thanks to Prof. Ana Paula Rosifini Alves Claro from UNESP-Guaratingueta, Brazil along with Dr. Paolo Soares and everyone at the Pontifical Catholic University of Paraná in Curitiba, Brazil who helped with the material analysis of my samples.

## TABLE OF CONTENTS

ABSTRACT.....	ii
ACKNOWLEDGEMENTS.....	iii
LIST OF FIGURES.....	vi
INTRODUCTION.....	1
HYPOTHESIS AND SPECIFIC AIMS.....	3
CHAPTER 1.....	5
LITERATURE REVIEW.....	5
1.1 Introduction.....	5
1.2 Thrombus Formation on Surfaces.....	6
1.3 Bacterial Adhesion to Surfaces.....	10
1.4 Surface Wetting and Superhydrophobic Surfaces.....	13
References.....	18
CHAPTER 2.....	22
FABRICATION AND CHARACTERIZATION OF TITANIA NANOTUBE ARRAYS.....	22
2.1 Introduction.....	22
2.2 Materials and Methods.....	26
2.3 Results and Discussion.....	29
2.4 Conclusion.....	42
References.....	43
CHAPTER 3.....	45
HEMOCOMPATIBILITY OF TITANIA NANOTUBE ARRAYS.....	45
3.1 Introduction.....	45
3.2 Materials and Methods.....	48
3.3 Results and Discussion.....	53
3.4 Conclusion.....	67
References.....	68
CHAPTER 4.....	71
BACTERIAL ADHESION ON TITANIA NANOTUBE ARRAYS.....	71
4.1 Introduction.....	71

4.2 Materials and Methods.....	74
4.3 Results and Discussion.....	77
4.4 Conclusion.....	87
References.....	89
CHAPTER 5.....	92
CONCLUSIONS AND FUTURE WORK.....	92
5.1 Conclusions.....	92
5.2 Future Work.....	94

## LIST OF FIGURES

Figure 2.3.1: SEM images showing titania nanotube arrays.....	30
Figure 2.3.2: Graph showing the average outer diameters of titania nanotube arrays..	31
Figure 2.3.3: SEM images showing titanium and titania nanotube arrays.....	33
Figure 2.3.4: Graph showing the average inner diameters and thicknesses of titania nanotube arrays.....	34
Figure 2.3.5: Graph showing the average contact angles of whole blood.....	35
Figure 2.3.6: Graph showing the advancing, receding, and estimated Young's contact angle of water.....	36
Figure 2.3.7: Figure showing XPS survey scans for titania surfaces.....	38
Figure 2.3.8: Figure showing XPS survey and high resolution carbon scans for titania surfaces.....	39
Figure 2.3.9: Figure showing GAXRD scans for titania surfaces.....	40
Figure 2.3.10: Figure showing GAXRD scans for titanium and titania surfaces.....	41
Figure 3.3.1: XPS scans showing albumin adsorption .....	55
Figure 3.3.2: XPS scans showing fibrinogen adsorption .....	55
Figure 3.3.3: Graphs showing cytotoxicity measurements obtained using LDH assay.	57
Figure 3.3.4: Fluorescence microscopy images of calcein-AM stained cells .....	58
Figure 3.3.5: Graph showing the percent surface area covered by calcein-AM stained cells .....	59
Figure 3.3.6: Fluorescence microscopy images of rhodamine phalloidin and DAPI stained cells .....	61
Figure 3.3.7: Graph showing the percent surface area covered by rhodamine-phalloidin stained cells.....	62
Figure 3.3.8: Graph showing the count of DAPI stained cells per $\mu\text{m}^2$ on titania surfaces.....	63

Figure 3.3.9: SEM images showing activated platelets on titania surfaces .....	64
Figure 3.3.10: Graph showing platelet counts on titania surfaces .....	65
Figure 3.3.11: Graph showing absorbance of hemoglobin onto titania surfaces .....	66
Figure 4.4.1: Fluorescence microscopy images of <i>S. aureus</i> .....	79
Figure 4.4.2: Counts of <i>S. aureus</i> cells after 6 and 24 h .....	80
Figure 4.4.3: Fluorescence microscopy images of <i>P. aeruginosa</i> .....	82
Figure 4.4.4: Counts of <i>P. aeruginosa</i> cells after 6 and 24 h .....	83
Figure 4.4.5: SEM images of <i>S. aureus</i> .....	85
Figure 4.4.6: SEM images of <i>P. aeruginosa</i> .....	86

## INTRODUCTION

The research presented here evaluates the potential of superhydrophobic and superhemophobic titania nanotube arrays as surfaces to reduce thrombosis and bacterial adhesion. Thrombosis and bacterial infections are common complications with medical devices. A thrombus will form on any surface that contacts blood when platelets adhere to the surface and aggregate as part of the human immune response. The thrombus can grow and restrict blood flow through the vessel or detach from the surface leading to strokes or myocardial infarctions. Bacterial colonies that grow on the surfaces of implants will prevent integration of the implant if left untreated. These complications limit the effectiveness of implanted medical devices.

Titania nanotube arrays have been proposed as a method to improve the performance of implanted devices. They have been shown to reduce bacteria adhesion and platelet aggregation compared to commercial titanium, a common biomaterial. Superhydrophobic surfaces have been investigated in a wide range of applications for their ability to reduce biofouling. Superhydrophobic surfaces have been shown to reduce the adhesion of bacteria to surfaces, among other organisms. There is little research, however, into how superhydrophobic nanotube arrays interact with bacteria or blood. Additionally, little investigation has been done into creating surfaces that are superhemophobic as well as superhydrophobic.

This master's thesis addresses the hypothesis that superhydrophobic titania nanotube arrays can function as superhemophobic surfaces and will exhibit reduced thrombogenicity and bacterial adhesion compared to pure titanium and unmodified titania

nanotube arrays. Superhemophobicity was induced by modifying the titania nanotube arrays with different silanes using chemical vapor deposition. The interactions of human blood plasma, *S. aureus* (gram-positive) bacteria, and *P. aeruginosa* (gram-negative) bacteria with the surfaces were investigated. The conclusions showed that superhemophobic and superhydrophobic titania nanotube arrays can be fabricated using well-researched techniques. The superhemophobic surfaces showed reduced adsorption of the blood proteins fibrinogen and albumin, lower platelet adhesion and activation, and reduced bacterial adhesion compared to the control surfaces. The results presented here indicate that superhemophobic titania nanotube arrays have the potential to improve the performance of implanted devices.

## HYPOTHESIS AND SPECIFIC AIMS

**Fundamental Hypothesis:** Superhemophobic titania nanotube arrays can reduce the attachment of platelets, leukocytes, blood proteins, and bacteria

**Hypothesis 1:** Titania nanotube arrays can be silanized to create a stable superhemophobic surface

**Specific Aim 1:** Fabrication and characterization of superhemophobic titania nanotube arrays. This specific aim is discussed in Chapter 2 and will cover:

- (a) Fabrication of uniform, vertically oriented, reproducible titania nanotube arrays
- (b) Modification of the surface chemistry of titania nanotube arrays to induce Superhemophobicity/superhydrophobicity
- (c) Characterization of titania nanotube arrays and measurement of contact angles of water and blood

**Hypothesis 2:** Superhemophobic titania nanotube arrays can improve hemocompatibility and reduce biofilm formation by reducing cell adhesion

**Specific Aim 2:** Investigation of protein adsorption, blood cell attachment, and bacterial adhesion to titania nanotube arrays. This specific aim is discussed in Chapters 3 and 4 and will cover:

- (a) Evaluation of cytotoxicity, platelet and leukocyte adhesion and activation, and adsorption of hemoglobin and blood proteins
- (b) Attachment and morphology of gram-positive and gram-negative bacteria

# CHAPTER 1

## LITERATURE REVIEW

### 1.1 Introduction

Medical devices can fail for several different reasons once they are implanted into a patient. The implant can be rejected by the immune system, where tissue inflammation surrounding the implant site causes enough pain that the implant must be removed. The implant site and implant itself can be colonized by bacteria, leading to the infections. The materials of which the implant is composed can elicit an allergic reaction from the patient. Or thrombi can form on the surfaces of blood-contacting devices, growing over time and leading to clot formation in the patient's blood vessels. Many researchers have investigated methods for mitigating these complications in order to improve the effectiveness of medical devices and the quality of life for patients. Much attention has gone into altering the surfaces of medical devices to improve biocompatibility. The earliest investigations into biocompatibility simply involved investigating different metals. These studies showed that titanium had a desirable combination of biocompatibility and strength so it became a common material choice for medical devices. Subsequent studies looked into methods of generating nanostructures, such as pillars or wires, on titanium surfaces. These studies showed that nanostructures tended to promote cell growth and reduce harmful immune responses. These nanostructures also emerged as a method for drug delivery. Anti-inflammatory drugs or antibiotics could be applied as a coating or embedded within the nanostructures and released once the device was implanted, reducing the risk of device failure. More recently, superhydrophobic surfaces

have gained interest as an application for medical devices for their potential to reduce the adhesion of the bacteria or platelets. Their attachment to the surfaces of medical devices is the first step in the infection or thrombus formation processes that can lead to device failure. To date there is limited data on the interactions between biological systems and superhydrophobic surfaces, however, so more work must be done to determine the potential applications of these surfaces.

## **1.2 Thrombus Formation on Surfaces**

Aortic stenosis – the obstruction of the aortic valve – is a common issue for patients with heart disease. It is often treated by implanting a mechanical or synthetic heart valve. This can be done through open heart surgery, but for cases where open heart surgery is risky a catheter fed through a blood vessel is used instead.<sup>1</sup> For both methods, valve failure through thrombosis is one of the most dangerous complications resulting from the surgery. If a thrombus forms on the leaflet of the valve, it can interfere with the movement of the leaflet, preventing it from opening or closing properly.<sup>1-3</sup> Also, the forces exerted by the leaflets on the blood and its components tend to damage the platelets and blood cells, further promoting thrombosis.<sup>4,5</sup> When red blood cells are exposed to shear forces, they change shape, becoming ellipsoidal. Eventually, if the Reynold's shear stress reaches a range of 150-400 N/m<sup>2</sup> the cell membrane of a red blood cell will tear and their contents will lyse into the bloodstream.<sup>4</sup> Viscous shear stress in excess of only 10 N/m<sup>2</sup>, a level typically reached in the flow fields around valve leaflets, is known to cause damage to the platelets, exposing a part of glycoprotein IIb/IIIa.<sup>4-6</sup> This protein binds to fibrinogen, which in turn binds with either other platelets or collagen in the wall of a blood vessel.<sup>7,8</sup>

Platelets damaged by shear forces will aggregate in this way to form clots, and unlike other methods of clot formation this cannot be treated with aspirin.<sup>6</sup>

Dual antiplatelet therapy (DAPT) is a common method for preventing and treating thrombosis. Patients are given aspirin and an anti-clotting drug, typically a drug that inhibit the production of P2Y<sub>12</sub> – a protein found on the surfaces of platelets that regulates blood clotting.<sup>6</sup> This treatment is often continued for years, but studies have shown no significant reduction in mortality or thrombosis for long term treatment compared to short term therapy of approximately 6 months or a regimen of aspirin. DAPT does not work for patients who are resistant to either aspirin or the blood thinning medications, and the use of the blood thinners increases a patient's risk of bleeding from other injuries. Additionally, clinical studies have found that it is difficult to confirm that patients are sticking to their medication regimens over longer periods of time.<sup>9</sup>

Thrombosis is associated with stent revascularization, a complication where vascular cells grow around the stent and constrict the flow of blood through the stent. This condition can occur with both drug-eluting stents and bare-metal stents. Recent research has focused on reducing the incidence of thrombosis in stents. Early stents - which were implanted through a vein and expanded - were made only of untreated metal and caused complications including artery occlusion and scar tissue formation in addition to thrombosis.<sup>10</sup> In response to these complications drug-eluting stents started to be developed. The first drug-eluting stents were coated with antibiotics, which were shown to reduce restenosis and revascularization around the implant area.<sup>10,11</sup> Clinical trials have shown that drug-eluting stents reduce restenosis and revascularization compared to untreated metal stents, but do not affect rates of long term thrombosis.<sup>12</sup> Additionally,

the rates of myocardial infarction deaths are unchanged between drug-eluting stents and bare metal stents.<sup>12</sup> Allergic reactions or sensitivity to the drug coatings have also caused myocardial infarctions, rejection, or death in some patients.<sup>12</sup> Analysis of the clinical trials has indicated that blood thinning medications or dual antiplatelet therapy, such as clopidogrel, should be taken continually after implantation of the stents. Without these medications, the risk of late stent thrombosis is comparable to that of bare metal stents.<sup>12,13</sup> Current research is focused on improving drug eluting stents to reduce the risk of late thrombosis and death further, but so far no approach has eliminated the need for dual antiplatelet therapy.<sup>10,12,14</sup>

Additionally, thrombosis formation can be caused by poor stent design, incomplete endothelialization of the stent once implanted, or an allergic reaction to a drug or coating on a stent. Patients with diabetes, renal issues, or those who do not respond well to blood thinners and anti-inflammatory medications are also at a higher risk of thrombosis formation.<sup>9</sup> Analysis of clinical trials has shown no significant difference between drug-eluting stents and other stents in preventing thrombosis formation.<sup>9,10,14</sup> Drug-eluting stents have helped reduce incidences of restenosis and acute vessel closure, which is why they are commonly used today.<sup>10</sup> Additionally, trials are being done to investigate biodegradable polymers for use in stents and alternate methods for drug delivering.<sup>15-17</sup> Results have shown that these stents perform around as well as biodegradable stents, but they are still far from being approved for widespread clinical use.<sup>18</sup> Another occurrence with which thrombosis is associated is heart disease. The propensity of thrombosis to cause heart disease is a major challenge for treatment, and is a common medical condition which can lead to heart attacks in patients.<sup>9</sup> Artificial heart valves are

commonly used to treat cases of heart disease. Because the structure of the heart valve has been extensively studied to inform the design of artificial heart valves – both mechanical and tissue-based – it is important to discuss the composition of a human heart valve.

Endocardial cells make up the outer layer of heart valves.<sup>7</sup> These cells form a barrier over the interstitial cells, and their surface is not thrombogenic. Much of the research into prosthetic valves has focused replicating this property of the endocardial surface, but so far there has not been a successful method for reducing thrombosis to the level of the natural heart valve. These endocardial cells also envelop the extra-cellular matrix of the valve leaflets, giving the leaflets their structure.<sup>7</sup> This extra-cellular matrix consist of collagen, elastin, and various proteoglycans.<sup>7</sup> Bundles of collagen fibers called fibrosa run through the leaflets and are what enable the leaflets to open and close.<sup>7</sup> The ventricularis layer is mainly composed of elastin and serves to maintain flexibility and the structure of the valve leaflets while they open and close.<sup>7</sup> Between the fibrosa and ventricularis is a layer called the spongiosa, which is composed of proteoglycans with some collagen fibers dispersed throughout. The proteoglycan matrix absorbs water, forming a gel that is able to absorb compressive stresses exerted on the leaflets by the flow of blood and the movement of the valves.<sup>7</sup> It also allows the fibrosa and ventricularis layers to shear across each other without sustaining damage.<sup>7</sup> The spongiosa layer also keeps the leaflet hydrated, which is important for maintaining flexibility in the leaflets.<sup>7</sup> A heart valve also contains interstitial cells which are long cells that form a connected, three-dimensional matrix in the valve.<sup>7</sup> Some of these interstitial cells secrete fibroblasts into the valve to maintain its integrity and repair damage to the valves.<sup>7</sup> Other interstitial

cells can contract similar to smooth muscle cells to resist the hemodynamic pressures on the valve.<sup>7</sup> The interstitial cells are important because they transmit signals from mechanical forces on the extra-cellular matrix to other cells in the heart valve, signaling needs for repair and cell differentiation.<sup>7</sup>

After implantation of a heart valve, complication can arise which will reduce the effectiveness of the treatment. Valvular stenosis is a common complication where platelets aggregate around the valve and narrow the path through which blood can flow.<sup>7</sup> Additionally, depending on where the platelets aggregate, they can cause a disease called valvar insufficiency where the leaflets of the valve do not completely close and seal properly, resulting of some backflow of the blood. Currently there is not a permanent way to prevent these complications. Most patients who receive heart valve are placed on a regimen of anticoagulant medications for the rest of their lives in order to prevent platelet aggregation. If the valves fail or are rejected by the immune system, the only option is surgical replacement of the valve.

### **1.3 Bacterial Adhesion to Surfaces**

Bacterial adhesion occurs in three stages. The adhesion forces are typically analyzed as Van der Waals forces between the cell walls of the bacterium and whatever surface it is contacting.<sup>19</sup> Negatively charged surfaces have been shown to reduce adhesion of bacteria, as the cell walls of bacteria are negatively charged under common environmental conditions.<sup>20-22</sup> Positively charged surfaces are shown to generally increase adhesion, but it has also been found that bacterial growth is slowed on these surfaces.<sup>20,23-26</sup> Initially, bacterial adhesion is characterized by the interactions between

a single bacterium and the surface. At this point, any attachment is reversible through cleaning or adjustments of environmental factors, such as the pH of the surface.<sup>24</sup> Once the bacterium contact the surface, the next stage of attachment binds the bacterium to the surface through the pili or other structures on the bacteria. The rate at which the binding occurs is again dependent on environmental factors, and is somewhat reversible depending on the environmental conditions.<sup>19,26</sup> This stage is characterized by aggregation of bacteria into colonies which will continue to grow on the surface. If left alone, these colonies will eventually form a biofilm, which is a three-dimensional colony with a protective covering of peptidoglycans.<sup>27</sup> At this stage the bacterial colony is difficult to dislodge from the surface. Materials with surface free energies below 30 mN/m have been shown to reduce adhesion of bacteria, and that generally materials with more hydrophilicity increase the adhesion of bacteria, though the relationship is not exact.<sup>24,27</sup> Surface texture has also been shown to affect bacteria adhesion depending on the size of the textures. Textures larger than the bacteria have been shown to promote adhesion, as the bacteria can fit in between the features and end up protected by the roughness.<sup>24,27</sup> If the roughness scale is smaller than the bacteria, however, it has been shown that adhesion is reduced.<sup>19,27</sup> Additionally, increasing the thickness of a surface coating has been shown to reduce adhesion up to approximately 100  $\mu\text{m}$ .<sup>19</sup> Materials with reduced Young's moduli have also been shown to reduce bacterial adhesion.<sup>19</sup>

If a biofilm does form on the surface, it can cause a serious infection. In the process of creating a biofilm the bacteria create an extracellular matrix that protects the bacteria and blocks antibiotics.<sup>27</sup> This makes these infections difficult to combat. Infectious bacteria fall into two categories: gram-positive and gram-negative.<sup>19,22,27,28</sup>

Gram-negative bacteria are known for their drug resistance and have been developing resistance to antibiotics.<sup>22,28</sup> Common gram-negative bacteria include *Escherichia coli* and *Pseudomonas aeruginosa*, the latter of which is commonly studied because of its prevalence and common infection associations.<sup>28</sup> Bacteria are characterized as either gram-positive or gram-negative by using the gram staining test.

Gram staining uses a violet stain and an iodine solution to stain the peptidoglycan in the cell membranes of bacteria.<sup>20</sup> Gram-positive will retain the violet stain under fluorescence microscopy due to their relatively thick cell membranes.<sup>19,20</sup> Gram-negative bacteria have thinner cell membranes, and so will not retain the stain due to the reduced amount of peptidoglycan present.<sup>20</sup> Often a secondary stain, which binds less strongly than the violet stain, is used to check for gram-negative bacteria.<sup>20</sup> The secondary stain will be too weak to displace the initial stain but will bind to the gram-negative bacteria, so they will appear to be a different color than violet under fluorescence microscopy, while the gram-positive bacteria will appear unchanged.<sup>19,20</sup>

The earliest strategies for combating bacterial infections involved the use of antibiotics or antibacterial metals. Antibiotics are effective, but their overuse has been shown to increase bacterial resistance, reducing their future effectiveness.<sup>19,29</sup> Copper, molybdenum, and silver have been shown to have antibacterial properties, as their ions will kill bacteria.<sup>27</sup> Eventually all the ions will diffuse from the material and it will no longer be antibacterial, so these materials are not effective long term. Titanium oxide has been shown to kill bacteria when activated by UV light.<sup>19,29</sup> Current research is focused on methods to activate titanium and other photocatalytic materials through other methods than UV light.<sup>19</sup>

## 1.4 Surface Wetting and Superhydrophobic Surfaces

Hydrophobicity and hydrophilicity are characterized by the contact angle: the angle drawn from a surface through a water droplet to the droplet's edge. If the angle is greater than  $90^\circ$  the surface is hydrophobic, and if the angle is less than  $90^\circ$  the surface is hydrophilic. Superhydrophobic surfaces have been defined as those with contact angles greater than  $150^\circ$  and roll-off angles below  $10^\circ$ . Superhydrophobic surfaces have been researched for a variety of uses, including water-repellent fabrics, ice-resistant surfaces, and specialized assay papers. For medical devices, these surfaces are of interest because of their ability to minimize contact with bodily fluids, such as blood, with the idea that minimizing contact with the fluids will reduce immune responses that can lead to device rejection.

Contact between a liquid and a surface takes two forms – the Wenzel state, where the liquid spreads out across the surface, and the Cassie-Baxter state, where a layer of air sits between the liquid and parts of the surface.<sup>30,31</sup> This happens because the overall system wants to be in the state with the lowest free energy. Liquids with lower surface tensions tend to spread out across surfaces, while materials with low solid surface energies tend to cause droplets to bead up. The combination of the solid surface energy and liquid surface tension will determine whether a particular solid and liquid will be in the Cassie-Baxter and Wenzel states.

Superhydrophobic surfaces are generally defined as surfaces with contact angles greater than  $150^\circ$  and roll-off angles below  $10^\circ$ .<sup>32</sup> Superhydrophobicity is only possible in the Cassie-Baxter state, as the maximum contact angle possible for the Wenzel state has been shown to be about  $120^\circ$ . For a surface to be superhydrophobic it needs to have

a low solid surface energy – to encourage water to bead up into droplets – and surface roughness. On a perfectly flat surface it would not be possible to have the air pockets between the droplet and the surface that are characteristic of the Cassie-Baxter state. Much of the research into superhydrophobic surfaces was inspired by Barthlott et al's work on lotus leaves.<sup>33–35</sup> They found that the combination of epicuticular wax secreted by the leaves and the tiny bumps on the order of nanometers that make up the leaves' surfaces allow water droplets to easily roll across the leaves.<sup>33</sup> As the droplets roll they pick up any dirt, dust, microorganisms, or other molecules that have attached to the leaves and carry them away, cleaning the leaves.<sup>33–35</sup> This allows the plant cells to be exposed to sunlight instead of being blocked by surface contaminants, ensuring the lotus plants can continue to grow.

Many applications have been suggested for superhydrophobic surfaces. Some surfaces that can transition between the Wenzel and Cassie-Baxter states through the application of an electric current.<sup>36</sup> The electric current changes the solid surface energy of the material, resulting in a surface that can be both hydrophilic and superhydrophobic. These surfaces are being investigated to make miniaturized labs, which would be able to use small amounts of chemicals and reagents to perform lab tests with minimal waste. These would have a wide application in the medical field, as blood tests, for example, could be done accurately with only a few drops of blood. The ability to control the superhydrophobicity of a surface can also be used to transfer droplets between surfaces without contamination – the superhydrophobicity can be turned off to pick up and move a droplet, and then can be reapplied to remove the droplet from the surface. Other applications include reducing the buildup of water turbine blades and steam engines,

increasing their efficiency.<sup>36</sup> Researchers have also created miniaturized engines and generators that use surface tension to generate electricity or mechanical energy, typically using a surface attached to a spring. As the surface changes between hydrophilicity and hydrophobicity, the surface is attracted to a fluid through capillary forces. The spring is extended and retracted, generating the electricity. Superhydrophobic fabrics have been created that repel stains as well, which can be used for protective suits and clothes.<sup>36</sup> Transparent superhydrophobic surfaces have been created by making sure the features on the surface are smaller than the wavelengths of light – allowing the light to pass through.<sup>36</sup> These can be used to coat and create self-cleaning solar panels and other surface that need to remain unobstructed but transparent to light.<sup>36</sup> This allows these surfaces to mimic the lotus leaf, and once applied the surfaces can retain the self-cleaning function as long as they remain undamaged. For all superhydrophobic applications, any damage to the features that create the surface roughness will reduce the effectiveness, as the roughness is necessary for any water droplet to be in the Cassie-Baxter state. Solar panels and similar surfaces that require little handling are thus ideal candidates for this application because they can be left alone and remain undamaged. Superhydrophobic silver surfaces have been created which can function as mirrors because of their reflectivity, but are easily damaged.<sup>36,37</sup> The surface roughness necessary to induce superhydrophobicity makes reflecting light difficult, so research to create reflective superhydrophobic surfaces from other materials is still ongoing.<sup>36,37</sup> The self-cleaning properties of superhydrophobic surfaces can also be used for any applications which require a surface to be submerged. Research has shown that superhydrophobic surfaces reduce the attachment of marine organisms, which is useful

for underwater pipes and the hulls of ships.<sup>36</sup> Many coatings currently used to reduce the fouling of ships are toxic to wildlife, whereas there are non-toxic superhydrophobic coatings, which is an additional benefit.<sup>36</sup> Superhydrophobic coatings also work within pipes, reducing the drag forces within the pipes and allowing water to flow more easily.<sup>36</sup> The main challenge facing any application of superhydrophobic surfaces is, as mentioned before, the ease with which these surfaces can be damaged. Nanoscale features can be destroyed with low amounts of force, and once damaged the features are difficult to repair. Currently researchers are looking into ways both to strengthen the features on superhydrophobic surfaces and create self-repairing surfaces, but so far no long term solution has been developed.

The research presented here evaluates the potential of superhydrophobic and superhemophobic titania nanotube arrays as surfaces to reduce thrombosis formation and bacterial adhesion. The fabrication titania nanotube arrays through electrochemical etching and anodization has been well-documented.<sup>38-40</sup> Superhemophobicity was induced by modifying the titania nanotube arrays with different silanes using chemical vapor deposition. The titania nanotube arrays were characterized using scanning electron microscopy (SEM), XPS, GAXRD, and both water and blood contact angle goniometry. The adsorption of human fibrinogen and albumin onto the surfaces were measured, along with the adhesion of platelets and leukocytes. The activation of platelets on the titania nanotube arrays was investigated using SEM. The adsorption of hemoglobin from whole human blood onto the surfaces was measured as well. The adhesion, morphology, and biofilm formation of *S. aureus* (gram-positive) and *P.*

*aeruginosa* (gram-negative) bacteria on the surfaces was measured using SEM and live/dead staining with fluorescence microscopy.

## REFERENCES

- (1) De Marchena, E.; Mesa, J.; Pomenti, S.; Marin Y Kall, C.; Marincic, X.; Yahagi, K.; Ladich, E.; Kutz, R.; Aga, Y.; Ragosta, M.; Chawla, A.; Ring, M. E.; Virmani, R. Thrombus Formation Following Transcatheter Aortic Valve Replacement. *JACC Cardiovasc. Interv.* **2015**, *8* (5), 728–739.
- (2) Hansson, N. C.; Grove, E. L.; Andersen, H. R.; Leipsic, J.; Mathiassen, O. N.; Jensen, J. M.; Jensen, K. T.; Blanke, P.; Leetmaa, T.; Tang, M.; Krusell, L. R.; Klaaborg, K. E.; Christiansen, E. H.; Terp, K.; Terkelsen, C. J.; Poulsen, S. H.; Webb, J.; Bøtker, H. E.; Nørgaard, B. L. Transcatheter Aortic Valve Thrombosis: Incidence, Predisposing Factors, and Clinical Implications. *J. Am. Coll. Cardiol.* **2016**, *68* (19), 2059–2069.
- (3) Makkar, R. R.; Fontana, G.; Jilaihawi, H.; Chakravarty, T.; Kofoed, K. F.; de Backer, O.; Asch, F. M.; Ruiz, C. E.; Olsen, N. T.; Trento, A.; Friedman, J.; Berman, D.; Cheng, W.; Kashif, M.; Jelnin, V.; Kliger, C. A.; Guo, H.; Pichard, A. D.; Weissman, N. J.; Kapadia, S.; Manasse, E.; Bhatt, D. L.; Leon, M. B.; Søndergaard, L. Possible Subclinical Leaflet Thrombosis in Bioprosthetic Aortic Valves. *N. Engl. J. Med.* **2015**, *373* (21), 2015–2024.
- (4) Ge, L.; Dasi, L. P.; Sotiropoulos, F.; Yoganathan, A. P. Characterization of Hemodynamic Forces Induced by Mechanical Heart Valves: Reynolds vs. Viscous Stresses. *Ann. Biomed. Eng.* **2008**, *36* (2), 276–297.
- (5) Simon, H. a; Leo, H.-L.; Carberry, J.; Yoganathan, A. P. Comparison of the Hinge Flow Fields of Two Bileaflet Mechanical Heart Valves under Aortic and Mitral Conditions. *Ann. Biomed. Eng.* **2004**, *32* (12), 1607–1617.
- (6) Elmariah, S.; Mauri, L.; Doros, G.; Galper, B. Z.; O'Neill, K. E.; Steg, P. G.; Kereiakes, D. J.; Yeh, R. W. Extended Duration Dual Antiplatelet Therapy and Mortality: A Systematic Review and Meta-Analysis. *Lancet* **2015**, *385* (9970), 792–798.
- (7) Flanagan, T. C.; Pandit, A.; Taylor, P.; Jockenhövel, S. Living Artificial Heart Valve Alternatives: A Review. *Eur. Cells Mater.* **2003**, *6* (0), 28–45.
- (8) Spijker, H. T.; Busscher, H. J.; Van Oeveren, W. Influence of Abciximab on the Adhesion of Platelets on a Shielded Plasma Gradient Prepared on Polyethylene. *Thromb. Res.* **2002**, *108* (1), 57–62.
- (9) Holmes, D. R.; Kereiakes, D. J.; Garg, S.; Serruys, P. W.; Dehmer, G. J.; Ellis, S. G.; Williams, D. O.; Kimura, T.; Moliterno, D. J. Stent Thrombosis. *J. Am. Coll. Cardiol.* **2010**, *56* (17), 1357–1365.
- (10) Garg, S.; Serruys, P. W. Coronary Stents: Current Status. *J. Am. Coll. Cardiol.* **2010**, *56* (10 SUPPL.), S1–S42.
- (11) Serruys, P. W.; Daemen, J. Response to Camenzind et Al: Commentary. *Circulation* **2007**, *115* (11), 1455.

- (12) Pfisterer, M.; Brunner-La Rocca, H. P.; Buser, P. T.; Rickenbacher, P.; Hunziker, P.; Mueller, C.; Jeger, R.; Bader, F.; Osswald, S.; Kaiser, C. Late Clinical Events After Clopidogrel Discontinuation May Limit the Benefit of Drug-Eluting Stents. An Observational Study of Drug-Eluting Versus Bare-Metal Stents. *J. Am. Coll. Cardiol.* **2006**, *48* (12), 2584–2591.
- (13) McFadden, E. P.; Stabile, E.; Regar, E.; Cheneau, E.; Ong, A. T. L.; Kinnaird, T.; Suddath, W. O.; Weissman, N. J.; Torguson, R.; Kent, K. M.; Pichard, A. D.; Satler, L. F.; Waksman, R.; Serruys, P. W. Late Thrombosis in Drug-Eluting Coronary Stents after Discontinuation of Antiplatelet Therapy. *Lancet* **2004**, *364* (9444), 1519–1521.
- (14) Waksman, R. Drug-Eluting Stents: Is New Necessarily Better? *Lancet* **2008**, *372* (9644), 1126–1128.
- (15) Zhang, J.; Liu, Y.; Luo, R.; Chen, S.; Li, X.; Yuan, S.; Wang, J.; Huang, N. In Vitro Hemocompatibility and Cytocompatibility of Dexamethasone-Eluting PLGA Stent Coatings. *Appl. Surf. Sci.* **2015**, *328*, 154–162.
- (16) Windecker, S.; Serruys, P. W.; Wandel, S.; Buszman, P.; Trznadel, S.; Linke, A.; Lenk, K.; Ischinger, T.; Klauss, V.; Eberli, F.; Corti, R.; Wijns, W.; Morice, M. C.; di Mario, C.; Davies, S.; van Geuns, R. J.; Eerdmans, P.; van Es, G. A.; Meier, B.; Jüni, P. Biolimus-Eluting Stent with Biodegradable Polymer versus Sirolimus-Eluting Stent with Durable Polymer for Coronary Revascularisation (LEADERS): A Randomised Non-Inferiority Trial. *Lancet* **2008**, *372* (9644), 1163–1173.
- (17) Ormiston, J. A.; Serruys, P. W.; Regar, E.; Dudek, D.; Thuesen, L.; Webster, M. W.; Onuma, Y.; Garcia-Garcia, H. M.; McGreevy, R.; Veldhof, S. A Bioabsorbable Everolimus-Eluting Coronary Stent System for Patients with Single de-Novo Coronary Artery Lesions (ABSORB): A Prospective Open-Label Trial. *Lancet* **2008**, *371* (9616), 899–907.
- (18) Stefanini, G. G.; Kalesan, B.; Serruys, P. W.; Heg, D.; Buszman, P.; Linke, A.; Ischinger, T.; Klauss, V.; Eberli, F.; Wijns, W.; Morice, M. C.; Di Mario, C.; Corti, R.; Antoni, D.; Sohn, H. Y.; Eerdmans, P.; Van Es, G. A.; Meier, B.; Windecker, S.; Jüni, P. Long-Term Clinical Outcomes of Biodegradable Polymer Biolimus-Eluting Stents versus Durable Polymer Sirolimus-Eluting Stents in Patients with Coronary Artery Disease (LEADERS): 4 Year Follow-up of a Randomised Non-Inferiority Trial. *Lancet* **2011**, *378* (9807), 1940–1948.
- (19) Zhang, X.; Shi, F.; Niu, J.; Jiang, Y.; Wang, Z. Superhydrophobic Surfaces: From Structural Control to Functional Application. *J. Mater. Chem.* **2008**, *18*, 621–633.
- (20) Poortinga, A. T.; Bos, R.; Norde, W.; Busscher, H. J. *Electric Double Layer Interactions in Bacterial Adhesion to Surfaces*; 2002; Vol. 47.
- (21) Kiremitci-Gumusderelioglu, M.; Pesmen, A. Microbial Adhesion to Ionogenic PHEMA, PU and PP Implants. *Biomaterials* **1996**, *17* (4), 443–449.

- (22) Speranza, G.; Gottardi, G.; Pederzoli, C.; Lunelli, L.; Canteri, R.; Pasquardini, L.; Carli, E.; Lui, A.; Maniglio, D.; Brugnara, M.; Anderle, M. Role of Chemical Interactions in Bacterial Adhesion to Polymer Surfaces. *Biomaterials* **2004**, *25* (11), 2029–2037.
- (23) Bélanger, M. C.; Marois, Y.; Roy, R.; Mehri, Y.; Wagner, E.; Zhang, Z.; King, M. W.; Yang, M.; Hahn, C.; Guidoin, R. Selection of a Polyurethane Membrane for the Manufacture of Ventricles for a Totally Implantable Artificial Heart: Blood Compatibility and Biocompatibility Studies. *Artif. Organs* **2000**, *24* (11), 879–888.
- (24) Zhang, X.; Wang, L.; Levänen, E. Superhydrophobic Surfaces for the Reduction of Bacterial Adhesion. *RSC Adv.* **2013**, *3* (30), 12003.
- (25) Jucker, B. a; Jucker, B. a; Harms, H.; Harms, H.; Zehnder, A. J. B.; Zehnder, A. J. B. Adhesion of the Positively Charged Bacterium. *Microbiology* **1996**, *178* (18), 5472–5479.
- (26) Gottenbos, B.; Van Der Mei, H. C.; Busscher, H. J.; Grijpma, D. W.; Feijen, J. Initial Adhesion and Surface Growth of *Pseudomonas Aeruginosa* on Negatively and Positively Charged Poly(methacrylates). *J. Mater. Sci. Mater. Med.* **1999**, *10* (12), 853–855.
- (27) Hori, K.; Matsumoto, S. Bacterial Adhesion: From Mechanism to Control. *Biochem. Eng. J.* **2010**, *48* (3), 424–434.
- (28) Neufeld, B. H.; Reynolds, M. M. Critical Nitric Oxide Concentration for *Pseudomonas Aeruginosa* Biofilm Reduction on Polyurethane Substrates. *Biointerphases* **2016**, *1111* (3), 31012.
- (29) Banerjee, I.; Pangule, R. C.; Kane, R. S. Antifouling Coatings: Recent Developments in the Design of Surfaces That Prevent Fouling by Proteins, Bacteria, and Marine Organisms. *Adv. Mater.* **2011**, *23* (6), 690–718.
- (30) Wenzel, R. N. Resistance of Solid Surfaces. *Ind. Eng. Chem.* **1936**, *28*, 988–994.
- (31) Cassie, B. D.; Cassie, A. B. D.; Baxter, S. Of Porous Surfaces,. *Trans. Faraday Soc.* **1944**, *40* (5), 546–551.
- (32) Sousa, C.; Rodrigues, D.; Oliveira, R.; Song, W.; Mano, J. F.; Azeredo, J. Superhydrophobic poly(L-Lactic Acid) Surface as Potential Bacterial Colonization Substrate. *AMB Express* **2011**, *1* (1), 34.
- (33) Barthlott, W.; Neinhuis, C. Purity of the Sacred Lotus, or Escape from Contamination in Biological Surfaces. *Planta* **1997**, *202* (1), 1–8.
- (34) Neinhuis, C.; Barthlott, W. Seasonal Changes of Leaf Surface Contamination in Beech , Oak , and Ginkgo in Relation to Leaf Micromorphology and Wvettabiity. *New Phytol.* **1998**, *138* (1), 91–98.
- (35) Neinhuis, C.; Barthlott, W. Characterization and Distribution of Water-Repellent , Self-Cleaning Plant Surfaces Author ( S ): C . NEINHUIS and W . BARTHLOTT Source : Annals of Botany , Vol . 79 , No . 6 ( June 1997 ), Pp . 667-677 Published by : Oxford University Press Stable URL : *Ann. Bot.* **1997**, *79* (6), 667–677.

- (36) Nosonovsky, M.; Bhushan, B. Superhydrophobic Surfaces and Emerging Applications: Non-Adhesion, Energy, Green Engineering. *Curr. Opin. Colloid Interface Sci.* **2009**, *14* (4), 270–280.
- (37) Shen, L.; Ji, A.; Shen, J. Silver Mirror Reaction as an Approach to Construct Superhydrophobic Surfaces with High Reflectivity. *Langmuir* **2008**, *24* (18), 9962–9965.
- (38) Leszczak, V.; Smith, B. S.; Popat, K. C. Hemocompatibility of Polymeric Nanostructured Surfaces. *J. Biomater. Sci. Polym. Ed.* **2013**, No. March 2013, 37–41.
- (39) Damodaran, V. B.; Bhatnagar, D.; Leszczak, V.; Popat, K. C. Titania Nanostructures: A Biomedical Perspective. *RSC Adv.* **2015**, *5* (47), 37149–37171.
- (40) Sorkin, J. A.; Hughes, S.; Soares, P.; Popat, K. C. Titania Nanotube Arrays as Interfaces for Neural Prostheses. *Mater. Sci. Eng. C* **2015**, *49*, 735–745.

## CHAPTER 2

### FABRICATION AND CHARACTERIZATION OF TITANIA NANOTUBE ARRAYS

#### 2.1 Introduction

##### 2.1.1 *Titanium as a Biomaterial*

Significant use of titanium alloys started with artificial joints. Titanium alloys combined with ultra-high-molecular-weight polyurethane were commonly used to replace knee and hip joints, but the polyurethane wore out quickly due to the friction from the titanium.<sup>1,2</sup> Other materials used for joint replacement either caused patients pain over long term use (alumina and steel) or had poor biocompatibility (cobalt based alloys).<sup>1,3-5</sup> In particular, metals such as cobalt would corrode and release ions when implanted in the body, and these ions proved to be toxic to the surrounding tissues.<sup>1,6</sup> Titanium exhibits strong corrosion resistance, and readily forms alloys with zirconium and niobium which improve its corrosion resistance.<sup>4,5</sup> These alloys also form oxide layers, which creates an inert surface on the titanium that minimizes interactions with the surrounding tissues. Titanium has been found to have strong wear resistance, and while its elastic modulus is lower than common steel alloys, this was found to be beneficial as it reduces stress shielding.<sup>1,3,5,6</sup> The titanium alloys were found to transfer more body weight to adjacent bones, reducing bone density loss.<sup>1</sup> Titanium alloys will still fail from fatigue over long periods of time however, so titanium is most commonly used in applications with lower stresses than joint replacements, such as plates, nails, heart valves, and stents.<sup>1,6,7</sup>

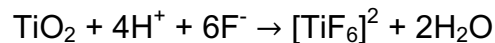
### **2.1.2 Surface Modification of Titania**

Nanoscale topographies have been investigated for their ability to improve biocompatibility. Researchers have investigated nanoscale pores, fibers, wires, particles, hydrogels, and arrays of tubes.<sup>8</sup> Nanotube arrays can readily be formed on titania through chemical etching and oxidation, and these arrays have been shown to have improved biocompatibility.<sup>8</sup> Previous studies have shown that titania nanotube arrays exhibit greater endothelialization and osseointegration, increased cell growth and deposition, improved hemocompatibility, and reduced thrombogenicity.<sup>9-11</sup> Other studies have looked into methods for using nanotube arrays for drug delivery, either to reduce the incidence of infections or to encourage implant acceptance and integration with the body.<sup>8,12</sup>

There are three main methods for manufacturing titania nanotube arrays. Templates in which titania can be deposited have been used to form nanotube arrays, after which the template can be removed using solvents.<sup>8</sup> The first nanotubes generated using this method were created using anodic aluminum oxide with uniform pores to create a polymer template.<sup>8,13</sup> The titanium oxide was then deposited on the polymer, which was removed with acetone to create the nanotube arrays with outer diameters of approximately 150 nm and thicknesses of about 50 nm.<sup>13</sup> Later researchers were able to create titania nanotube arrays using a zinc oxide template instead of aluminum. These were easier to manufacture because the template could be removed during the deposition of the titanium oxide if it was done with liquid phase deposition, and gel-like nanotube arrays could also be generated using this method.<sup>13</sup> The nanotubes created through this method, however, have closed ends – meaning they cannot be used for drug delivery –

and there is not a way for their length to be controlled.<sup>13</sup> Because of this, negative templates were developed which allowed researchers to control the length of the nanotube arrays. These templates were able to generate uniform nanotube arrays with diameters ranging between 100-200 nm, but the size was limited by the pore size of the materials used to create the templates.<sup>13</sup> This method could not create nanotubes with smaller diameters, and again could only create nanotubes with closed ends.<sup>13</sup>

Electrochemical anodization is also commonly used to grow titania nanotubes from a titania base.<sup>8,13</sup> In this process, titanium oxide is the anode while a platinum sheet functions as a cathode. When a voltage, typically between 20-60 V, is applied to these metals in the presence of an electrolyte containing fluorine, nanotube arrays will grow on the surface of the titanium oxide.<sup>8</sup> The chemical process that generates these nanotube arrays is controlled by the following two equations.<sup>8</sup>



Nanotube arrays created through anodization have been shown to have uniform orientation without requiring any extra effort to create this uniformity.<sup>8</sup> Additionally, the size and geometry of the nanotube arrays can be varied by adjusting the contents of the electrolyte or the voltage applied during the anodization.<sup>8</sup> This means that nanotube arrays with a range of characteristics can be created relatively easily, making this a commonly used process for generating nanotube arrays. The nanotube arrays created using anodization must be annealed after generation to transform the initial amorphous crystal structure into anatase and rutile phases.<sup>8</sup> A disadvantage of this need for annealing is that the temperatures needed to properly anneal the nanotube arrays can

damage the nanotubes if not properly controlled, which adds to the inherent fragility of the nanotube arrays.<sup>8</sup>

Nanotube arrays can also be formed through a hydrothermal process where titania powders are mixed in a sodium hydroxide solution and heating the mixture to at least 110°C.<sup>8</sup> The sodium hydroxide breaks the bonds between the titanium and oxygen, and then when the mixture is washed with hydrochloric acid the sodium is removed and titania nanotube arrays are formed.<sup>8</sup> This method has been used to create nanotubes with very small diameters – below 10 nm – in a tightly packed array.<sup>8</sup> Additionally, the hydrochloric acid wash has been found to remove impurities in the nanotube arrays, resulting in nanotubes made of nearly pure titanium oxide.<sup>8</sup> However, the resulting nanotube arrays are not highly ordered like the ones created through electrochemical anodization.<sup>8</sup>

### **2.1.3 Silanization**

Silanes are a class of molecules that contain silicon atoms saturated with other atoms, typically hydrogen, the simplest being SiH<sub>4</sub>. They are widely used to modify surfaces because of their ability to covalently bond with metals, glass, and ceramics. Silanes can change how a surface holds a charge, how it adheres to other materials, and how it interacts with liquids. This last modification has been investigated by many research teams because silanes can be used to alter the surface energy while remaining inert under many conditions.

Superhydrophobic surfaces have been found to reduce the adhesion of some bacteria compared to hydrophilic and hydrophobic surfaces.<sup>14,15</sup> The bacteria that did adhere to the superhydrophobic surfaces were also easily removed through rinsing.<sup>15</sup>

Other silanized superhydrophobic surfaces were shown to have reduced absorption of fibrinogen and albumin, which in turn reduced the adhesion of bacteria that bind to those proteins.<sup>14</sup> Silanized titania nanotube arrays have been shown to reduce platelet aggregation as well.<sup>16</sup> Other silanized titanium surfaces were shown to improve titanium's corrosion resistance due to the reduced attachment of the bacteria that cause the corrosion.<sup>17</sup>

## **2.2. Materials and Methods**

### ***2.2.1 Fabrication of Superhemophobic Titania Nanotube Arrays***

Titania nanotube arrays were fabricated from titanium sheets (0.1 cm thick) cut into 2.5 cm x 2.5 cm squares. The titanium substrates were first cleaned in acetone using a sonicator for 7 mins. They were then rinsed with M90 detergent and cleaned with isopropyl alcohol in a sonicator for 3 mins. The titania nanotube arrays were fabricated using the anodization process described elsewhere.<sup>18-22</sup> The electrolyte used for anodization was composed of 95% v/v diethylene glycol (DEG, Alfa) and 2% v/v hydrofluoric acid (HF, Alfa) by volume in de-ionized (DI) water. The titanium sheet was used as the anode and platinum foil was used as the cathode. The anodization was done for 24 hrs at 60 V. After anodization, the titania nanotube arrays were rinsed three times with DI water, dried with nitrogen gas, and annealed for 3 hrs at 530°C with a ramp rate of 15°C in ambient oxygen. The titania nanotube arrays (and unmodified titanium) were further cut into 0.5 cm X 0.5 cm which were used for all subsequent studies.

Superhemophobic titania nanotube arrays were fabricated by modifying the surface using chemical vapor deposition. Prior to surface modification, titania nanotube

arrays were etched in plasma atmosphere at 200 V in 10 cm<sup>3</sup>/min of oxygen gas for 10 mins. The titania nanotube arrays were placed on a hot plate next to a glass slide with 100-120 μl of either octadecyltrichlorosilane (referred to as S1, Gelest) or (heptadecafluoro-1,1,2,2-tetrahydrodecyl)trichlorosilane (referred to as S2, Gelest). These silanes were chosen in order to have an examples from two classes of silanes – alkyl-silanes and fluoro-silanes. The titania nanotube arrays and glass slide were covered with a glass bowl, and heated for 1 hr at 120°C. The superhemophobic titania nanotube arrays were then rinsed with DI water, dried and stored in desiccator until further use.

Superhydrophilic titania nanotube arrays were fabricated by binding poly-ethylene glycol to the nanotube surfaces. As with the superhydrophobic arrays, the titania nanotube arrays were first etched with plasma at 200 V in 10 cm<sup>3</sup>/min of oxygen gas for 10 mins. The titania nanotube arrays were placed in plastic petri dishes and covered with enough 2-[methoxy(polyethyleneoxy)propyl]trimethoxysilane (referred to as S2, Gelest), approximately 200 μl.

The characterization results for the substrates used for the hemocompatibility studies (Chapter 3) and the bacteria adhesion studies (Chapter 4) are both presented here. The following nomenclature will be used in this chapter for the substrates: unmodified titanium (referred to as Ti), unmodified titania nanotube arrays (referred to as NT), titania nanotube arrays coated with the two superhemophobic silanes (referred to as NT-S1 and NT-S2), and the superhydrophilic titania nanotube arrays (referred to as NT-S3). Prior to all the biological experiments, the substrates were sterilized. They were incubated in ethanol for 30 mins, followed by rinsing with DI water.

### **2.2.2 Characterization of Titania Nanotube Arrays**

The surface morphology was characterized using a field emission scanning electron microscope (SEM, JEOL JSM-6500). All surfaces were coated with a 10 nm layer of gold prior to imaging and imaged at 15 kV.<sup>20,22-24</sup> The average nanotube diameter was measured using ImageJ.

The hemophobicity and hydrophobicity were characterized by measuring the contact angle of whole blood on different surfaces. An approximately 10  $\mu$ l droplet of blood or 20  $\mu$ l droplet of water was formed on the tip of a syringe and lowered until it contacted and detached onto the surface. An image of the droplet was taken using a goniometer (Ramé-Hart Model 250) connected to a camera.<sup>23</sup> Images were captured within 5 secs of contact between the droplet and the surface. Images for advancing and receding contact angles were also taken by slowly adding and removing water from the droplet, and roll off angles were acquired by placing a droplet on the surface and tilting the goniometer. The images were analyzed using the goniometer software to measure the contact angles.

The surface chemistry was characterized using X-ray photoelectron spectroscopy (XPS). Scans were taken for all four substrates. Survey spectra were collected from 0 to 1100 eV with a pass energy of 187.85 eV. High resolution spectra were collected for titanium and oxygen using a pass energy of 10 eV. Surface elemental composition was calculated using peak fit analysis in the Multipack software.<sup>25</sup>

The presence of anatase and rutile crystal phases on different substrates was detected through GAXRD (Bruker D8).<sup>18</sup> XRD scans were collected at  $\theta=1.5^\circ$  and  $2\theta$  ranges were chosen based on significant peak intensities. Detector scans were run at a

step size of 0.01 with a time per step of 1 sec. Peaks were filtered and correlated to crystal structures using DIFFRACT.EVA software.

## **2.3 Results and Discussion**

### **2.3.1 Characterization of Titania Nanotube Arrays**

SEM was used to characterize surface morphology of titania nanotube arrays. The results indicate that vertically oriented and uniformly distributed titania nanotube arrays with an average diameter of 155.9 nm (**Figure 2.3.1**). The nanotube arrays were further modified with S1 and S2 to make them superhemophobic. The results indicate no visible changes in the morphology of the nanotube arrays after modification, however, the average diameter increased to 167.2 nm for NT-S1 ( $p \leq 0.05$ ) and 169.8 nm for NT-S2 ( $p \leq 0.05$ ) (**Figure 2.3.2**). The diameter increase was expected as the silanes are deposited on the outside walls of the titania nanotube arrays.

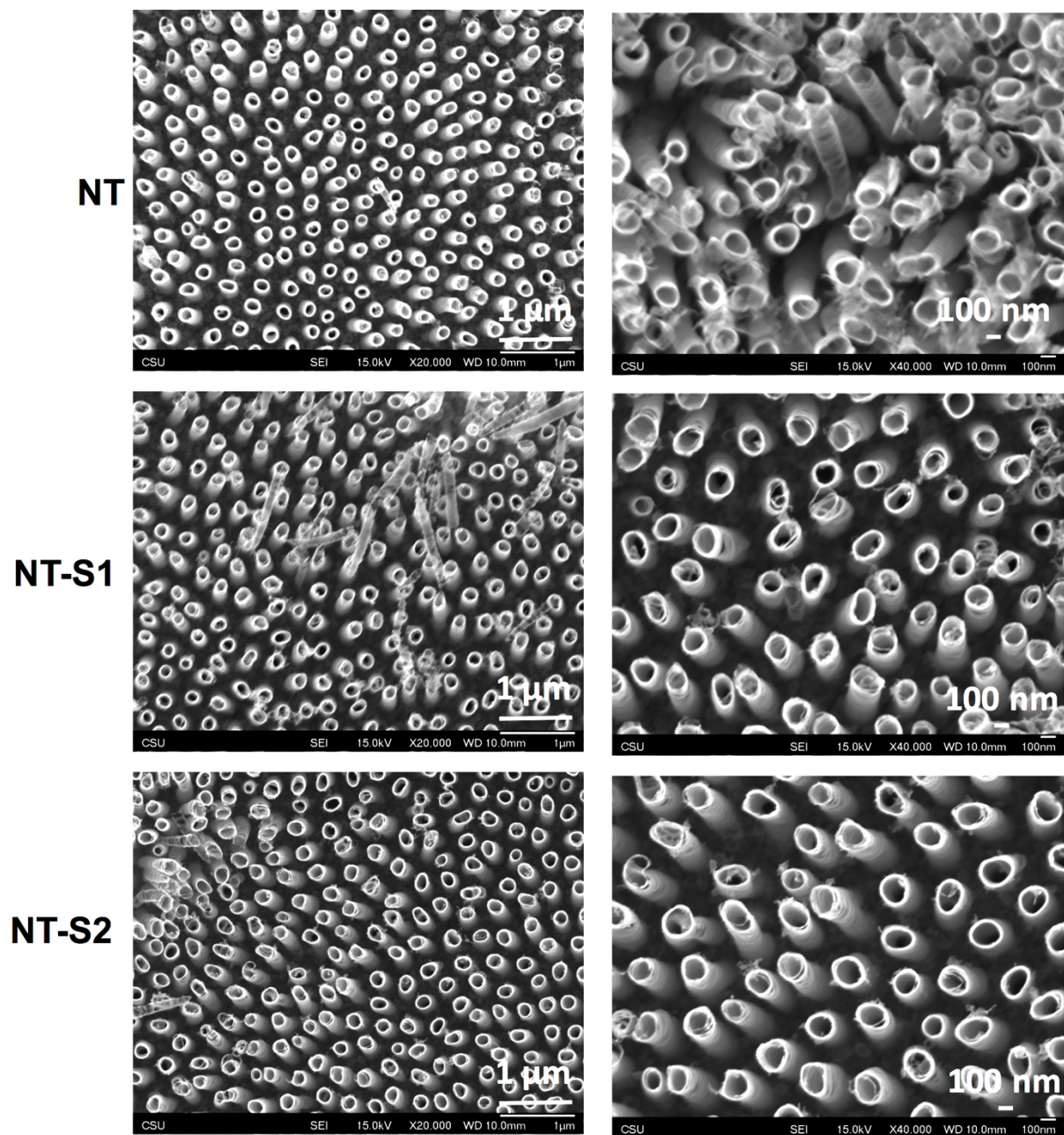


**Figure 2.3.1:** SEM images of titania nanotube arrays fabricated by anodization and modified using chemical vapor deposition.

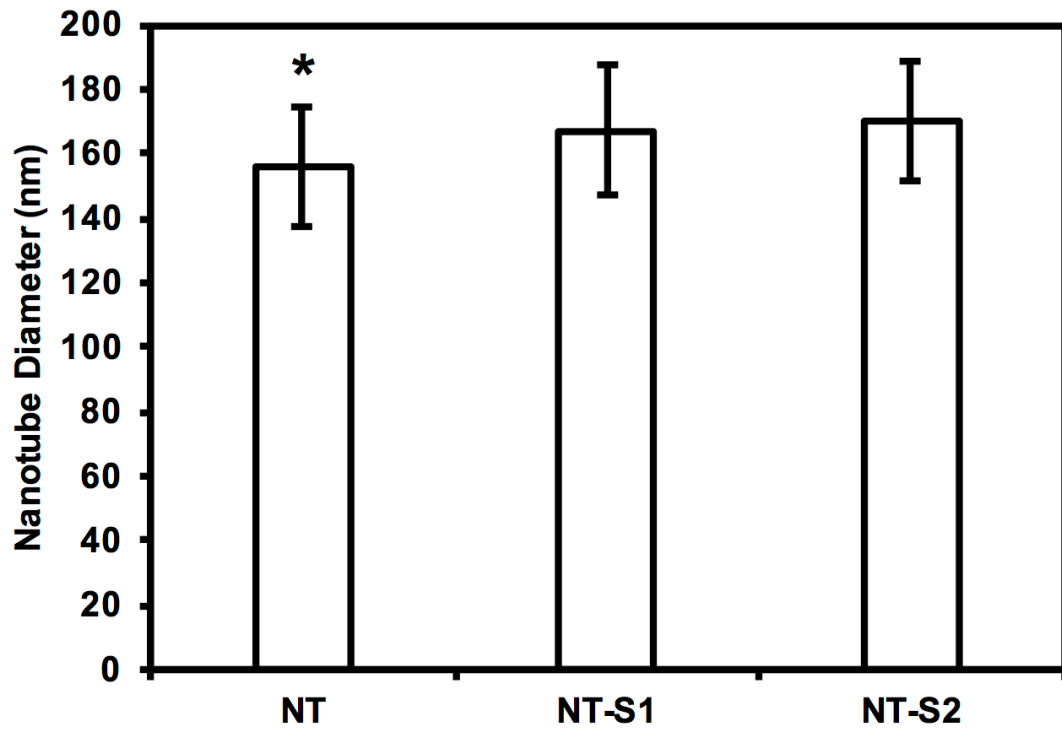


**Figure 2.3.2:** Average diameter of titania nanotube arrays before and after modification. The average diameters for NT were smaller than NT-S1 or NT-S2 diameters ( $p \leq 0.05$ ).

The titania nanotube arrays used for the bacteria studies (NT-S2 and NT-S3) were found to have an average inner diameter of 150 nm, were vertically oriented, and were uniformly distributed across the titania surface (**Figure 2.3.3 and 2.3.4**). After modification with S1 and S2, the average inner diameter of the nanotube decreased to 140 nm ( $p \leq 0.05$ ) and ( $p \leq 0.05$ ) 147 nm respectively (**Figure 2.3.4**). The orientation and distribution of the silanized nanotubes remained unchanged, as expected (**Figure 2.3.3**). The average wall thickness of the nanotube arrays also increased after modification, going from 27 nm (NT) to 33 nm (NT-S3) ( $p \leq 0.05$ ) and 38 nm (NT-S2) ( $p \leq 0.05$ ). This change was expected due to the bonding of the silanes with the titania surface.

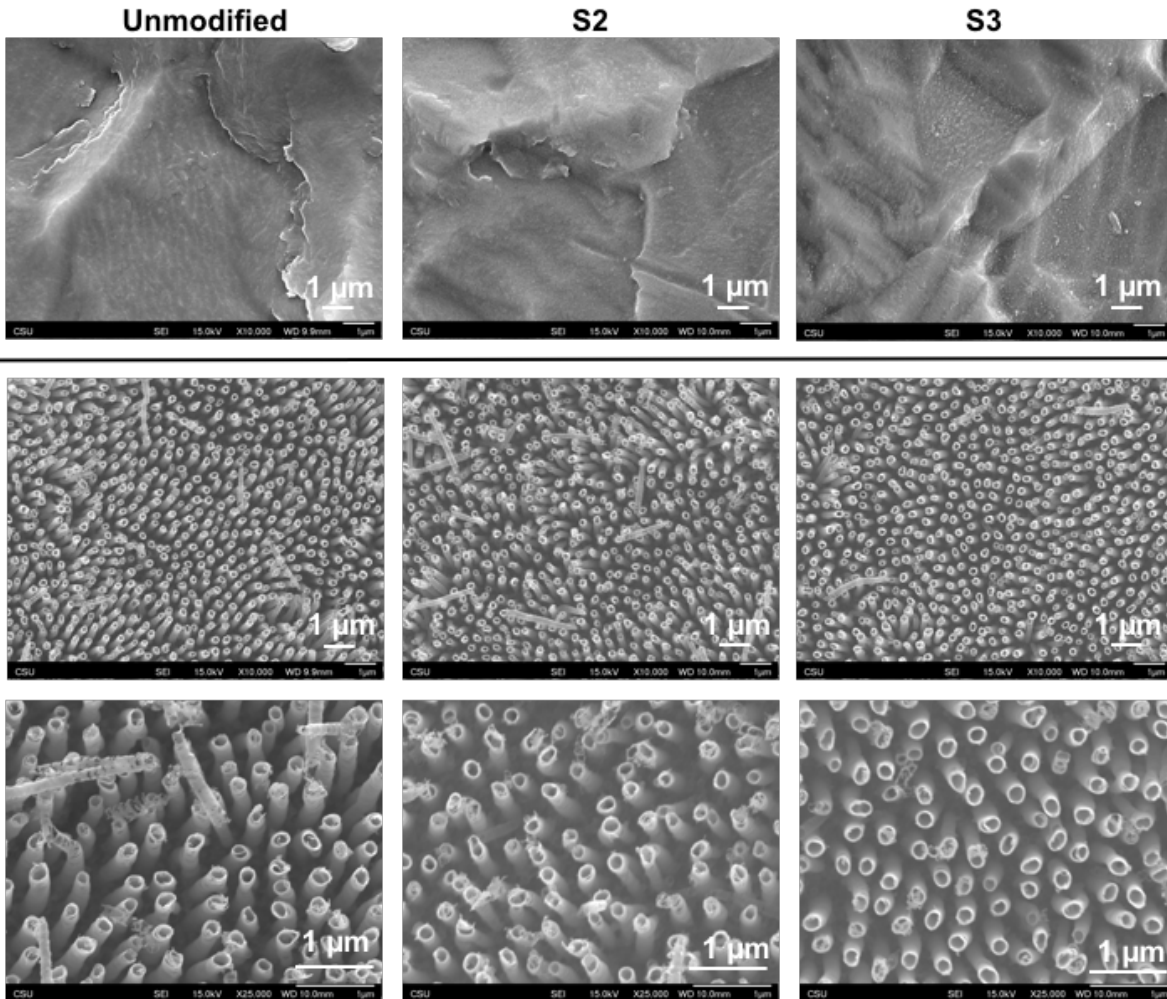


**Figure 2.3.3:** SEM images of titania nanotube arrays

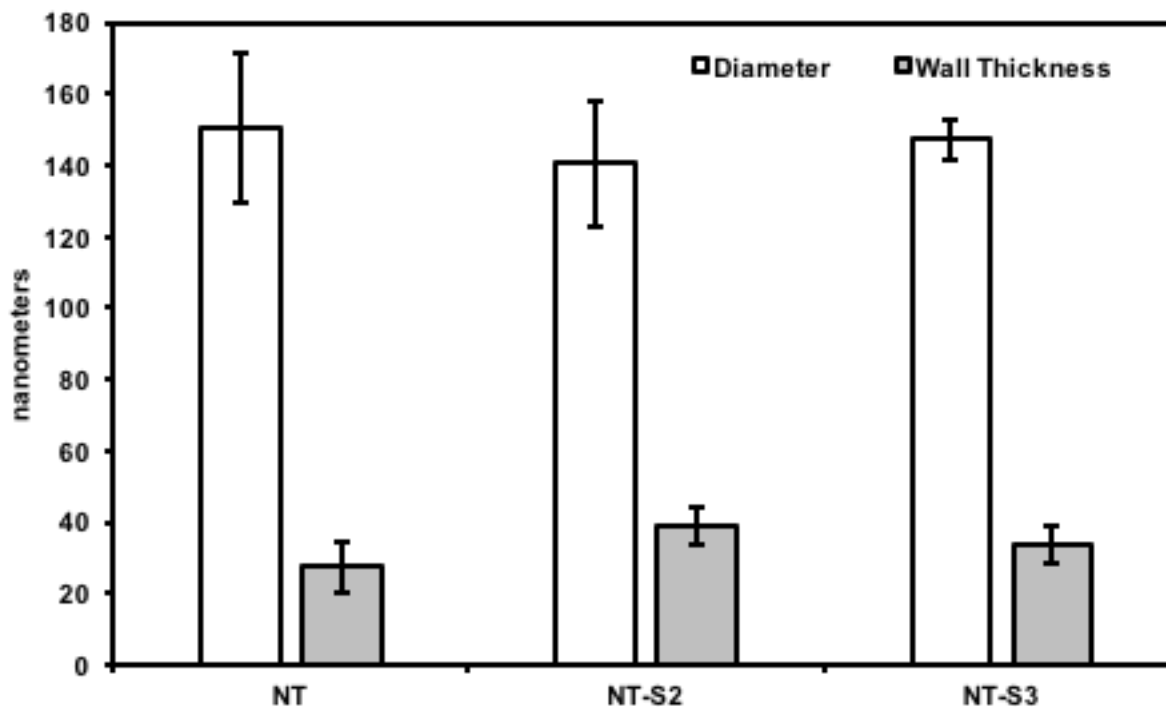


**Figure 2.3.4:** Average inner diameter and thickness of titania nanotube arrays

Contact angle goniometry was used to characterize the surface hemophobicity. The results indicate a static contact angle of 61° for Ti, 28° for NT, 154° for NT-S1, and 157° for NT-S2 (**Figure 2.3.5**). The contact angle measurements for NT-S1 and NT-S2 were significantly higher than Ti and NT ( $p < 0.05$ ) (**Figure 2.3.5**). The roll off angles were measured as 16° for NT-S1 and 9° for NT-S2, while the blood did not roll off the Ti or NT surfaces. A contact angle greater than 150° and roll off angle less than 10° indicates that a surface is superhemophobic. This means that the NT-S2 is the most superhemophobic, followed by NT-S1. A droplet on a textured surface will enter either the Wenzel state or the Cassie-Baxter state. The Wenzel state is where the droplet spreads throughout the surface features, completely wetting the surface.<sup>16</sup> This state is expected for Ti and NT. The Cassie-Baxter state is when air pockets remain among the surfaces features, leading

to the droplet being suspended above the surface. The Cassie-Baxter state is characterized by high contact angles due to the reduced contact between the droplet and surface due to the presence of the air pockets. This state is expected for NT-S1 and NT-S2. We hypothesize that by minimizing the contact between blood and a surface we can reduce the formation of clots.

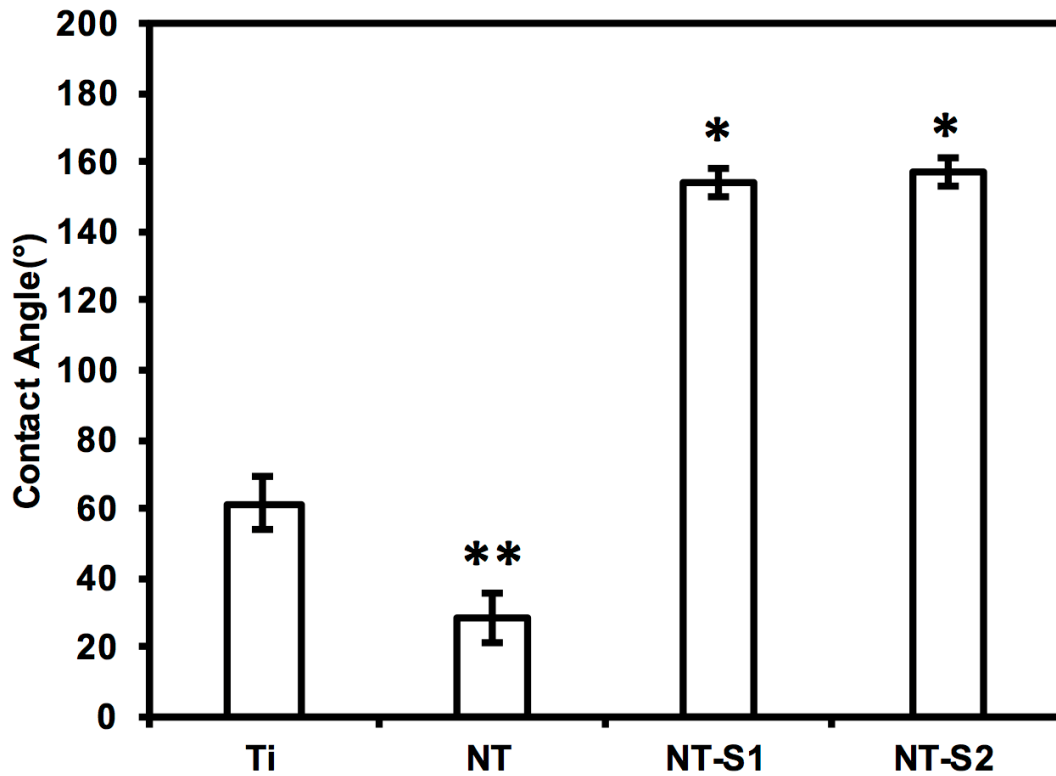


**Figure 2.3.5:** Average whole blood contact angles for different surfaces. The contact angles for NT-S1 and NT-S2 are significantly higher than that for Ti and NT ( $p \leq 0.05$ )

For the substrates used in the bacteria studies, the results indicate an approximate Young's contact angle of  $75^\circ$  for Ti,  $26^\circ$  for NT,  $164^\circ$  for NT-S2, and  $7^\circ$  for NT-S3 (**Figure 2.3.6**). The contact angles for all the substrates were significantly different from each other ( $p < 0.05$ ). Additionally, the average roll-off angle for NT-S2 was measured as  $8^\circ$ , while the NT and NT-S3 substrates did not have roll-off angles. The water droplets did

not roll-off the Ti substrates until the tilt angle on the goniometer reached the receding angle for the substrate, at which point the droplet slid on the surface. The NT-S1 substrates can be considered superhydrophobic as they exhibit contact angles greater than  $150^\circ$  with a roll-off angle under  $10^\circ$ .

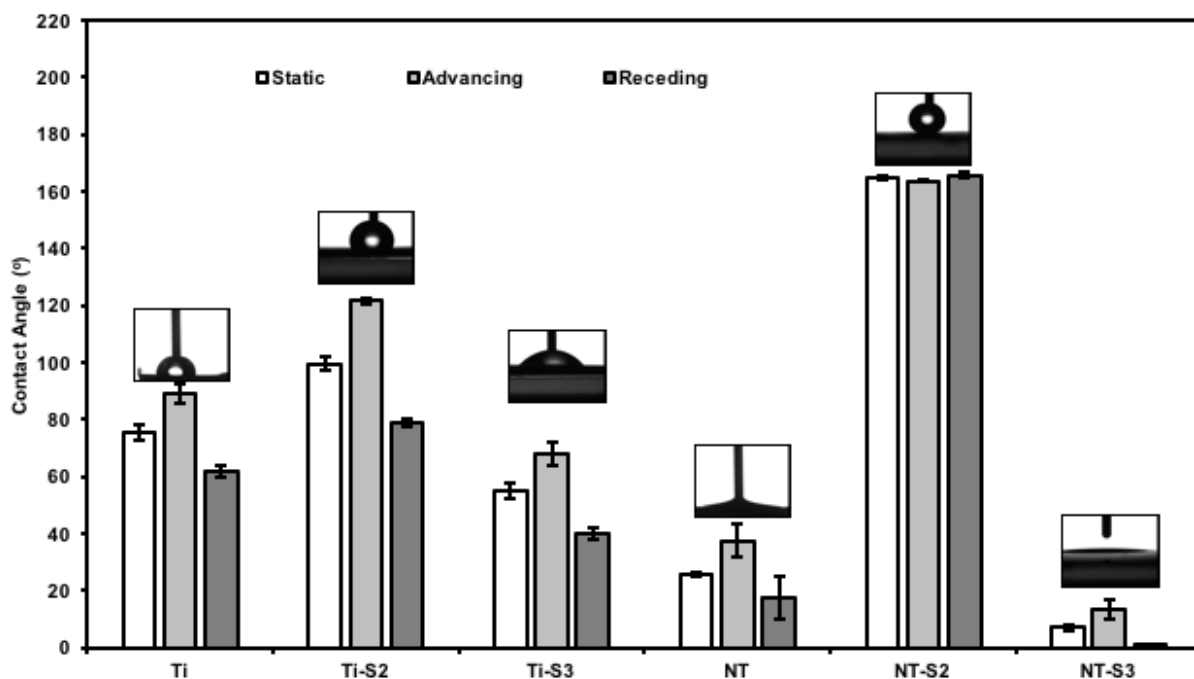


**Figure 2.3.6:** Advancing, receding, and estimated Young's contact angle for water on different titania surfaces

XPS was used to characterize the surface chemistry of different substrates. XPS will show the relative compositions of different elements on the surface of a material. The results indicate O1s, Ti2p<sub>3/2</sub>, and C1s peaks present on all four surfaces (**Figure 2.3.7**). The C1s peak was present on Ti because contamination in the XPS chamber and some trace amounts of carbon present on the Ti surface. The C1s peak was reduced on NT because of the electrochemical etching and oxidation process. Further, the C1s peak increased for both NT-S1 and NT-S2 since the silanes contain significant amounts of carbon. Similarly, the Ti2p<sub>3/2</sub> peak is present on Ti, and the peak increases on NT because of the anodization process exposing a higher amount of titanium. After silanization, the Ti2p<sub>3/2</sub> peak decreased for both NT-S1 and NT-S2. Additionally, Si1s peaks are present on both NT-S1 and NT-S2 since both the silanes contain silicon, along with a F1s peak on NT-S2 since S2 contains fluorine (**Figure 2.3.7**). The Ti2p peak decreases after silanization because the silanes are deposited on the surfaces, reducing the relative composition of titanium on the surface.

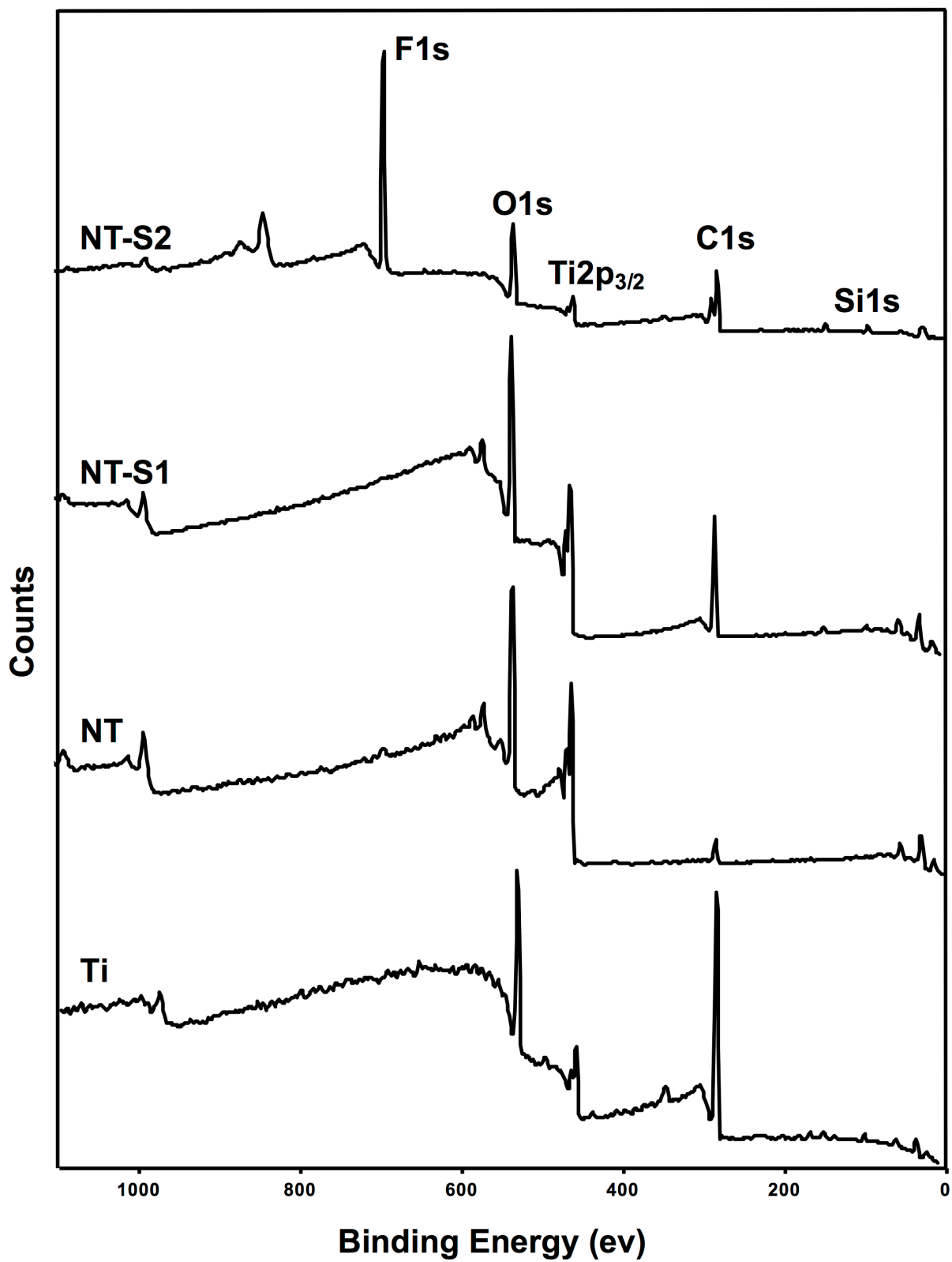


**Figure 2.3.7:** XPS survey scans for Ti, NT, NT-S1, and NT-S2 surfaces

For the substrates used in the bacteria studies, O1s, Ti2p<sub>3/2</sub>, and C1s peaks were present on all surfaces (**Figure 2.3.8**). The NT samples showed a lower C1s peak than Ti because the anodization and etching process removes some of the carbon naturally present on the surface. The NT-S2 and NT-S3 samples then had higher C1s peaks than the NT samples because the silanes contain carbon and had bonded to the titania nanotube arrays. The NT-S2 samples also had a large fluorine peak along with a C-F peak due to the fluorinated silane used on the samples. The presence of these peaks confirms that the silanes were successfully deposited on the titania nanotube arrays.

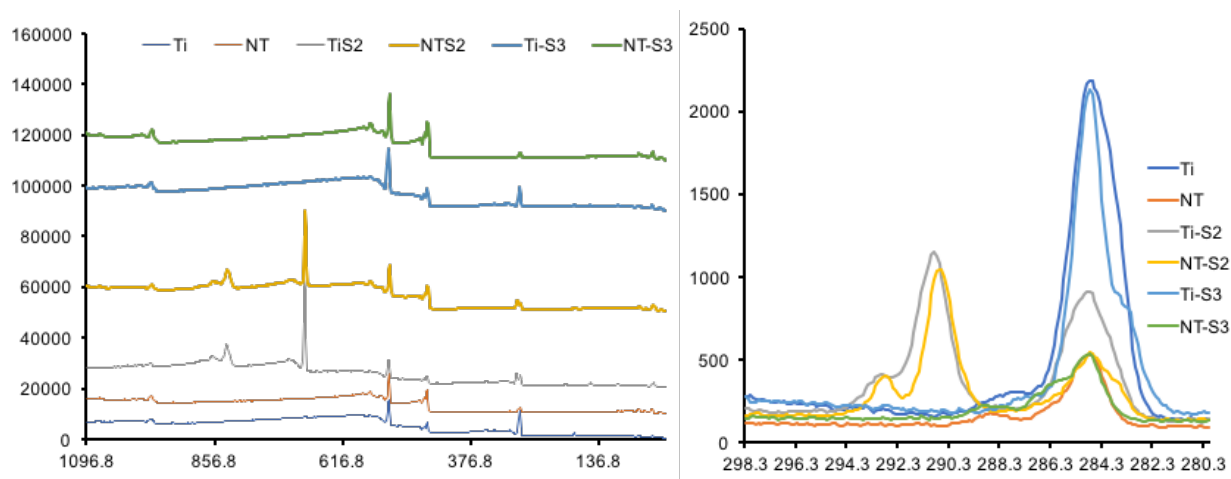


**Figure 2.3.8:** XPS survey and carbon scans Ti, NT, NT-S2, and NT-S3 surfaces

GAXRD was used to characterize the crystal structures on different surfaces. NT, NT-S1, and NT-S2 all have anatase and rutile crystal phases that are not present on Ti (**Figure 2.3.9**). These crystal phases are formed during the annealing process for the surfaces. The rutile phases are the most stable phase, but previous work has shown that a higher presence of rutile phases will cause the nanotube arrays to fall apart.<sup>18</sup> The anatase crystal structures have been shown to be metastable compared to rutile phase crystals, and to be biocompatible, which is important for this application.<sup>26,27</sup> However,

the crystal structure does not differ between the NT, NT-S1, and NT-S2 surfaces. The results indicate that the silanization does not affect the crystal structure of the titania nanotube arrays.

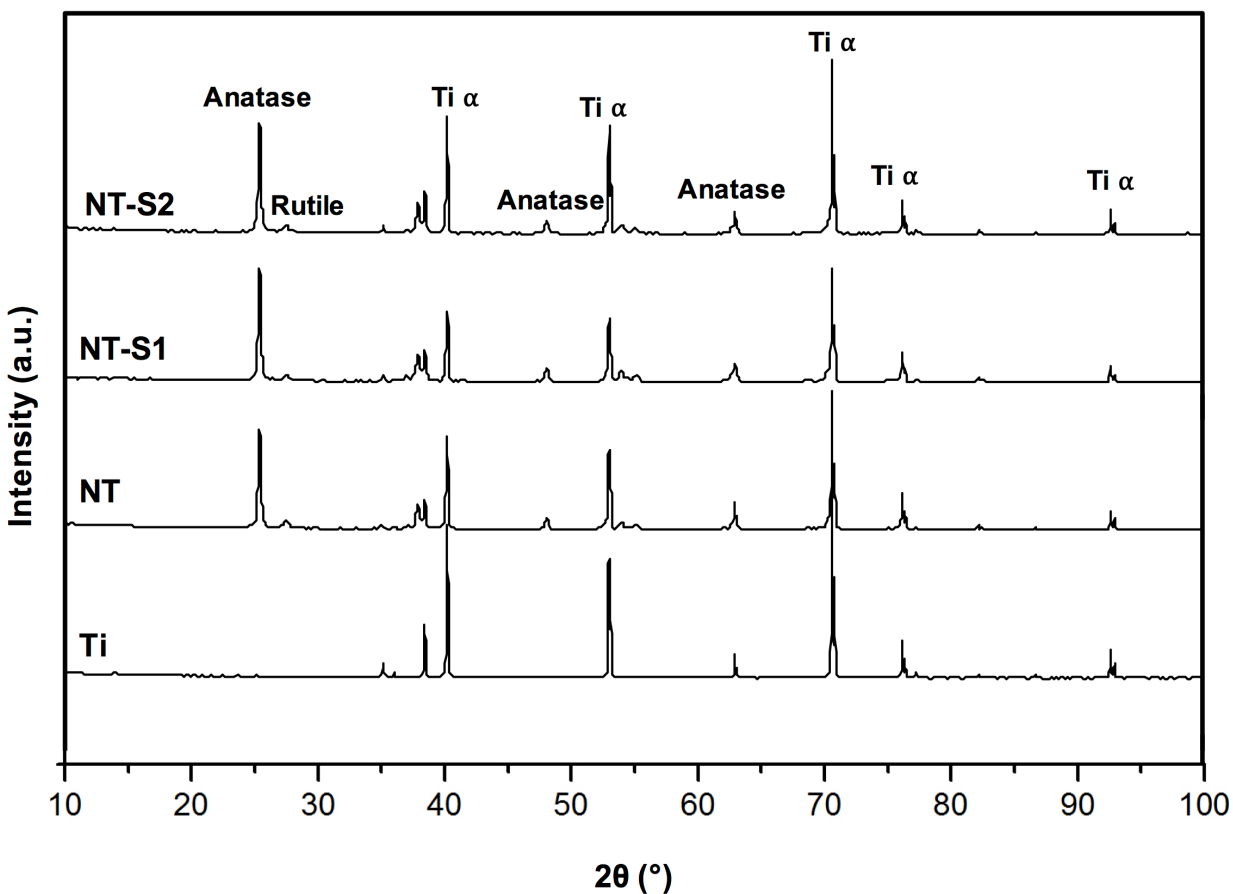


**Figure 2.3.9:** XRD scans for Ti, NT, NT-S1, and NT-S2 surfaces.

For the substrates used in the bacteria studies, the titania nanotube arrays exhibit anatase and rutile crystal structures which are not present on the unmodified titania surfaces (**Figure 2.3.10**). These crystal phases are the result of the anodization, etching, and annealing process which forms the nanotube arrays. The crystal phases were unchanged between the silanized and uncoated titania nanotube arrays, indicating

that the silanization process does not affect the underlying crystal structure of the nanotube arrays.

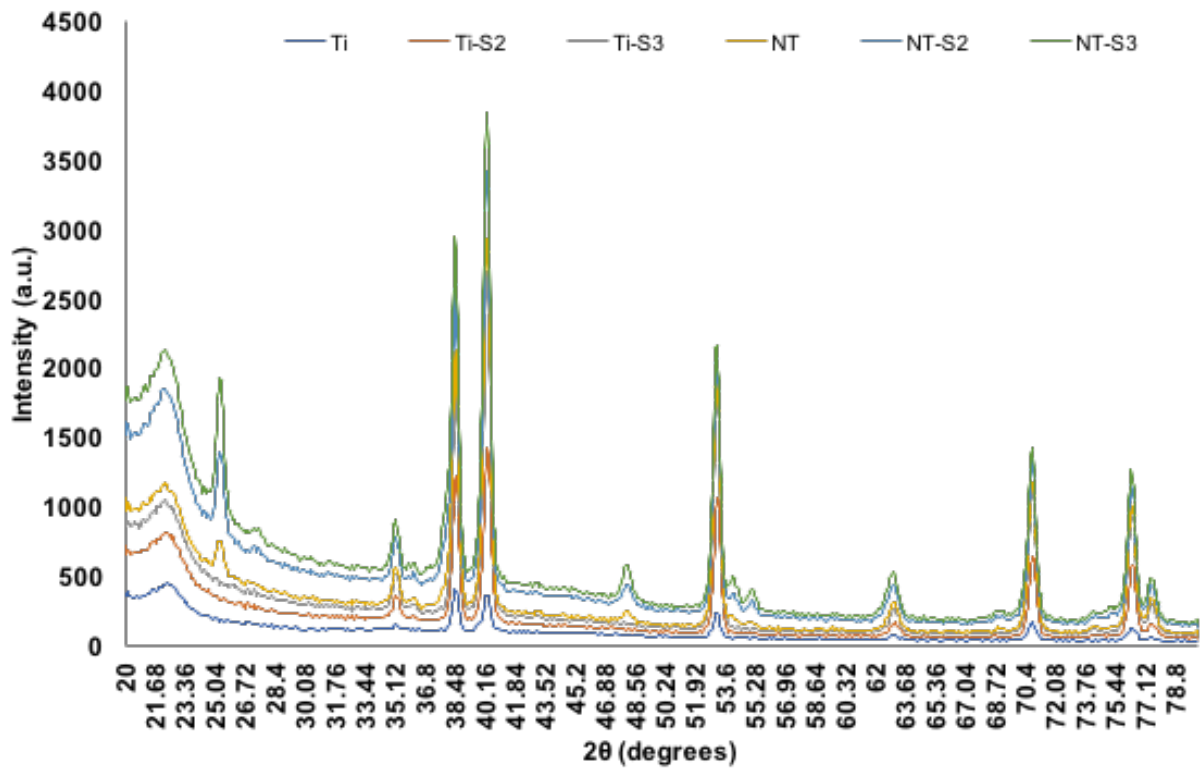


Figure 2.3.10: GAXRD scans for titanium and nanotube array samples.

## 2.4 Conclusion

Titanium is commonly used as a biomaterial due to its resistance to wear and corrosion, biocompatibility, and versatility. Significant research has gone into modifying the surface of titanium in order to further improve its biocompatibility. Cellular responses have been shown to change based on the material properties, topography, and surface chemistry of titanium. Superhydrophobic surfaces and titania nanotube arrays have both been shown to improve some aspects of biocompatibility. This research investigated the surface chemistry and characteristics of two superhydrophobic titania arrays. The nanotube arrays were fabricated using an electrochemical etching and anodization technique with a water based, diethylene glycol and hydrofluoric acid electrolyte. The resulting titania nanotube arrays were cleaned and annealed at 530° C. The titania nanotube arrays were then etched with atmospheric oxygen plasma and coated with silanes using both chemical vapor and liquid deposition techniques. The SEM images showed that the titania nanotube arrays were highly ordered and vertically oriented. The silanized nanotubes were found to be superhydrophobic when the alkane or fluorinated silanes were used, and superhydrophilic when the trimethoxysilane was used. Chemical bonding of the silanes was confirmed using XPS spectra. The XRD data showed that the underlying crystal structure of the titania nanotube arrays was unchanged by the silanization process, indicating that the underlying mechanical properties are unchanged. The results show the characteristics of the titania nanotube arrays are consistent with previous studies and may improve biocompatibility.

## REFERENCES

- (1) Long, M.; Rack, H. J. Titanium Alloys in Total Joint Replacement--a Materials Science Perspective. *Biomaterials* **1998**, *19* (18), 1621–1639.
- (2) Paschali, E. P. De Radation Potential. *Biomed. Mater.* **1995**, *29*, 1499–1505.
- (3) Yoshimitsu Okazaki, Y. I.; Kyo, K.; Tateishi, T. Corrosion Resistance and Corrosion Fatigue Strength of New Titanium Alloys for Medical Implants without V and Al. *Mater. Sci. Eng. A* **1996**, *213*, 138–147.
- (4) Okazaki, Y.; Rao, S.; Ito, Y.; Tateishi, T. Corrosion Resistance, Mechanical Properties, Corrosion Fatigue Strength and Cytocompatibility of New Ti Alloys without Al and V. *Biomaterials* **1998**, *19* (13), 1197–1215.
- (5) Yue, S.; Pilliar, R. M.; Weatherly, G. C. The Fatigue Strength of Porous-Coated Ti-6%Al-4%V Implant Alloy. *J Biomed Mater Res* **1984**, *18* (9), 1043–1058.
- (6) Santavirta, S.; Konttinen, Y. T.; Lappalainen, R.; Anttila, A.; Goodman, S. B.; Lind, M.; Smith, L.; Takagi, M.; Gómez-Barrena, E.; Nordsletten, L.; Xu, J. W. Materials in Total Joint Replacement. *Curr. Orthop.* **1998**, *12* (1), 51–57.
- (7) Wang, K. The Use of Titanium for Medical Applications in the USA. *Mater. Sci. Eng. A* **1996**, *213* (1–2), 134–137.
- (8) Damodaran, V. B.; Bhatnagar, D.; Leszczak, V.; Popat, K. C. Titania Nanostructures: A Biomedical Perspective. *RSC Adv.* **2015**, *5* (47), 37149–37171.
- (9) Brammer, K. S.; Choi, C.; Frandsen, C. J.; Oh, S.; Johnston, G.; Jin, S. Comparative Cell Behavior on Carbon-Coated TiO<sub>2</sub> Nanotube Surfaces for Osteoblasts vs. Osteo-Progenitor Cells. *Acta Biomater.* **2011**, *7* (6), 2697–2703.
- (10) Brammer, K. S.; Oh, S.; Cobb, C. J.; Bjursten, L. M.; Heyde, H. van der; Jin, S. Improved Bone-Forming Functionality on Diameter-Controlled TiO<sub>2</sub> Nanotube Surface. *Acta Biomater.* **2009**, *5* (8), 3215–3223.
- (11) Brammer, K. S.; Frandsen, C. J.; Jin, S. TiO<sub>2</sub> Nanotubes for Bone Regeneration. *Trends Biotechnol.* **2012**, *30* (6), 315–322.
- (12) Popat, K. C.; Eltgroth, M.; LaTempa, T. J.; Grimes, C. A.; Desai, T. A. Titania Nanotubes: A Novel Platform for Drug-Eluting Coatings for Medical Implants? *Small* **2007**, *3* (11), 1878–1881.
- (13) Tan, A. W.; Pingguan-Murphy, B.; Ahmad, R.; Akbar, S. A. Review of Titania Nanotubes: Fabrication and Cellular Response. *Ceram. Int.* **2012**, *38* (6), 4421–4435.
- (14) Zhang, X.; Wang, L.; Levänen, E. Superhydrophobic Surfaces for the Reduction of Bacterial Adhesion. *RSC Adv.* **2013**, *3* (30), 12003.

- (15) Lin, C.; Tang, P.; Zhang, W.; Wang, Y.; Zhang, B.; Wang, H.; Zhang, L. Effect of Superhydrophobic Surface of Titanium on Staphylococcus Aureus Adhesion. *J. Nanomater.* **2011**, 2011.
- (16) Movafaghi, S.; Leszczak, V.; Wang, W.; Sorkin, J. A.; Dasi, L. P.; Popat, K. C.; Kota, A. K. Hemocompatibility of Superhemophobic Titania Surfaces. *Adv. Healthc. Mater.* **2016**, 1600717.
- (17) Mahalakshmi, P. V.; Vanithakumari, S. C.; Gopal, J.; Mudali, U. K.; Raj, B. Enhancing Corrosion and Biofouling Resistance through Superhydrophobic Surface Modification. *Curr. Sci.* **2011**, 101 (10), 1328–1336.
- (18) Sorkin, J. A.; Hughes, S.; Soares, P.; Popat, K. C. Titania Nanotube Arrays as Interfaces for Neural Prostheses. *Mater. Sci. Eng. C* **2015**, 49, 735–745.
- (19) Capellato, P.; Escada, A. L.; Popat, K. C.; Claro, A. P. Interaction between Mesenchymal Stem Cells and Ti-30Ta Alloy after Surface Treatment. *J Biomed Mater Res A* **2013**, 2147–2156.
- (20) Capellato, P.; Smith, B. S.; Popat, K. C.; Claro, A. P. R. A. Fibroblast Functionality on Novel Ti30Ta Nanotube Array. *Mater. Sci. Eng. C* **2012**, 32 (7), 2060–2067.
- (21) Smith, B. S.; Yoriya, S.; Johnson, T.; Popat, K. C. Dermal Fibroblast and Epidermal Keratinocyte Functionality on Titania Nanotube Arrays. *Acta Biomater.* **2011**, 7 (6), 2686–2696.
- (22) Smith, B. S.; Capellato, P.; Kelley, S.; Gonzalez-Juarrero, M.; Popat, K. C. Reduced in Vitro Immune Response on Titania Nanotube Arrays Compared to Titanium Surface. *Biomater. Sci.* **2013**, 1 (3), 322–332.
- (23) Leszczak, V.; Popat, K. C. Improved in Vitro Blood Compatibility of Polycaprolactone Nanowire Surfaces. *ACS Appl. Mater. Interfaces* **2014**, 6 (18), 15913–15924.
- (24) Riedel, N. A.; Williams, J. D.; Popat, K. C. Ion Beam Etching Titanium for Enhanced Osteoblast Response. *J. Mater. Sci.* **2011**, 46 (18), 6087–6095.
- (25) Smith, B. S.; Yoriya, S.; Grissom, L.; Grimes, C. A.; Popat, K. C. Hemocompatibility of Titania Nanotube Arrays. *J. Biomed. Mater. Res. - Part A* **2010**, 95 A (2), 350–360.
- (26) Zhang, D.; Li, G.; Wang, H.; Chan, K. M.; Yu, J. C. Biocompatible Anatase Single-Crystal Photocatalysts with Tunable Percentage of Reactive Facets. *Cryst. Growth Des.* **2010**, 10 (3), 1130–1137.
- (27) Hasan, M. M.; Haseeb, A. S. M. A.; Saidur, R.; Masjuki, H. H. Effects of Annealing Treatment on Optical Properties of Anatase TiO<sub>2</sub> Thin Films. *Eng. Technol.* **2008**, 30, 221–225.

## CHAPTER 3

### HEMOCOMPATIBILITY OF TITANIA NANOTUBE ARRAYS

#### 3.1 Introduction

Materials that come into contact with blood have several issues which can cause medical devices to fail. For example, thrombosis is a major challenge for vascular stents as it obstructs the flow of blood.<sup>1,2</sup> Leaflets of artificial heart valves are also prone to thrombosis, preventing them from opening or closing properly.<sup>3-5</sup> Also, the forces exerted by the leaflets on the blood and its components tend to damage the platelets, further promoting thrombosis.<sup>6,7</sup> Catheters may be obstructed by blood clots formed on the material surface and are one of the leading sources for bloodstream infections.<sup>8</sup> Due to complications such as these, hemocompatibility is a challenge for blood-contacting medical devices. There is not a single material that is truly compatible with blood and its components.<sup>9</sup> When blood contacts a material, proteins from the plasma in the blood, particularly fibrinogen, will begin to adsorb on the surface within a few minutes of contact.<sup>10</sup> The fibrinogen will convert into fibrin, which along with other blood serum proteins will promote the attachment of platelets on the material surface. After adhering, the platelets will begin to activate, forming a platelet-immune complex.<sup>10,11</sup> The platelet-immune complexes signal leukocytes to attach on the material surface as part of the immune response, leading to further clot formation<sup>12,13</sup>. The clot can remain on the surface and grow restricting the blood flow, or it can detach from the material surface into the bloodstream, travelling throughout the body and potentially causing major complications for the patient.<sup>10,12</sup>

To deal with these adverse effects, patients receiving these medical devices are often prescribed blood thinning medications. These medications must be continued for the rest of the patient's life and increase the risks of heart failure and internal bleeding, and thus are not an ideal solution. One other method employed in clinical situations is to pre-clot the medical device surface by exposing it to the patient's blood prior to implantation.<sup>14</sup> This method, however, can only be used for porous implants such as vascular grafts, so is not applicable for valves and catheters.<sup>14</sup> Further, over time the pre-clotted material surface will wear off, exposing the device to the same issues discussed previously. Thus, there is an unmet need to prevent these complications by designing hemocompatible materials for blood contacting medical devices.

Recent studies have examined several strategies to improving material hemocompatibility.<sup>11,15-17</sup> Heparin has been investigated as a coating for blood contacting devices, particularly for stents and catheters.<sup>18-21</sup> It is a common blood thinning medication and has been shown to improve the hemocompatibility of stents by reducing the activation of thrombin, an enzyme that begins clot formation.<sup>19,22</sup> However, because of its dense negative charge, it is also thought to initiate the intrinsic pathway of blood coagulation.<sup>23</sup> Polymers modified with surface coatings, such as polyethylene terephthalate coated with polydopamine, have been investigated in attempts to enhance hemocompatibility.<sup>16,24</sup> The addition of different coatings has been shown to reduce blood cell adhesion and plasma protein adsorption.<sup>17,24,25</sup> Additionally, carbon films have been studied because of their biological inertness and inherent hemocompatibility.<sup>26</sup> All these strategies have shown some increase in hemocompatibility, but are not effective over long periods of time.<sup>20</sup> Thus, there is a need to develop material surfaces that interact

with blood and its components appropriately and remain hemocompatible over long time periods.

In this study, we have developed superhemophobic surfaces as a potential approach for enhancing the hemocompatibility of titanium based blood contacting medical devices. Titanium has been shown to be biocompatible but blood clots readily form on titanium devices, leading to their failure.<sup>27</sup> Superhemophobic surfaces were fabricated by first modifying the topography and then the chemistry of titanium surfaces. The surface topography was modified by fabricating titania nanotube arrays on titanium surface. Previous studies have shown enhanced hemocompatibility of these titania nanotubes arrays.<sup>10,28</sup> These titania nanotube arrays were further modified with alkyl and fluorinated silanes using a chemical vapor deposition technique to fabricate superhemophobic surfaces. Platelet adhesion studies on these surfaces have shown promising results, however, the way in which blood and its individual components interacts with these surfaces is not known.<sup>29</sup> In this study, superhemophobic surfaces were characterized using scanning electron microscopy (SEM), contact angle goniometry, X-ray photoelectron spectroscopy (XPS) and X-ray diffraction (XRD). Protein adsorption, material surface cytotoxicity, platelet/leukocyte adhesion, platelet activation and hemolysis was investigated on superhemophobic surfaces. The results presented here indicate improved hemocompatibility of superhemophobic surfaces when compared to that of control surfaces.

## **3.2 Materials and Methods**

The following nomenclature will be used in this chapter for the substrates: unmodified titanium (referred to as Ti), unmodified titania nanotube arrays (referred to as NT), superhydrophobic titania nanotube arrays coated with octadecyltrichlorosilane (Gelest) (referred to as NT-S1), superhydrophobic titania nanotube arrays coated with (heptadecafluoro-1,1,2,2-tetrahydrodecyl)trichlorosilane (Gelest) (referred to as NT-S2). Prior to all the biological experiments, the substrates were sterilized. They were incubated in ethanol for 30 mins, followed by rinsing with DI water.

### ***3.2.1 Protein Adsorption on Different Surfaces***

Protein adsorption on sterilized substrates was characterized using the process described elsewhere.<sup>11</sup> Sterilized substrates were incubated in 48-well plates with 100 µg/ml of a protein solution on a horizontal shaker plate (100 rpm) at 37°C and 5% CO<sub>2</sub> for 2 hrs. The two proteins investigated were human serum albumin (Pierce Biotechnology) and fibrinogen (Pierce Biotechnology). After 2 hrs of incubation, the protein solution was aspirated followed by 3 rinses with PBS to remove any non-adherent proteins. The adsorbed proteins on the surface was characterized using X-ray photoelectron spectroscopy (XPS). High resolution spectra were collected for carbon and nitrogen using a pass energy of 10 eV. Peak fit analysis was done using the Multipack software.<sup>34</sup> Further, the protein-adsorbed substrates were air dried and coated with a 10 nm layer of gold and imaged at 15 kV.

### **3.2.2 Isolation of Human Platelet Rich Plasma (PRP)**

Whole blood from healthy individual volunteers, acquired through venipuncture, was drawn into standard 6ml vacuum tubes coated with the anti-coagulant ethylenediaminetetraacetic acid (EDTA). The protocol for blood isolation from healthy individuals was approved by Colorado State University Institutional Review Board. The first tube was discarded to account for the skin plug and locally activated platelets resulting from the needle insertion, following the protocol described elsewhere.<sup>10,11,33</sup> Whole blood was isolated by centrifuging the tubes at 150 g for 15 mins to separate the PRP from the red blood cells. The PRP was then collected and pooled in a separate tube for further use. All the studies discussed below were repeated at least three time with blood drawn from a minimum of three different healthy individuals, however, for each experiment the PRP was only pooled from the same donor. This is because there is donor-to-donor variability in the number of platelets and it is not possible to compare the absolute values from different donors.

### **3.2.3 Cytotoxicity of Different Surfaces**

The cytotoxicity of the different substrates was investigated using a Cayman LDH assay (Cayman Chemical). Sterilized samples were incubated with 500  $\mu$ l of human PRP at 37°C and 5% CO<sub>2</sub> for 2 hrs in a 48-well plate so that all the samples are completely immersed in PRP. After incubation, 100  $\mu$ l of the PRP was placed in a new clear polystyrene U-bottom 96-well plate (Greiner Bio-One). 100  $\mu$ l of the LDH reaction solution, mixed according to the manufacturer's instructions, was added to each well.<sup>33</sup> The 96-well plate was placed in an incubator at 37°C and 5% CO<sub>2</sub> for 30 mins. The

absorbance of the PRP-assay solution was then read at 490 nm using a plate reader (BMG Labtech).

### **3.2.4 Cell Adhesion on Different Surfaces**

Cell adhesion was characterized using fluorescence microscopy. The adhered cells were stained using calcein-AM stain (Invitrogen). Sterilized substrates were incubated in a 48-well plate with 500  $\mu$ l of PRP at 37°C and 5% CO<sub>2</sub> on a horizontal shaker plate at 100 rpm for 2 hrs. After incubation, the PRP was aspirated from the substrates. The substrates were rinsed 3 times with sterile PBS to remove any unattached platelets. This was followed by incubating the substrates with a 2  $\mu$ M calcein-AM solution at 37°C and 5% CO<sub>2</sub> (in PBS) for 30 mins. The substrates were rinsed once more with PBS and imaged using a fluorescence microscope (Zeiss).<sup>28,32</sup> ImageJ was used to calculate the cell coverage on the substrates.

The calcein-AM stain will stain both platelets and leukocytes green, so additional studies were performed to distinguish between the two cell types. Cell adhesion was characterized by staining the cell cytoskeleton protein actin using rhodamine-phalloidin (Invitrogen). Cell nuclei were stained with DAPI (4',6-diamidino-2-phenylindole, Invitrogen). The DAPI will stain cell nuclei blue in leukocytes, whereas the rhodamine-phalloidin will stain the actin red in both platelets and leukocytes, thus distinguishing the two cell types. Substrates were incubated in PRP using the same conditions as described earlier. After incubation, the PRP was aspirated off and the substrates were rinsed twice in sterile PBS. The substrates were moved to a new 48-well plate and fixed in a solution of 3.7% formaldehyde in PBS at room temperature for 15 mins. The substrates were

rinsed twice in sterile PBS, sitting for 5 mins in PBS each time. Next the substrates were moved to clean wells and submerged in a permeative of 1% Triton X in PBS for 3 mins.<sup>10,28,32</sup> The substrates were rinsed twice more in sterile PBS and moved to a new 48-well plate. 200  $\mu$ l of rhodamine phalloidin (actin) solution in PBS (at a concentration of 1:200) was added to each well.<sup>33</sup> The substrates were incubated in this solution for 25 mins. Next, 21  $\mu$ l of DAPI stain was added to each well and the substrates were incubated for 5 more mins. The substrates were then rinsed twice in sterile PBS and imaged using a fluorescence microscope. ImageJ was used to calculate the actin cell coverage and number of nuclei on the substrates.

### **3.2.5 Platelet Activation on Different Surfaces**

Sterilized substrates were incubated with 500  $\mu$ l of human PRP at 37°C for 2 hrs on a shaker plate. The substrates were rinsed in sterile PBS to remove any unattached platelets. The substrates were then incubated in a primary fixative - a solution of 3% glutaraldehyde (Sigma), 0.1 M sodium cacodylate (Polysciences), and 0.1 M sucrose (Sigma) in DI water for 45 mins. Then the substrates were placed in the secondary fixative – 0.1 M sodium cacodylate and 0.1 M sucrose in DI water – for 10 mins. Next the substrates were dehydrated in consecutive solutions of ethanol – 35, 50, 70, 95, and 100% - for 10 mins each. The last dehydration step was to soak the solution in hexamethyldisilazane (HMDS) (Sigma) for 10 mins.<sup>10,28,32,34</sup>

The substrates were coated with 10 nm of gold and imaged using SEM at 2 kV. The platelets were characterized into un-activated, short-dendritic, and long-dendritic morphologies.<sup>11</sup> Un-activated platelets were defined to be spherical with compact central

bodies. Short-dendritic platelets were defined to be partially activated with small dendrites extending from the bodies. Long-dendritic platelets were defined to be fully activated with substantial dendrites extending from the bodies.

### **3.2.6 Hemolysis on Different Surfaces**

Hemolysis was investigated using the process described elsewhere.<sup>11</sup> Whole human blood was drawn and a 5  $\mu$ l drop was placed on each sterilized substrate in a 24-well plate. The substrates were left alone for 15, 30, and 60 mins. After the designated time, 500  $\mu$ l of DI water was added to the wells. The substrates were agitated gently on a horizontal shaker plate for 5 mins to dissolve any un-clotted blood, releasing the free hemoglobin. The absorbance of the solution was then measured using a plate reader at 540 nm.

### **3.2.7 Statistical Analysis**

Protein adsorption was reconfirmed on 3 different samples of each substrate. The LDH assay, calcein-AM stains, and rhodamine-phalloidin, and DAPI stains were repeated twice with five samples of each substrate ( $n = 10$ ). SEM images for platelet activation were taken for six of each substrate ( $n = 6$ ). At least five images were taken for each sample and quantified to evaluate the level of platelet activation ( $n=30$ ). The hemolysis studies were repeated three times with five samples of each surface ( $n = 15$ ). The quantitative results were analyzed using either one-way or two-way anova tests as appropriate. Results were considered statistically significant with a p-value < 0.05.

The studies were repeated with blood drawn from a minimum of three different healthy individuals. The data that is presented (i.e., the arithmetic mean and standard deviation) is only from one donor (from a minimum of three repetitive samples of each surface). This is because there is donor-to-donor variability in the number of platelets and it is not possible to compare the absolute values from different donors. However, similar trends were observed for blood used from each donor, which implies the reproducibility of the trends observed in our experiments.

### **3.3 Results and Discussion**

Hemocompatibility is a challenge for all medical devices since to date there is not a material that is truly compatible with blood. Contact between a material with blood may lead to complications including clots forming on the material surface. These clots can detach, causing heart failure and strokes among other complications. Additionally, the clots may not detach, instead continuing to grow on the material surface causing inflammation and eventually leading to device failure. Current strategies for reducing clot formation have significant drawbacks. In this study, we propose superhemophobic surfaces for enhancing hemocompatibility by modifying the material's surface topography and chemistry.

#### ***3.3.1 Protein Adsorption on Different Surfaces***

Protein adsorption on different surfaces was investigated by incubating the surfaces in solutions of human serum albumin and human fibrinogen and using XPS to determine how much protein was adsorbed onto the surface (**Figure 3.3.1**). Albumin is

a passivating protein which, when present on a surface, reduces the tendency of platelets to adhere on a surface. The high-resolution C1s scans indicated three peaks: C-C, C-N, and N-C=O for all the substrates. A C-F peak is present for only the NT-S2 due to the presence of fluorine in S2. The N-C=O peak is the amide peak, and is the characteristic peak for proteins on the surface.<sup>11</sup> The results indicate that the Ti had the highest albumin adsorption, followed by NT, NT-S1 and NT-S2. (**Figure 3.3.1**). Previous studies have shown that titania nanotubes exhibit reduced protein adsorption compared to unmodified titanium.<sup>11</sup> The high-resolution N1s peak, which is characteristic to proteins as it is not inherently present on any surface, followed similar trend as that of N-C=O peak (**Figure 3.3.1**). The XPS scans of the surfaces exposed to albumin show that there was not significant adsorption on the NT-S1 and NT-S2 surfaces, while the albumin easily adsorbed onto the Ti and NT (**Figure 3.3.1**). Fibrinogen is the main protein involved in thrombosis. When fibrinogen adsorbs onto a surface, it allows platelets to adhere, recruit leukocytes, and activate, which are the initial steps in clot formation. Fibrinogen is long and narrow protein, contrasting with albumin's globular structure, so it adsorbed more on all surfaces as compared to albumin. However, the fibrinogen adsorption followed similar trend as that of albumin adsorption with higher adsorption on Ti, followed by NT, NT-S1 and NT-S2 (**Figure 3.3.2**). Again, the XPS scans of surfaces exposed to fibrinogen that there was not significant adsorption on the NT-S1 and NT-S2 surfaces, while the fibrinogen was adsorbed onto the Ti and NT (**Figure 3.3.2**).

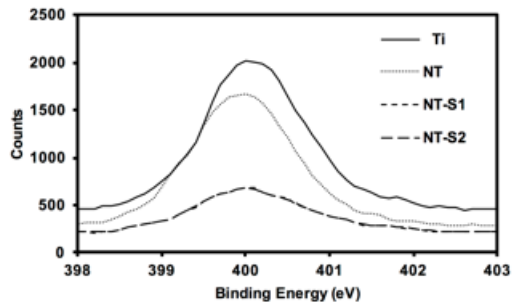
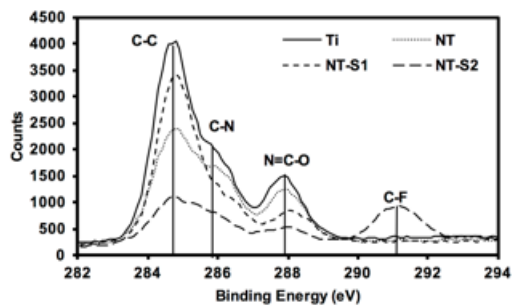


**Figure 3.3.1:** High resolution C1s and N1s scans for albumin adsorption on different surfaces

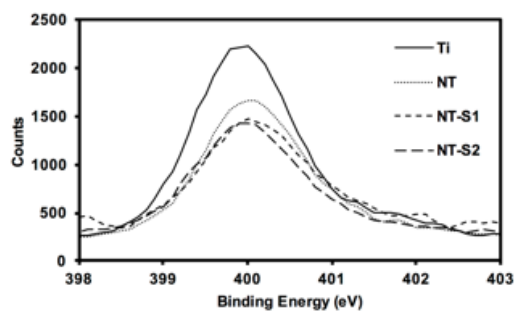
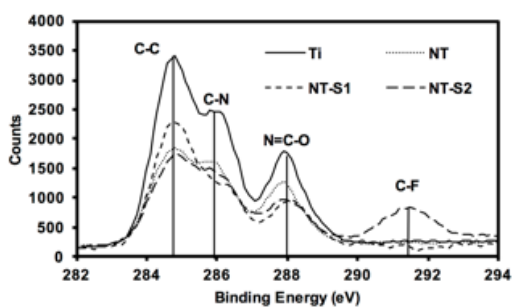


**Figure 3.3.2:** High resolution C1s and N1s scans for albumin adsorption on different surfaces

### **3.3.2 Cytotoxicity of Different Surfaces**

An LDH (lactose dehydrogenase) assay was used to investigate the cytotoxicity of different surfaces. LDH is a chemical generated by cells when they are exposed to toxic environments. When the cells die the LDH is released, and thus the amount of LDH can be measured to determine how toxic a given substrate is. The assay catalyzes a reaction which uses the LDH present in a solution to create a formazan salt that absorbs at 490 nm. Because the amount of absorbance will be proportional to the amount of LDH present, the absorbance reading will indicate the cytotoxicity of the substrate. The results indicate that the PRP exposed to NT-S1 and NT-S2 showed higher amounts of LDH present compared to Ti and NT ( $p < 0.05$ ) (**Figure 3.3.3**). None of the substrates, however, caused enough LDH to be released to be considered cytotoxic. (Note: the high absorbance values for LDH were due to the use of path correction feature in the manufacturer provided software for the plate reader).

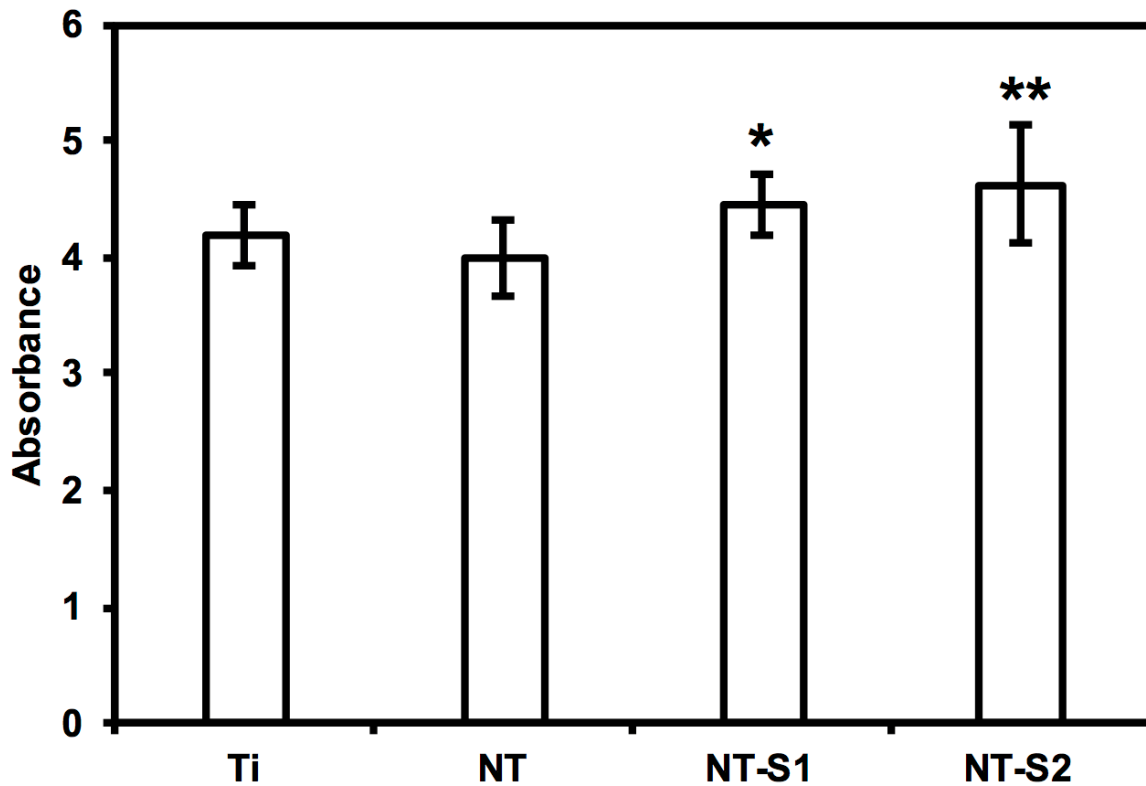


**Figure 3.3.3:** Cytotoxicity of different surfaces measured using LDH assay. NT-S1 and NT-S2 have significantly higher cytotoxicity than Ti and NT ( $p \leq 0.05$ ).

### 3.3.3 Cell Adhesion on Different Surfaces

Platelet and leukocyte adhesion was investigated by fluorescence microscopy. Platelet adhesion has previously been shown to be reduced on titania nanotube arrays compared to unmodified titanium.<sup>10</sup> It was expected that the modification of titania nanotube arrays with silanes would further reduce the adhesion of platelets. The results indicate that NT-S1 and NT-S2 had lower cell adhesion compared to Ti and NT (**Figure 3.3.4**). The percent area of adhered platelets was calculated from the fluorescence microscopy images (**Figure 3.3.5**). Ti had the highest cell coverage, followed by NT. The NT-S1 and NT-S2 surfaces had lower cell coverage compared to Ti and NT ( $p \leq 0.05$ )

(Figure 3.3.5). This result was expected because the superhydrophobicity of the NT-S1 and NT-S2 that minimizes the contact between the PRP and surface. Additionally, the reduced fibrinogen adsorption on NT-S1 and NT-S2 also will affect platelet adhesion.

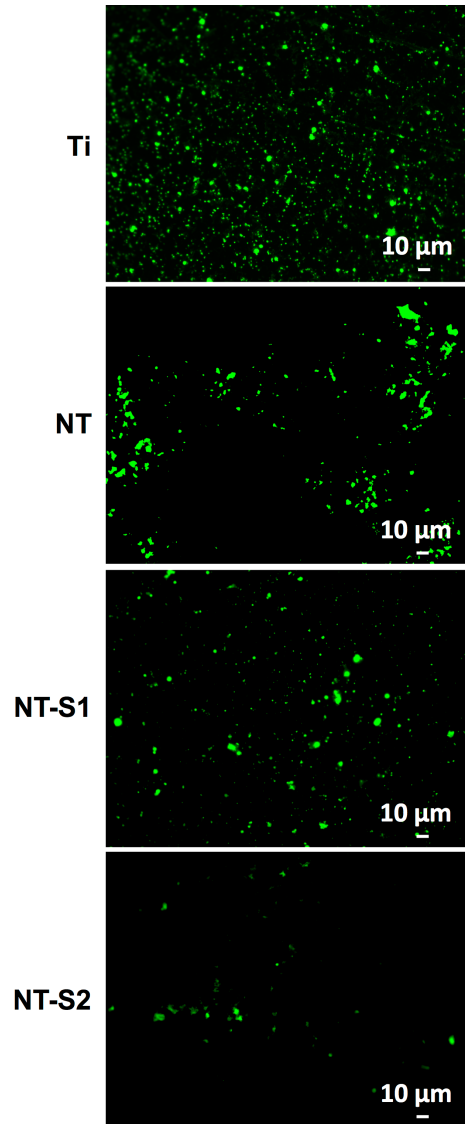


**Figure 3.3.4:** Fluorescence microscopy images of calcein-AM stained cells on different surfaces.

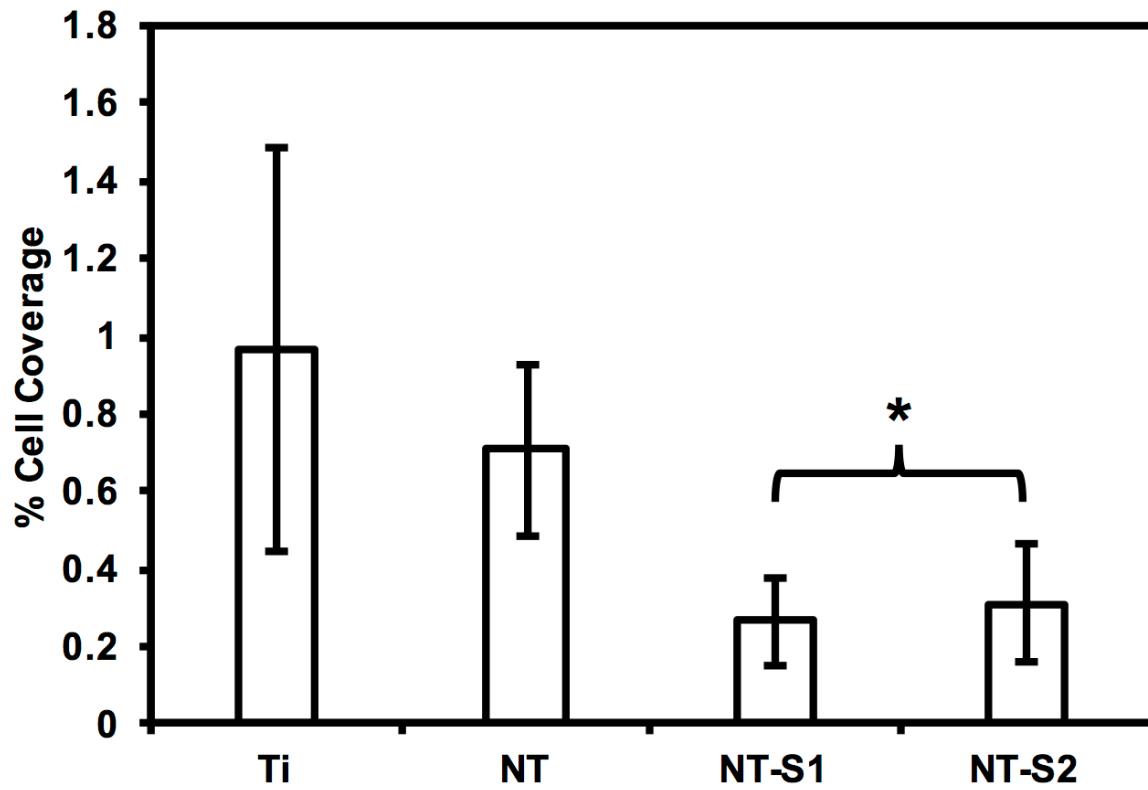


**Figure 3.3.5:** The percentage surface area covered by cells on different surfaces. NT-S1 and NT-S2 have significantly lower cell adhesion than Ti or NT ( $p \leq 0.05$ ).

PRP contains two types of cells – platelets and leukocytes. However, the calcein stain does not distinguish between the two types of cell since it stains the cytoplasm of cells. The adhesion of leukocytes and platelets was determined by staining the cells with rhodamine-phalloidin and DAPI, which stain cell cytoskeleton (actin) and cell nuclei respectively. Since platelets do not have nucleus, the DAPI stain indicates leukocytes, whereas the rhodamine-phalloidin will stain both platelets and leukocytes. The results of rhodamine-phalloidin stained images indicate that NT-S1 and NT-S2 had lower cell adhesion compared to Ti and NT (**Figures 3.3.6 and 3.3.7**). However, the DAPI stained images indicate that Ti had fewer leukocytes compared to NT, NT-S1, and NT-S2 ( $p \leq 0.05$ ) (**Figure 3.3.6 and 3.3.8**). The higher leukocyte adhesion on titania nanotube arrays was likely due to the presence of nanotopography on the surface, as previous studies have shown that surface roughness promotes the adhesion of leukocytes.<sup>33</sup> It was expected that data from the calcein stain and actin/DAPI stained samples would show more similarities than were found. The discrepancies could be caused by the fact that depending on the day, the platelets and leukocytes contained in the PRP would differ. This could be addressed in future studies by pooling plasma taken from several volunteers. As it is, the data showed that the superhemophobic titania nanotube arrays were consistently better than unmodified titanium, but were not consistently better at reducing platelet adhesion compared to unmodified nanotube arrays.

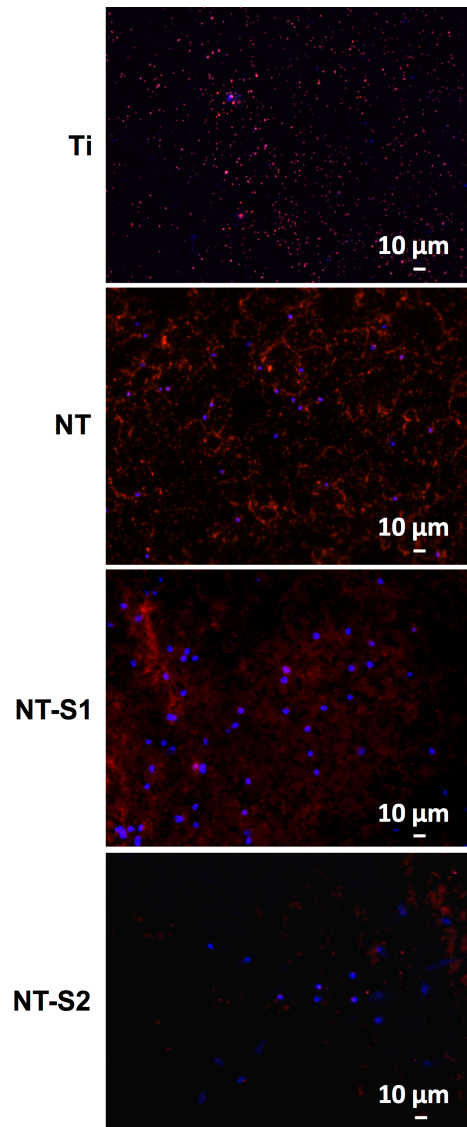


**Figure 3.3.6:** Fluorescence microscopy images of rhodamine-phalloidin and DAPI stained cells on different surfaces.

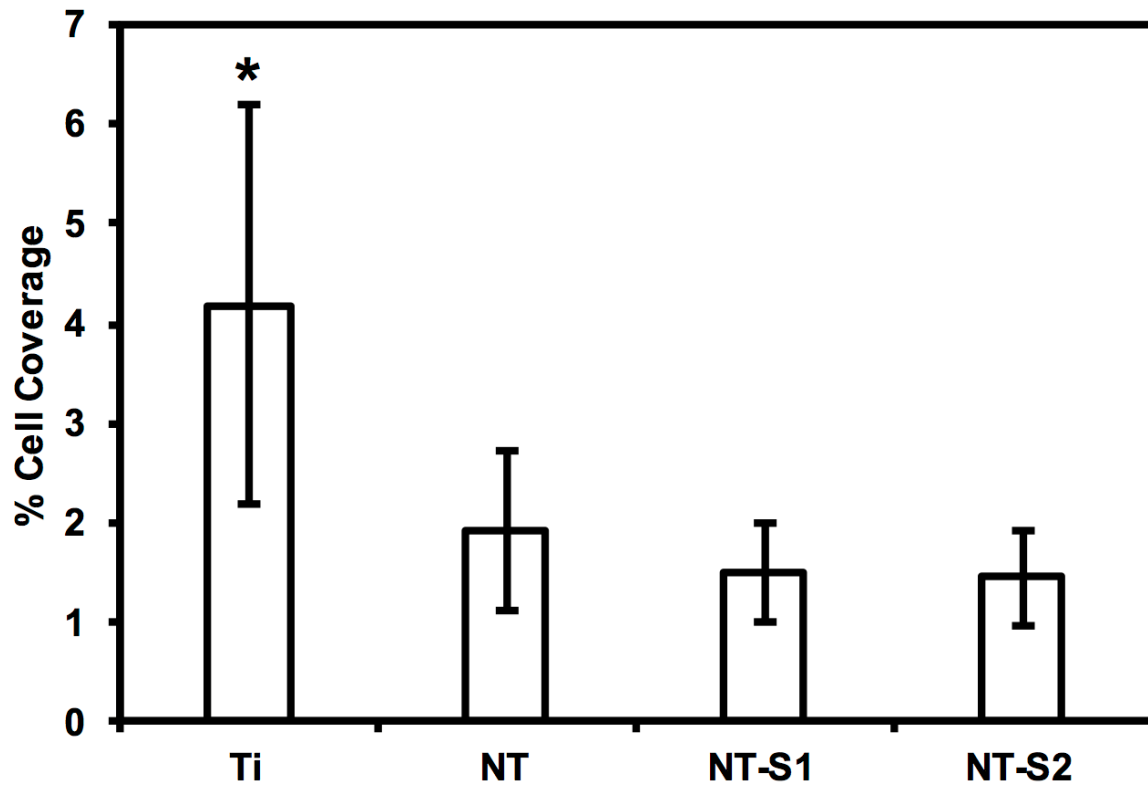


**Figure 3.3.7:** The percentage surface area covered by rhodamine-phalloidin stained cells on different surfaces.

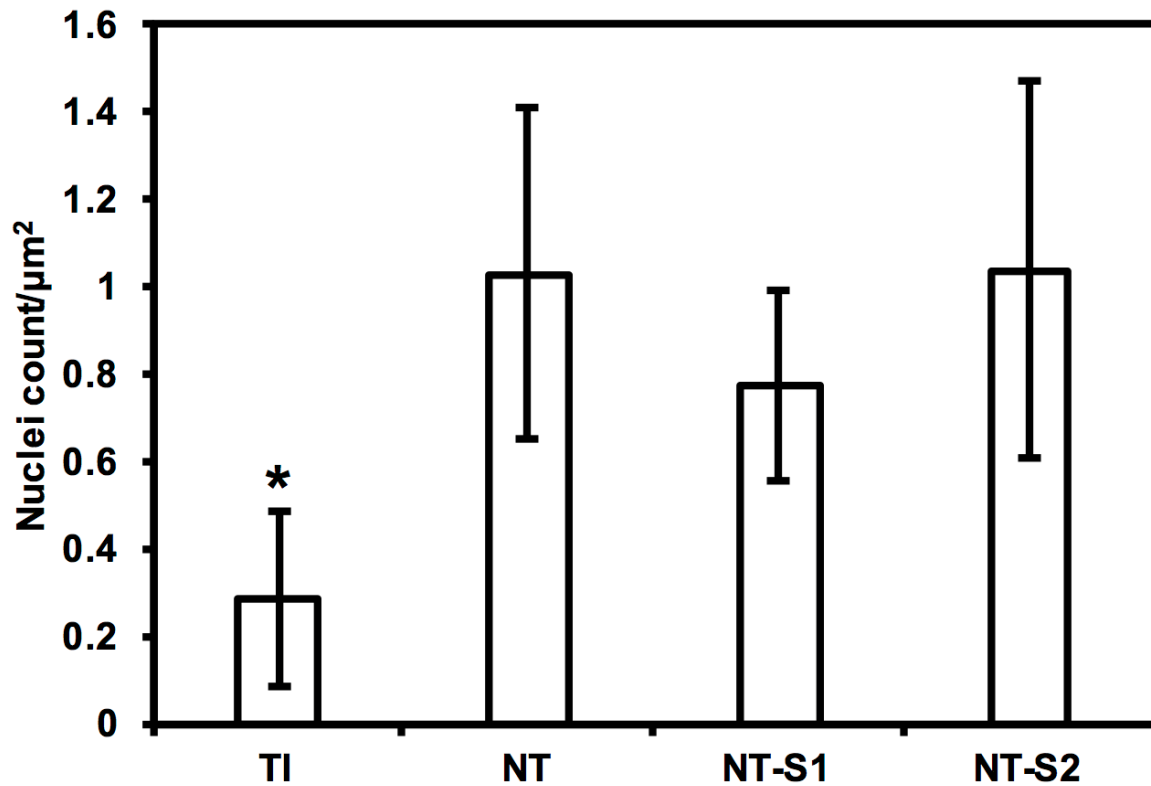


**Figure 3.3.8:** Count of DAPI stained cells per  $\mu\text{m}^2$  on different surfaces. Ti samples show significantly lower leukocyte adhesion than NT, NT-S1 and NT-S2 ( $p \leq 0.05$ ).

### 3.3.4 Platelet Activation on Different Surfaces

SEM was used to investigate platelet activation on different surfaces. The degree of platelet activation was characterized through changes in the platelet shapes, extension of dendrites, and aggregation. A larger number of activated and aggregated platelets indicates a greater propensity for thrombosis. The SEM images were also used to count the number of un-activated, partially activated, and fully activated platelets. Platelet aggregation was seen on both the Ti and NT surfaces (**Figure 3.3.9**). The results indicate that Ti and NT had fewer un-activated platelets than partially or fully activated platelets ( $p \leq 0.05$ ) (**Figure 3.3.10**). Minimal platelet aggregation and adhesion was seen on NT-S1

and NT-S2 (**Figure 3.3.9**). Of the platelets that were attached, there were no significant differences between the number of activated and un-activated platelets NT-S1 and NT-S2 (**Figure 3.3.10**).

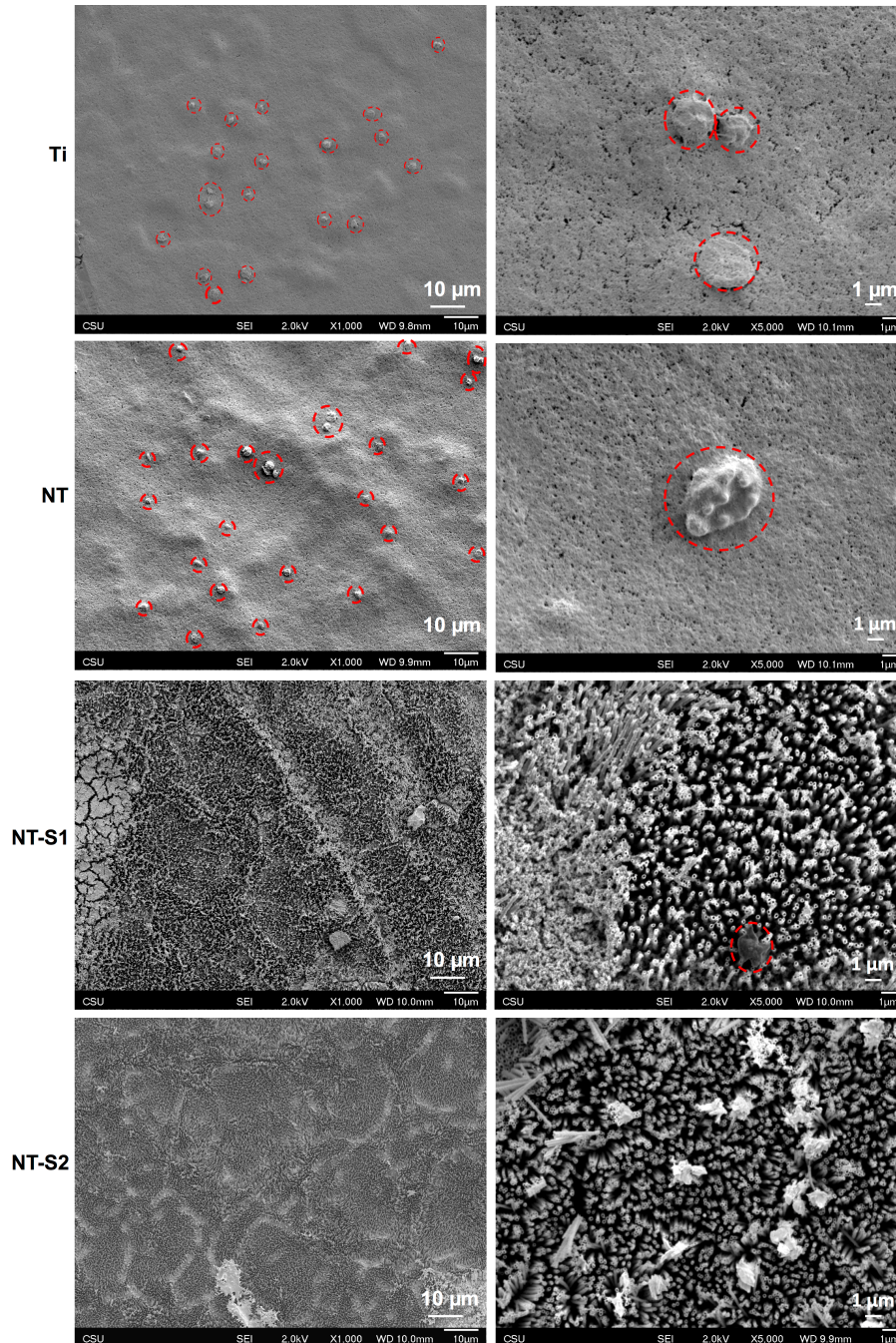


**Figure 3.3.9:** SEM images of cells on different surfaces.

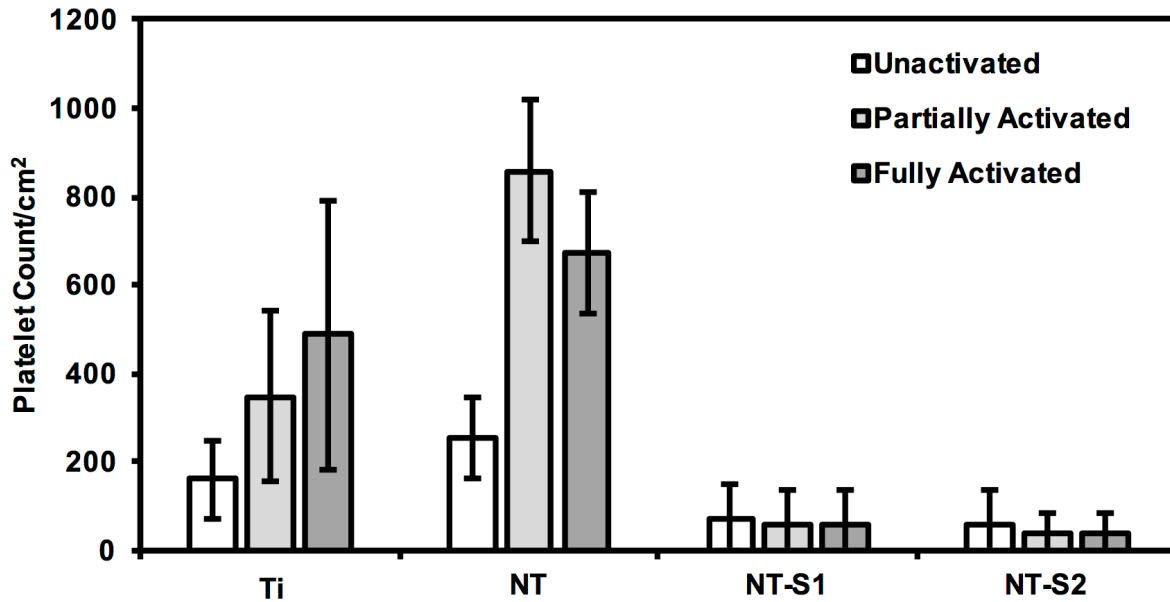


**Figure 3.3.10:** Platelet count on different surfaces. For Ti and NT, the number of un-activated platelets was significantly lower than partially activated and fully activated platelets ( $p \leq 0.05$ ). NT-S1 and NT-S2 had lower counts of all morphologies of platelets ( $p \leq 0.05$ ).

### 3.3.5 Hemolysis on Different Surfaces

The hemolysis of whole human blood on the different substrates was investigated by allowing drops of blood to clot on different surfaces for 15, 30, and 60 minutes and then measuring the absorbance of hemoglobin in the un-clotted blood. After the specific time interval, DI water was added to the well plate to lyse the red blood cells in un-clotted blood and release their hemoglobin. The absorbance of the solution is directly proportional to the amount of hemoglobin dissolved in the DI water, so a higher absorbance value means that there is more hemoglobin dissolved in the water, corresponding to less hemoglobin on the surface. After 15 mins of blood clotting, Ti and NT had lower amounts of free hemoglobin than NT-S1 and NT-S2 indicating more clotting on the surface ( $p \leq 0.05$ ) (**Figure 3.3.11**). The trends were similar after 30 and 60 mins of

hemolysis on different surfaces. However, after 60 mins there was significantly lower amounts of free hemoglobin on Ti and NT, indicating significant hemolysis on these surfaces ( $p \leq 0.05$ ), whereas the amount of free hemoglobin for NT-S1 and NT-S2 was the same, indicating minimal hemolysis on these surfaces. This was expected because the superhemophobic surfaces have minimal contact with the blood due to the air pockets trapped between the blood and surface. (Note: the high absorbance values for hemoglobin were due to the use of path correction feature in the manufacturer provided software for the plate reader).

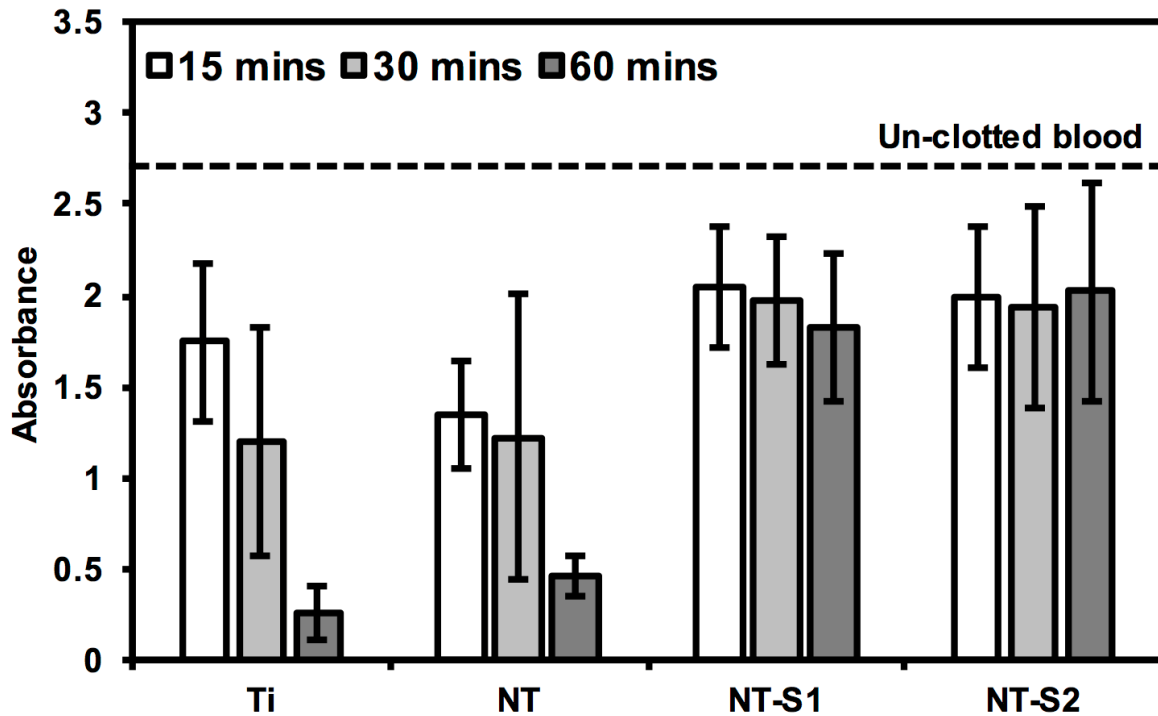


**Figure 3.3.11:** Absorbance of hemoglobin on different surfaces for up to 60 mins. The dotted line represents the absorbance of free hemoglobin in un-clotted blood. A lower absorbance value indicates more hemoglobin absorbed onto the surface.

### **3.4. Conclusion**

Hemocompatibility remains a challenge for any blood-contacting medical device. Thrombosis is a major complication for stents, heart valves, and similar devices as it will obstruct the flow of blood. Reducing the incidence of thrombosis and clot formation on device surfaces is important to reduce device failure. Though there is no truly hemocompatible material, titania nanotube arrays have been shown to enhance hemocompatibility. Previous work with superhydrophobic titania nanotube arrays has shown promising reductions in PRP cell adhesion, but the interactions of individual blood components have not been reported. In this work, we have fabricated superhemophobic titania nanotube arrays using anodization of titanium followed by modifying the surface chemistry by chemical vapor deposition of two silanes. The hemocompatibility of these surfaces was evaluated by measuring blood protein adsorption, cytotoxicity, platelet/leukocyte adhesion, platelet activation, and hemolysis. The results indicate that albumin, fibrinogen, and hemoglobin adsorption was reduced on superhemophobic surfaces as compared unmodified surfaces, and that none of the surfaces were cytotoxic. Further, the superhemophobic surfaces significantly reduced PRP cell adhesion compared to unmodified titanium but not titania nanotube arrays. These results indicate that superhemophobic surfaces are a potential approach for enhancing hemocompatibility of blood-contacting devices, but more work is needed. The interactions of blood with superhemophobic surfaces should be investigated further, including for longer time periods than the 1-3 hour periods investigated in this study.

## REFERENCES

- (1) Schmidt, W.; Behrens, P.; Brandt-Wunderlich, C.; Siewert, S.; Grabow, N.; Schmitz, K. P. In Vitro Performance Investigation of Bioresorbable Scaffolds - Standard Tests for Vascular Stents and beyond. *Cardiovasc. Revascularization Med.* **2016**, *17* (6), 375–383.
- (2) Liu, H.; Pan, C.; Zhou, S.; Li, J.; Huang, N.; Dong, L. Improving Hemocompatibility and Accelerating Endothelialization of Vascular Stents by a Copper-Titanium Film. *Mater. Sci. Eng. C* **2016**, *69*, 1175–1182.
- (3) Hansson, N. C.; Grove, E. L.; Andersen, H. R.; Leipsic, J.; Mathiassen, O. N.; Jensen, J. M.; Jensen, K. T.; Blanke, P.; Leetmaa, T.; Tang, M.; Krusell, L. R.; Klaaborg, K. E.; Christiansen, E. H.; Terp, K.; Terkelsen, C. J.; Poulsen, S. H.; Webb, J.; B??tger, H. E.; N??rgaard, B. L. Transcatheter Aortic Valve Thrombosis: Incidence, Predisposing Factors, and Clinical Implications. *J. Am. Coll. Cardiol.* **2016**, *68* (19), 2059–2069.
- (4) Makkar, R. R.; Fontana, G.; Jilaihawi, H.; Chakravarty, T.; Kofoed, K. F.; de Backer, O.; Asch, F. M.; Ruiz, C. E.; Olsen, N. T.; Trento, A.; Friedman, J.; Berman, D.; Cheng, W.; Kashif, M.; Jelnin, V.; Kliger, C. A.; Guo, H.; Pichard, A. D.; Weissman, N. J.; Kapadia, S.; Manasse, E.; Bhatt, D. L.; Leon, M. B.; S??ndergaard, L. Possible Subclinical Leaflet Thrombosis in Bioprosthetic Aortic Valves. *N. Engl. J. Med.* **2015**, *373* (21), 2015–2024.
- (5) De Marchena, E.; Mesa, J.; Pomenti, S.; Marin Y Kall, C.; Marincic, X.; Yahagi, K.; Ladich, E.; Kutz, R.; Aga, Y.; Ragosta, M.; Chawla, A.; Ring, M. E.; Virmani, R. Thrombus Formation Following Transcatheter Aortic Valve Replacement. *JACC Cardiovasc. Interv.* **2015**, *8* (5), 728–739.
- (6) Ge, L.; Dasi, L. P.; Sotiropoulos, F.; Yoganathan, A. P. Characterization of Hemodynamic Forces Induced by Mechanical Heart Valves: Reynolds vs. Viscous Stresses. *Ann. Biomed. Eng.* **2008**, *36* (2), 276–297.
- (7) Simon, H. a; Leo, H.-L.; Carberry, J.; Yoganathan, A. P. Comparison of the Hinge Flow Fields of Two Bileaflet Mechanical Heart Valves under Aortic and Mitral Conditions. *Ann. Biomed. Eng.* **2004**, *32* (12), 1607–1617.
- (8) Timsit, J.-F.; Dubois, Y.; Minet, C.; Bonadona, A.; Lugosi, M.; Ara-Somohano, C.; Hamidfar-Roy, R.; Schwebel, C. New Materials and Devices for Preventing Catheter-Related Infections. *Ann. Intensive Care* **2011**, *1*, 34.
- (9) Werner, C.; Maitz, M. F.; Sperling, C. Current Strategies towards Hemocompatible Coatings. *J Mater Chem* **2007**, *17*, 3376–3384.
- (10) Smith, B. S.; Capellato, P.; Kelley, S.; Gonzalez-Juarrero, M.; Popat, K. C. Reduced in Vitro Immune Response on Titania Nanotube Arrays Compared to Titanium Surface. *Biomater. Sci.* **2013**, *1* (3), 322–332.
- (11) Leszczak, V.; Smith, B. S.; Popat, K. C. Hemocompatibility of Polymeric Nanostructured Surfaces. *J. Biomater. Sci. Polym. Ed.* **2013**, No. March 2013, 37–41.
- (12) Anderson, J. M.; Rodriguez, A.; Chang, D. T. Foreign Body Reaction to Biomaterials. *Semin. Immunol.* **2008**, *20* (2), 86–100.
- (13) Franz, S.; Rammelt, S.; Scharnweber, D.; Simon, J. C. Immune Responses to Implants - A Review of the Implications for the Design of Immunomodulatory Biomaterials. *Biomaterials* **2011**, *32* (28), 6692–6709.

- (14) Hisagi, M.; Nishimura, T.; Ono, M.; Gojo, S.; Nawata, K.; Kyo, S. New Pre-Clotting Method for Fibrin Glue in a Non-Sealed Graft Used in an LVAD: The KYO Method. *J. Artif. Organs* **2010**, *13* (3), 174–177.
- (15) Riedel, N. A.; Smith, B. S.; Williams, J. D.; Popat, K. C. Improved Thrombogenicity on Oxygen Etched Ti6Al4V Surfaces. *Mater. Sci. Eng. C* **2012**, *32* (5), 1196–1203.
- (16) Bender, E. A.; Adorne, M. D.; Colomé, L. M.; Abdalla, D. S. P.; Guterres, S. S.; Pohlmann, A. R. Hemocompatibility of Poly( $\epsilon$ -Caprolactone) Lipid-Core Nanocapsules Stabilized with Polysorbate 80-Lecithin and Uncoated or Coated with Chitosan. *Int. J. Pharm.* **2012**, *426* (1–2), 271–279.
- (17) Kuznetsova, N. R.; Sevrin, C.; Lespineux, D.; Bovin, N. V.; Vodovozova, E. L.; Mészáros, T.; Szebeni, J.; Grandfils, C. Hemocompatibility of Liposomes Loaded with Lipophilic Prodrugs of Methotrexate and Melphalan in the Lipid Bilayer. *J. Control. Release* **2012**, *160* (2), 394–400.
- (18) Lin, W. C.; Liu, T. Y.; Yang, M. C. Hemocompatibility of Polyacrylonitrile Dialysis Membrane Immobilized with Chitosan and Heparin Conjugate. *Biomaterials* **2004**, *25* (10), 1947–1957.
- (19) Chou, C.-C.; Hsin, S.-W.; Lin, H.-C.; Yeh, C.-H.; Wu, R.; Cherng, W.-J. Oxidized Dopamine as the Interlayer between Heparin/collagen Polyelectrolyte Multilayers and Titanium Substrate: An Investigation of the Coating's Adhesion and Hemocompatibility. *Surf. Coatings Technol.* **2016**, *303*, 277–282.
- (20) Chou, C. C.; Zeng, H. J.; Yeh, C. H. Blood Compatibility and Adhesion of Collagen/heparin Multilayers Coated on Two Titanium Surfaces by a Layer-by-Layer Technique. *Thin Solid Films* **2013**, *549*, 117–122.
- (21) Weber, N.; Wendel, H. P.; Ziemer, G. Hemocompatibility of Heparin-Coated Surfaces and the Role of Selective Plasma Protein Adsorption. *Biomaterials* **2002**, *23* (2), 429–439.
- (22) Zheng, Z.; Wang, W.; Huang, X.; Lv, Q.; Fan, W.; Yu, W.; Li, L.; Zhang, Z. Fabrication, Characterization, and Hemocompatibility Investigation of Polysulfone Grafted With Polyethylene Glycol and Heparin Used in Membrane Oxygenators. *Artif. Organs* **2016**, *40* (11), E219–E229.
- (23) Blezer, R.; Fouache, B.; Willems, G. M.; Lindhout, T. Activation of Blood Coagulation at Heparin-Coated Surfaces. *J. Biomed. Mater. Res.* **1997**, *37* (1), 108–113.
- (24) Jin, X.; Yuan, J.; Shen, J. Zwitterionic Polymer Brushes via Dopamine-Initiated ATRP from PET Sheets for Improving Hemocompatible and Antifouling Properties. *Colloids Surfaces B Biointerfaces* **2016**, *145*, 275–284.
- (25) Hamerli, P.; Weigel, T.; Groth, T.; Paul, D. Surface Properties of and Cell Adhesion onto Allylamine-Plasma-Coated Polyethylenterephthalat Membranes. *Biomaterials* **2003**, *24* (22), 3989–3999.
- (26) Roy, R. K.; Choi, H. W.; Yi, J. W.; Moon, M. W.; Lee, K. R.; Han, D. K.; Shin, J. H.; Kamijo, A.; Hasebe, T. Hemocompatibility of Surface-Modified, Silicon-Incorporated, Diamond-like Carbon Films. *Acta Biomater.* **2009**, *5* (1), 249–256.
- (27) Damodaran, V. B.; Bhatnagar, D.; Leszczak, V.; Popat, K. C. Titania Nanostructures: A Biomedical Perspective. *RSC Adv.* **2015**, *5* (47), 37149–37171.

- (28) Smith, B. S.; Yoriya, S.; Johnson, T.; Popat, K. C. Dermal Fibroblast and Epidermal Keratinocyte Functionality on Titania Nanotube Arrays. *Acta Biomater.* **2011**, 7 (6), 2686–2696.
- (29) Movafaghi, S.; Leszczak, V.; Wang, W.; Sorkin, J. A.; Dasi, L. P.; Popat, K. C.; Kota, A. K. Hemocompatibility of Superhemophobic Titania Surfaces. *Adv. Healthc. Mater.* **2016**, 1600717.
- (30) Smith, B. S.; Yoriya, S.; Grissom, L.; Grimes, C. A.; Popat, K. C. Hemocompatibility of Titania Nanotube Arrays. *J. Biomed. Mater. Res. - Part A* **2010**, 95 A (2), 350–360.
- (31) Leszczak, V.; Popat, K. C. Improved in Vitro Blood Compatibility of Polycaprolactone Nanowire Surfaces. *ACS Appl. Mater. Interfaces* **2014**, 6 (18), 15913–15924.
- (32) Riedel, N. A.; Bechara, S. L.; Popat, K. C.; Williams, J. D. Ion Etching for Sharp Tip Features on Titanium and the Response of Cells to These Surfaces. *Mater. Lett.* **2012**, 81, 158–161.
- (33) Capellato, P.; Smith, B. S.; Popat, K. C.; Claro, A. P. R. A. Fibroblast Functionality on Novel Ti30Ta Nanotube Array. *Mater. Sci. Eng. C* **2012**, 32 (7), 2060–2067.
- (34) Riedel, N. A.; Williams, J. D.; Popat, K. C. Ion Beam Etching Titanium for Enhanced Osteoblast Response. *J. Mater. Sci.* **2011**, 46 (18), 6087–6095.

## CHAPTER 4

### BACTERIAL ADHESION ON TITANIA NANOTUBE ARRAYS

#### 4.1 Introduction

Bacterial infections are a serious issue for medical devices. An infection occurs when bacteria colonize the device surface, forming what is known as a biofilm.<sup>1-4</sup> The biofilm's purpose is to protect the bacteria by blocking antibiotics, making these infections difficult to combat.<sup>4-6</sup> The polymers composing the biofilms have been shown to slow the rate at which antibiotics can diffuse into the colony, which reduces their effectiveness.<sup>5</sup> This effect of slowing the penetration of molecules can allow the active compounds in certain drugs to react with other molecules in the environment. These reactions can deactivate the drugs, rendering them unable to affect the bacteria. Biofilms are structured with channels to allow nutrients for bacteria to circulate, which keeps the bacteria colony viable and growing.<sup>7</sup> Researchers have shown that some of the sections of the biofilm will be undernourished and the bacteria in those areas will go into a starved state. In this state bacteria interact less with their environment, which means these bacteria will interact less with any drugs present, reducing the effectiveness of the drugs.<sup>7</sup> Additionally, the overuse of antibiotics is giving rise to bacteria strains which are resistant to common drugs used in treatment.<sup>2,5</sup> Currently, more than half of the infections acquired in hospitals are estimated to come from biofilms.<sup>7,8</sup>

Infectious bacteria fall into two categories: gram-positive and gram-negative.<sup>1,5,6,9</sup> The categories are based on the reaction of the bacteria to the gram stain, which attaches to peptidoglycan.<sup>10</sup> Bacteria whose cells walls contain peptidoglycan will retain the stain

(gram-positive), while the stain will not bind to bacteria with no peptidoglycan in their cell walls.<sup>10</sup> Gram-negative bacteria are known for their drug resistance and have been developing resistance to antibiotics.<sup>2</sup> Common gram-negative bacteria include *Escherichia coli* and *Pseudomonas aeruginosa*, the latter of which is often studied because of its prevalence and association with device-related infections.<sup>2</sup> *S. aureus* is a gram-positive bacteria that is found naturally on human skin, and is associated with device-related infections.<sup>8</sup> *S. aureus* is often studied due to its prevalence and the danger they pose for patients when they cause infections in the bloodstream.<sup>8,11,12</sup> Because the different types of bacteria must be treated with different drugs, an approach to reducing infection and biofilm formation that does not depend on the bacteria's composition would be very beneficial.

Due to their prevalence and the complications they cause, several methods have been developed to prevent bacterial infections from occurring. The most common method is to apply prophylactic antibiotics to the implant site at the end of surgery in order to sterilize the wounds. This has been shown both to reduce the occurrence of bacterial infections and cut the severity of those that do occur.<sup>13</sup> When infections do develop after implant surgeries, they are typically treated with antibiotic regimens. However, growth of bacteria and inflammation to the surrounding tissues will interfere with the integration of the implants, persistent infections typically require replacement of the implant.<sup>13</sup> One recent approach is to create surfaces which are coated with drugs in order to release them directly to the implant site.<sup>14,15</sup> Some drugs, such as the antibiotic Neomycin, are inactivated as they travel through the body; Neomycin will be inactivated if it moves through the liver.<sup>16</sup> Drug-eluting surfaces are able to deliver the drugs directly to the area

of the body where they are needed and have shown some positive results.<sup>15</sup> Other surfaces doped with silver ions have shown similar anti-bacterial properties, as silver is a commonly used antimicrobial agent.<sup>13</sup> The challenge for these approaches is to remain effective in the long term, as eventually any antimicrobial coating will be depleted from the surface.<sup>17,18</sup> Additionally, any bacteria resistant to the chosen antimicrobial agent will be unaffected by these treatments.<sup>13,15,19</sup> Thus investigations are being done into new approaches for combating infections without relying on antimicrobial coatings.

Superhydrophobic surfaces are being investigated for their anti-biofouling properties as the low solid surface energies of these surfaces reduces the adhesion of contaminants and water, making them easy to clean.<sup>20,21</sup> Biofouling is the attachment of any microorganism to a surface.<sup>22,23</sup> Superhydrophobic materials are typically made either by bonding molecules with low surface energies to a roughened surface or by roughening the surface of a material which is already hydrophobic.<sup>3,20,24,25</sup> Some previous work has shown that superhydrophobic surfaces tend to reduce the attachment of a range of bacteria strains, but other results show attachment and biofilm formation, indicating that more research is needed.<sup>26-28</sup> There is consensus that reduced protein adsorption on superhydrophobic surfaces helps reduce the attachment of bacteria.<sup>21</sup> Proteins have been shown to adsorb easily on surfaces that are mildly hydrophobic or mildly hydrophilic.<sup>5,29</sup> An adsorbed protein film can provide a surface to which a bacterium can easily attach.<sup>1</sup> Superhydrophobic surfaces exhibit reduced protein adsorption and any proteins that do adhere are easy to remove.<sup>9</sup> This in turn makes it more difficult for bacteria to attach and form biofilms.

In this research the adhesion of *S. aureus* and *P. aeruginosa* to superhydrophobic and superhydrophilic titania nanotube arrays was investigated. Titanium was chosen because it is a common biocompatible material used in medical devices. The surfaces were created by first anodizing and chemically etching titanium to form the titania nanotube arrays. Next the surface chemistry was altered by bonding silane to the surfaces of the nanotube arrays. Chemical vapor deposition was used to create the superhydrophilic surfaces while liquid deposition was used to create the superhydrophobic surfaces. The surfaces were characterized using scanning electron microscopy (SEM) to determine topography, contact angle goniometry to determine wettability, X-ray photoelectron spectroscopy (XPS) to characterize surface chemistry, and X-ray diffraction (XRD) to determine crystallinity. The numbers of attached bacteria after 6 h and 24 h were then measured using SEM and fluorescence microscopy. The results showed fewer bacteria attached to the superhydrophobic surfaces when compared to the control surfaces. The superhydrophilic surfaces did not show significant differences in the number of bacteria compared to the unmodified titania nanotube arrays.

## **4.2 Materials and Methods**

### **4.2.1 Preparation of Bacteria Cultures**

Stock cultures of *P. aeruginosa* and *S. aureus* were grown overnight in nutrient broth media (Oxoid, referred to as NBM). The bacteria cultures were obtained from 10 ml tubes from bacteria solutions stored in glycerol (30% v/v, Sigma) at a concentration of 15% v/v and stored in a -80° freezer. Prior to each study, one 10 ml tube was thawed at room temperature for approximately 1 hour and then centrifuged for 10 min at 4700 rpm

and 21°C. The centrifuging caused the bacteria to collect in a pellet at the bottom of the tube, after which the remaining glycerol solution was discarded. The pellet was resuspended in 5 ml of NBM which had been warmed in a 37°C water bath. Next 35 ml of additional NBM, warmed in a 37°C water bath, were added to the bacteria solution. This mixture was stored overnight in a 37°C incubator on a shaker plate set to low. The culture was incubated until the optical density (OD) at 600 nm was approximately 1. The culture was then diluted with warm NBM until the OD at 600 nm was approximately 0.35.

The following nomenclature will be used in this chapter for the substrates: unmodified titanium (referred to as Ti), unmodified titania nanotube arrays (referred to as NT), superhydrophobic titania nanotube arrays coated with (heptadecafluoro-1,1,2,2-tetrahydrodecyl)trichlorosilane (Gelest) (referred to as NT-S1), and the superhydrophilic titania nanotube arrays coated with 2-[methoxy(polyethyleneoxy)propyl]trimethoxysilane (referred to as NT-S2). Prior to all the biological experiments, the substrates were sterilized. They were incubated in ethanol for 30 mins, followed by rinsing with DI water.

#### ***4.2.4 Bacteria Adhesion and Biofilm Formation***

Fluorescence microscopy was used to quantify the number of bacteria that adhered to the surface. Sterilized Ti, NT, NT-S1, and NT-S2 substrates were placed in 24-well plates. 1 ml of the prepared bacterial culture was added to each well. The well plates were placed in a sterile plastic bag and stored in a 37°C incubator for 6 and 24 h periods. After the incubation period was complete, the media was removed from each well and the samples were rinsed three times with sterile phosphate buffer solution (PBS). The substrates were then moved to a clean 48-well plate.

After incubation, the media was removed from the wells and the substrates were rinsed three times with sterile PBS. The fluorescence stain was made by adding 3  $\mu$ l of propidium iodide (Fisher Scientific, referred to as PI) and 3  $\mu$ l of Syto 9 stain (Fisher Scientific) per 1 ml of sodium chloride solution. 300  $\mu$ l of the stain solution was then added to each new well. The well plates were incubated for 20 min at 37°C, at which point the stain solution was removed and the samples were washed once more with PBS. The substrates were then imaged with an Olympus IX73 fluorescence microscope with the Olympus CellSens software.

#### **4.2.5 Bacteria Morphology**

Scanning electron microscopy was used to examine the attachment of bacteria and formation of biofilms on the substrates. The sterilized substrates were placed in a 24-well plate and covered with 1 ml of the prepared bacteria solution. The well plate was then placed in a sterile plastic bag and incubated at 37°C for 6 h or 24 h. Once the incubation period was ended the media was removed and the substrates were rinsed three times with sterile PBS to remove any bacteria that did not adhere to the substrates.

The adhered bacteria were fixed using a process described previously.<sup>30,31</sup> The substrates were soaked in a primary fixative made of 0.1 M sucrose, 0.1 M sodium cacodylate, and 3% glutaraldehyde (v/v) in DI water for 45 mins. The substrates were then moved to the secondary fixative composed of 0.1 M sucrose and 0.1 M sodium cacodylate in DI water. The substrates were kept in this fixative for 12 h overnight. The substrates were then dehydrated in a series of ethanol/DI water baths – 35%, 50%, 70%,

95%, and 100% ethanol (v/v) – for 10 mins each. The substrates were then moved to a sterile well plate and stored in a desiccator until imaging.

#### **4.2.6 Statistical Analysis**

Surface characterization was reconfirmed on 2 different samples of each substrate. SEM images and contact angle measurements were taken for 6 samples of each substrate ( $n = 6$ ). The fluorescence stains were repeated three times for each bacteria and period of time on three substrates each time ( $n=9$ ). SEM fixing was repeated three times for each bacteria and period of time on three substrates each time ( $n = 9$ ). The quantitative results were analyzed using one-way and two-way anova tests as appropriate. Results were considered statistically significant with a p-value  $< 0.05$ .

### **4.3 Results and Discussion**

#### **4.3.1 Bacteria Adhesion and Biofilm Formation**

Fluorescence microscopy was used to investigate the attachment of *P. aeruginosa* and *S. aureus* bacteria to the substrates. Two separate stains were used to differentiate between bacteria which were living at the time of the stain and bacteria which had died. Propidium iodide is absorbed by both living and dead bacteria, but the Syto-9 stain is only absorbed by living bacteria. Syto-9 stain appears green under fluorescence imaging and propidium iodide appears red under fluorescence imaging. The use of these two stains enables the living and dead bacteria to be distinguished from each other.

The results for *S. aureus* similarly indicate that adhesion of bacteria was highest on Ti after both 6 h and 24 h (**Figures 4.3.1 and 4.3.2**) ( $p<0.05$ ). The NT samples showed

reduced adhesion compared to the Ti samples ( $p < 0.05$ ). The NT-S2 samples showed somewhat reduced attachment after 6 h compared to the NT samples, but the results were mixed and not always significantly different. After 6 h, the NT-S2 substrates had fewer dead bacteria ( $p < 0.05$ ) and similar numbers of live bacteria compared to the NT substrates. After 24 h, the NT-S2 and NT had similar numbers of bacteria adhered, but the NT-S2 samples had more dead bacteria while the NT samples had more live bacteria ( $p < 0.05$ ). The NT-S1 substrates showed reduced attachment of *S. aureus* compared to all other substrates for both time periods tested ( $p < 0.05$ ). The results showed that the Ti and NT-S1 samples behaved as expected – Ti having the highest bacterial adhesion and the superhydrophobic substrate reducing adhesion are results consistent with previous studies. The hydrophilic and superhydrophilic substrates showed reduced adhesion compared to titania, which is also consistent with previous studies on unmodified titania nanotube arrays. The NT and NT-S2 substrate did have some unexpected results. The NT substrates had similar numbers of dead bacteria between 6 and 24 h, but the number of live bacteria was lower after 24 h than 6 h. For the NT-S2 samples, the decrease in live bacteria from 6 to 24 h was accompanied by an increase in the number of dead bacteria, indicating that some of the adhered bacteria had simply died. The reason for the decrease in live bacteria on the NT substrates is unclear, so further investigation is needed to determine whether this is due to some property inherent to the NT substrates.

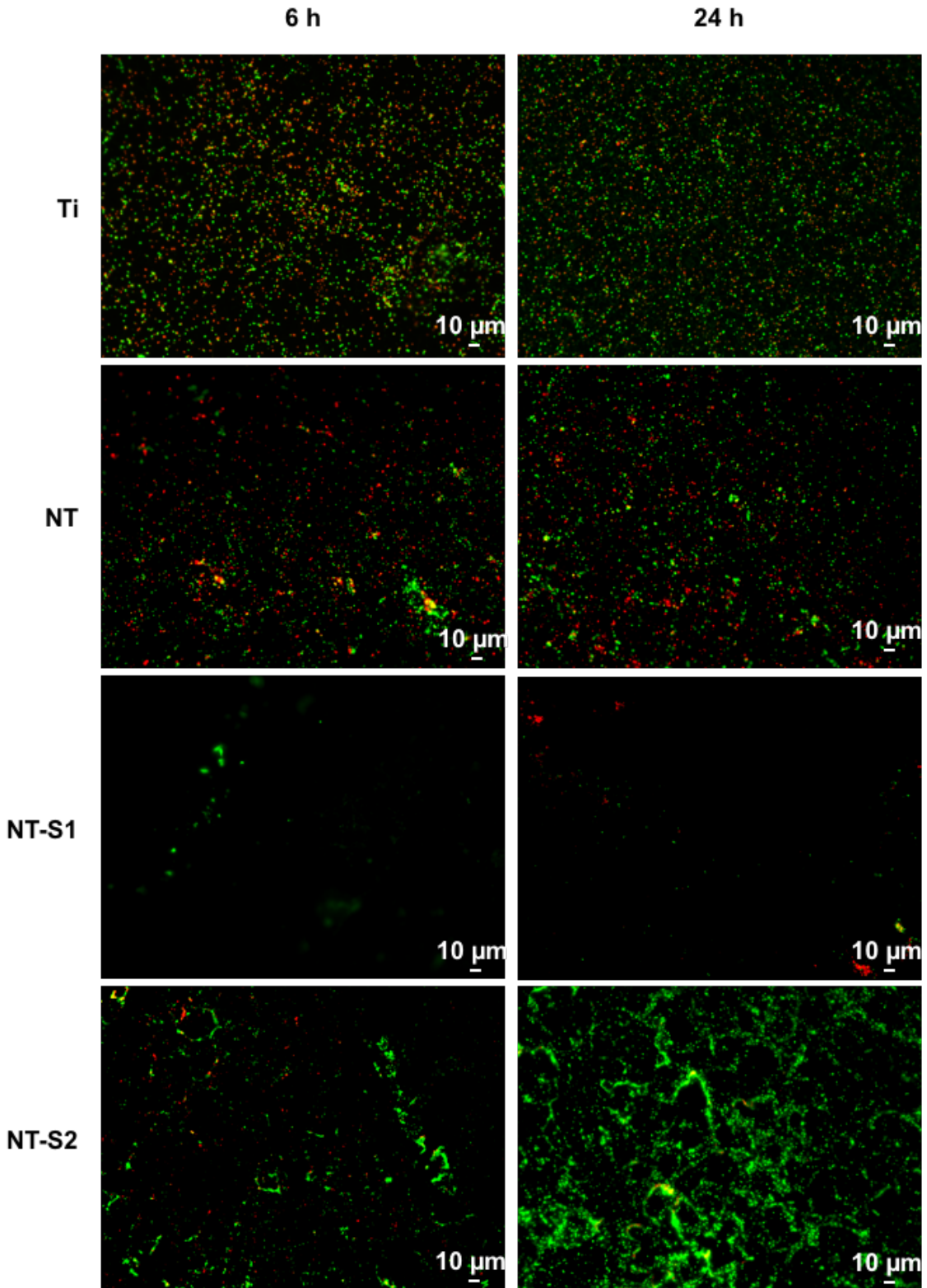


**Figure 4.3.1:** Fluorescence images of *S. aureus* on different surfaces

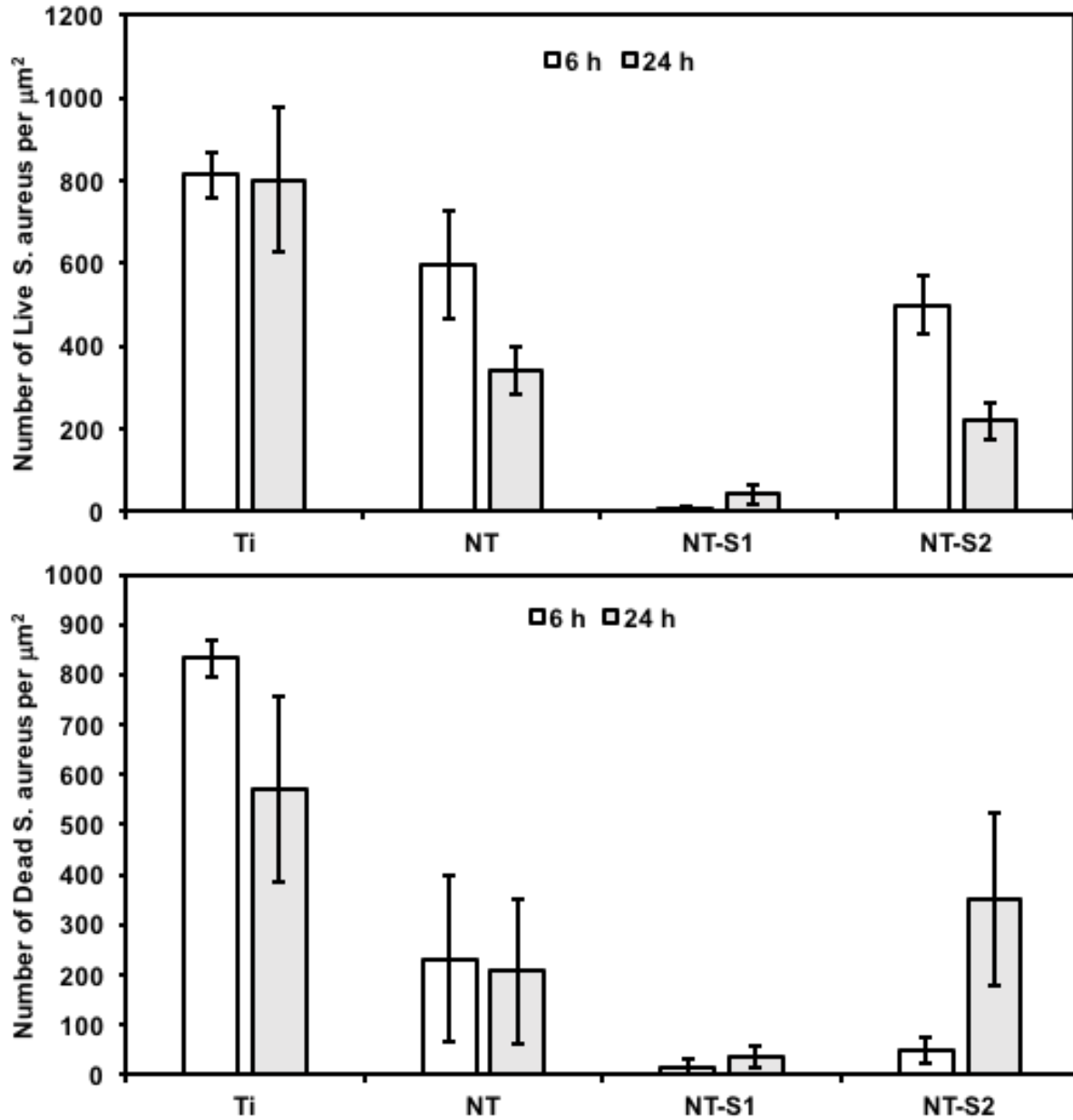


**Figure 4.3.2:** Counts of *S. aureus* on different surfaces after 6 and 24 h

The results for *P. aeruginosa* showed that adhesion on Ti was highest after both 6 h and 24 h (Figure 4.3.3 and 4.3.4). The NT samples showed reduced attachment of both live and dead bacteria compared to Ti ( $p < 0.05$ ), which is consistent with previous studies (56). The number of dead bacteria on the NT-S2 samples was lower than on the

NT samples after 6 h ( $p < 0.05$ ), but there was no significant difference after 24 h. The NT and NT-S2 substrates had similar numbers of live bacteria after both 6 and 24 h ( $p > 0.05$ ). The superhydrophobic NT-S1 substrates showed reduced attachment of both live and dead bacteria compared to all other substrates for both time periods ( $p < 0.05$ ). As with the gram-positive *S. aureus*, the Ti and NT-S1 substrates behaved as expected, having the highest and lowest numbers of adhered *P. aeruginosa*. As the NT-S2 samples only had fewer dead bacteria after 6 h, with no significant differences after 24 h, these results indicate that superhydrophilic titania nanotube arrays do not have much effect on the adherence of *P. aeruginosa*. The numbers of both live and dead *P. aeruginosa* attached to the Ti, NT, and NT-S2 substrates were greater after 24 h compared to 6 h, which was expected due to the increased incubation time. The NT-S1 substrates showed an increase in attached live bacteria, but no significant difference in the numbers of dead bacteria after 24 h. This could indicate that the dead bacteria were not strongly attached to the superhydrophobic substrate and were removed during the staining procedure, but more investigation would be needed to confirm this explanation.

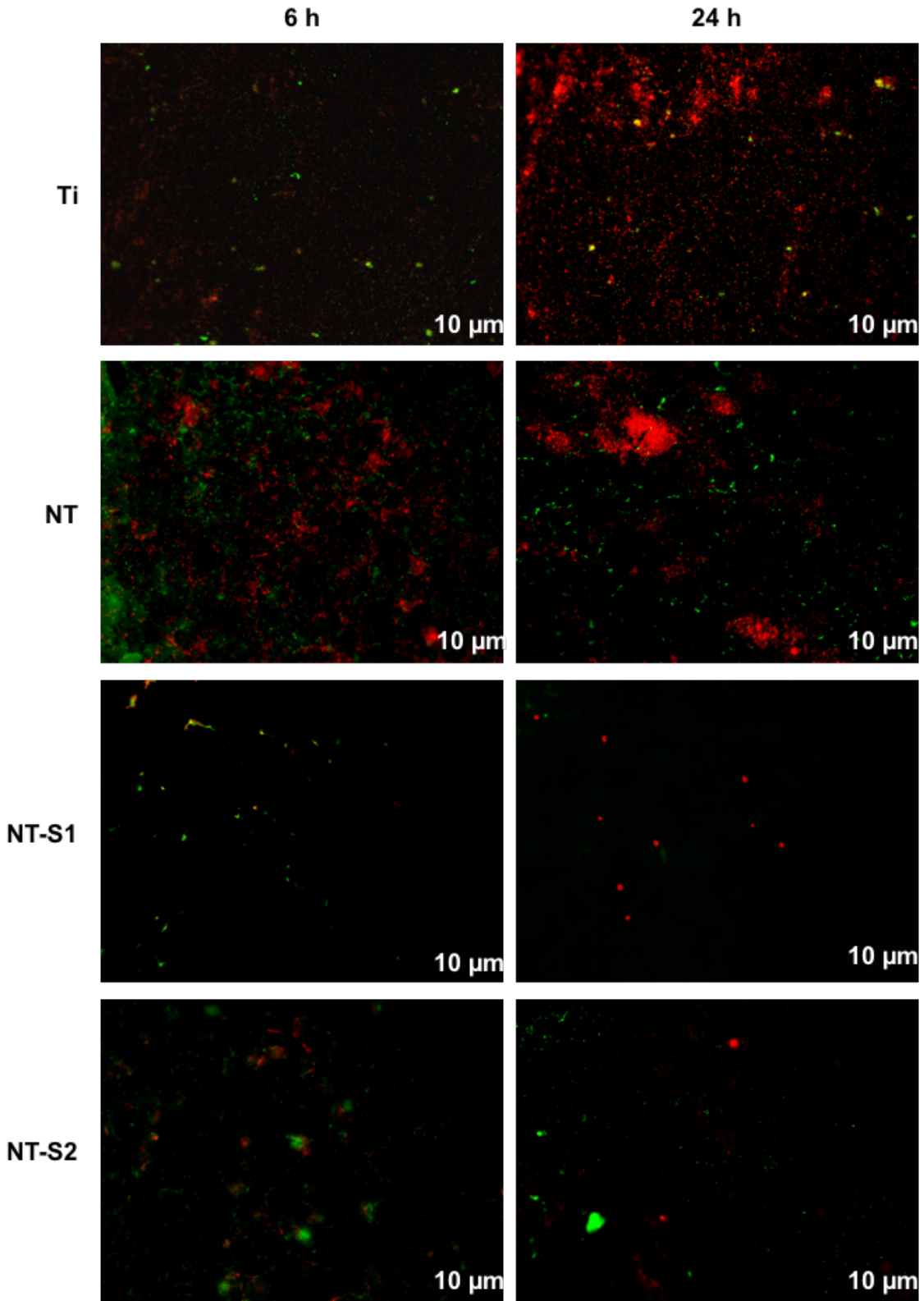


**Figure 4.3.3:** Fluorescence images of *P. aeruginosa* on different surfaces

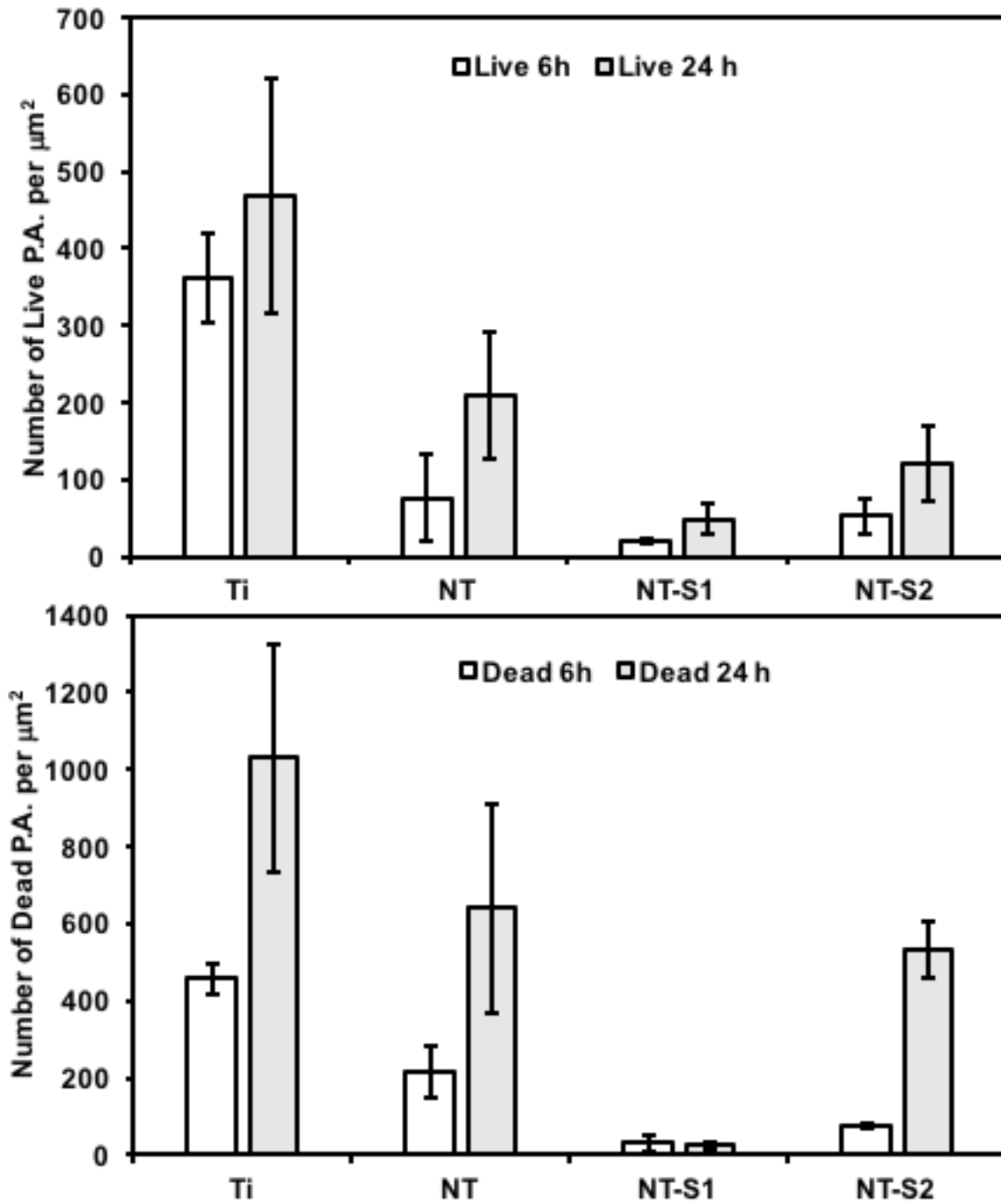


**Figure 4.3.4:** Counts of *P. aeruginosa* on different surfaces after 6 and 24 h

### **4.3.2 Bacteria Morphology**

SEM was used to investigate the morphology of *P. aeruginosa* and *S. aureus* on the substrates. The bacteria were expected to colonize and form biofilms on the Ti substrates with reduced adhesion on the other substrates. The results for *S. aureus* showed more attached bacteria on all substrates after 24 h compared to 6 h, which was expected (**Figure 4.3.5**). Consistent with the fluorescence results, the Ti substrates had the most adhered bacteria. After 24 h, large colonies formed across the Ti surface with some initial biofilm formation. The other substrates showed no biofilm formation, with some colony formation evident on the NT substrates after 24 h. The *S. aureus* remained mostly in small groups and showed little aggregation on the NT-S1 and NT-S2 samples. The *P. aeruginosa* results were similar to the fluorescence results as well. No substrates showed significant colony formation after 6 h (**Figure 4.3.6**). On Ti, the bacteria had nearly covered the surfaces and formed biofilms after 24 h. The NT-S2 substrates showed some colony formation after 24 h. On the NT and NT-S1 samples, the adhered bacteria were still mostly individual cells with little aggregation after 24 h. The SEM results also show the impact of flaws in the titania nanotube arrays, as bacteria can be seen adhered within the grooves or in the spaces between nanotube arrays. This indicates that both the microstructure and surface chemistry of the surfaces contribute to repelling the bacteria.

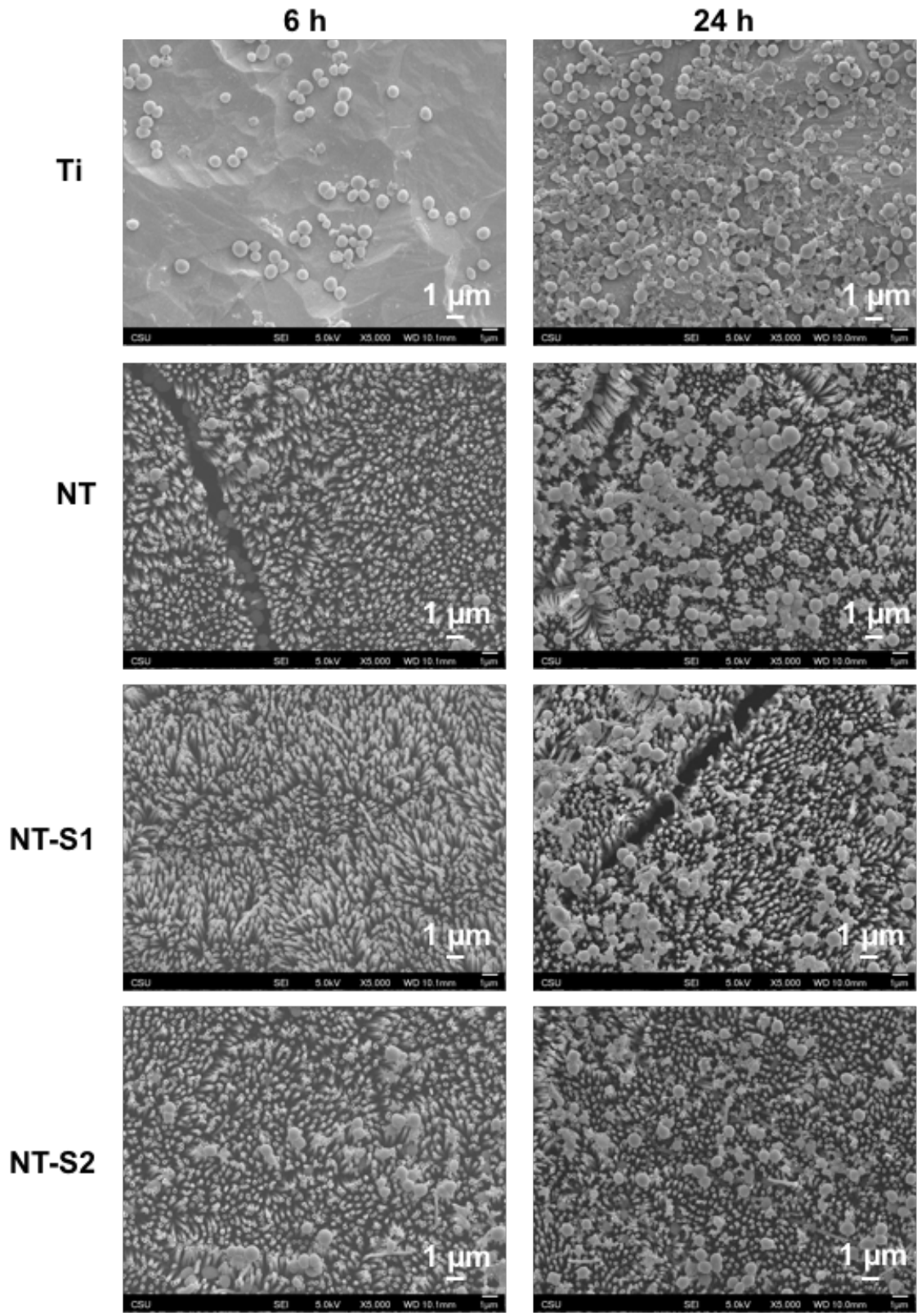


**Figure 4.3.5:** SEM images of *S. aureus* on different surfaces

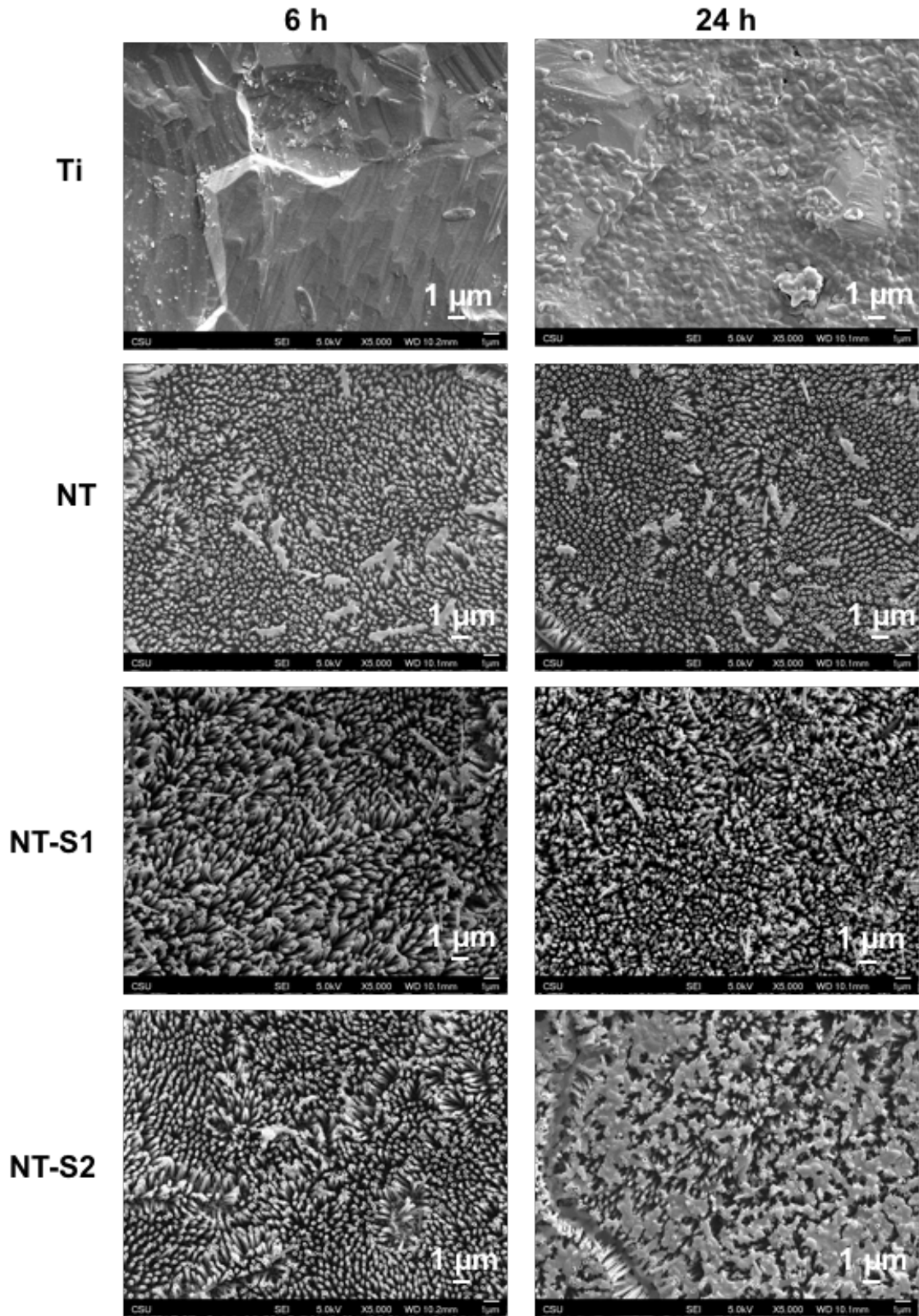


Figure 4.3.6: SEM images of *P. aeruginosa* on different surfaces

#### 4.4 Conclusion

Combating bacterial infections is a challenge for any patient who receives an implanted medical device. Reducing the occurrence of bacterial infections is important in order to reduce device failure and improve patients' quality of life. Due to the increase in antibiotic-resistant bacteria strains, new approaches that do not create bacterial resistance are needed for infection rates to be reduced. Titania nanotube arrays have shown some ability to reduce bacterial adhesion, but there is little research on how superhydrophilic surfaces affect bacterial adhesion. Additionally, there is some research on the effect superhydrophobic surfaces have on bacterial adhesion, but the results so far have been mixed. In this work we have fabricated superhydrophobic and superhydrophilic titania nanotube arrays by anodizing and chemically etching titanium and then modifying the surface chemistry through silanization. The adhesion of gram-positive *S. aureus* and gram-negative *P. aeruginosa* bacteria was investigated by incubating the substrates in bacteria solutions for 6 h and 24 h. The number of adhered bacteria were calculated using SEM imaging, along with fluorescence staining using propidium iodide and Syto-9 stains to distinguish between living and dead bacteria. The results showed fewer bacteria adhered to the superhydrophobic surfaces than any other surface, while the superhydrophilic surfaces were not significantly better than unmodified titania nanotube arrays at reducing the adhesion of bacteria. It is important to note that the superhydrophilic surfaces had some bacteria attached after 24 h and did not repel bacteria completely. This implies that these surfaces slow the rate at which bacteria attach to the surface and over time a biofilm would still be expected to form on these surfaces. Future work will investigate the attachment of bacteria beyond 24 h, and also

ways in which superhydrophobicity and superhydrophilicity can be combined with other techniques, such as drug release, to create surfaces which can both repel bacteria and eliminate any that do adhere. Additionally, other strains of bacteria, including gram-indeterminate bacteria which do not fall into the traditional gram staining categories, should be tested, along with other silanes for the superhydrophilic and superhydrophobic surfaces.

## REFERENCES

- (1) Hori, K.; Matsumoto, S. Bacterial Adhesion: From Mechanism to Control. *Biochem. Eng. J.* **2010**, *48* (3), 424–434.
- (2) Neufeld, B. H.; Reynolds, M. M. Critical Nitric Oxide Concentration for *Pseudomonas Aeruginosa* Biofilm Reduction on Polyurethane Substrates. *Biointerphases* **2016**, *1111* (3), 31012.
- (3) Sousa, C.; Rodrigues, D.; Oliveira, R.; Song, W.; Mano, J. F.; Azeredo, J. Superhydrophobic poly(L-Lactic Acid) Surface as Potential Bacterial Colonization Substrate. *AMB Express* **2011**, *1* (1), 34.
- (4) Kiremitci-Gumusderelioglu, M.; Pesmen, A. Microbial Adhesion to Ionogenic PHEMA, PU and PP Implants. *Biomaterials* **1996**, *17* (4), 443–449.
- (5) Speranza, G.; Gottardi, G.; Pederzolli, C.; Lunelli, L.; Canteri, R.; Pasquardini, L.; Carli, E.; Lui, A.; Maniglio, D.; Brugnara, M.; Anderle, M. Role of Chemical Interactions in Bacterial Adhesion to Polymer Surfaces. *Biomaterials* **2004**, *25* (11), 2029–2037.
- (6) Zhang, X.; Shi, F.; Niu, J.; Jiang, Y.; Wang, Z. Superhydrophobic Surfaces: From Structural Control to Functional Application. *J. Mater. Chem.* **2008**, *18*, 621–633.
- (7) Costerton, J. W. Bacterial Biofilms: A Common Cause of Persistent Infections. *Science (80-. )*. **1999**, *284* (5418), 1318–1322.
- (8) Zago, C. E.; Silva, S.; Sanitá, P. V.; Barbugli, P. A.; Dias, C. M. I.; Lordello, V. B.; Vergani, C. E. Dynamics of Biofilm Formation and the Interaction between *Candida Albicans* and Methicillin-Susceptible (MSSA) and -Resistant *Staphylococcus Aureus* (MRSA). *PLoS One* **2015**, *10* (4), 1–15.
- (9) Banerjee, I.; Pangule, R. C.; Kane, R. S. Antifouling Coatings: Recent Developments in the Design of Surfaces That Prevent Fouling by Proteins, Bacteria, and Marine Organisms. *Adv. Mater.* **2011**, *23* (6), 690–718.
- (10) Poortinga, A. T.; Bos, R.; Norde, W.; Busscher, H. J. *Electric Double Layer Interactions in Bacterial Adhesion to Surfaces*; 2002; Vol. 47.
- (11) Abe, S.; Ishihara, K.; Okuda, K. Prevalence of Potential Respiratory Pathogens in the Mouths of Elderly Patients and Effects of Professional Oral Care. *Arch. Gerontol. Geriatr.* **2001**, *32* (1), 45–55.
- (12) Harris, L. G.; Tosatti, S.; Wieland, M.; Textor, M.; Richards, R. G. *Staphylococcus Aureus* Adhesion to Titanium Oxide Surfaces Coated with Non-Functionalized and Peptide-Functionalized poly(L-Lysine)-Grafted- Poly(ethylene Glycol) Copolymers. *Biomaterials* **2004**, *25* (18), 4135–4148.
- (13) Trujillo, N. A.; Oldinski, R. A.; Ma, H.; Bryers, J. D.; Williams, J. D.; Popat, K. C. Antibacterial Effects of Silver-Doped Hydroxyapatite Thin Films Sputter Deposited on Titanium. *Mater. Sci. Eng. C* **2012**, *32* (8), 2135–2144.

- (14) Zhang, J.; Liu, Y.; Luo, R.; Chen, S.; Li, X.; Yuan, S.; Wang, J.; Huang, N. In Vitro Hemocompatibility and Cytocompatibility of Dexamethasone-Eluting PLGA Stent Coatings. *Appl. Surf. Sci.* **2015**, *328*, 154–162.
- (15) Liu, H.; Pan, C.; Zhou, S.; Li, J.; Huang, N.; Dong, L. Improving Hemocompatibility and Accelerating Endothelialization of Vascular Stents by a Copper-Titanium Film. *Mater. Sci. Eng. C* **2016**, *69*, 1175–1182.
- (16) Papat, K. C.; Eltgroth, M.; LaTempa, T. J.; Grimes, C. A.; Desai, T. A. Titania Nanotubes: A Novel Platform for Drug-Eluting Coatings for Medical Implants? *Small* **2007**, *3* (11), 1878–1881.
- (17) Head, S. J.; Bogers, A. J. J. C.; Kappetein, A. P. Drug-Eluting Stent Implantation for Coronary Artery Disease: Current Stents and a Comparison with Bypass Surgery. *Curr. Opin. Pharmacol.* **2012**, *12* (2), 147–154.
- (18) Holmes, D. R.; Kereiakes, D. J.; Garg, S.; Serruys, P. W.; Dehmer, G. J.; Ellis, S. G.; Williams, D. O.; Kimura, T.; Moliterno, D. J. Stent Thrombosis. *J. Am. Coll. Cardiol.* **2010**, *56* (17), 1357–1365.
- (19) Stefanini, G. G.; Kalesan, B.; Serruys, P. W.; Heg, D.; Buszman, P.; Linke, A.; Ischinger, T.; Klauss, V.; Eberli, F.; Wijns, W.; Morice, M. C.; Di Mario, C.; Corti, R.; Antoni, D.; Sohn, H. Y.; Eerdmans, P.; Van Es, G. A.; Meier, B.; Windecker, S.; Jüni, P. Long-Term Clinical Outcomes of Biodegradable Polymer Biolimus-Eluting Stents versus Durable Polymer Sirolimus-Eluting Stents in Patients with Coronary Artery Disease (LEADERS): 4 Year Follow-up of a Randomised Non-Inferiority Trial. *Lancet* **2011**, *378* (9807), 1940–1948.
- (20) Fadeeva, E.; Truong, V. K.; Stiesch, M.; Chichkov, B. N.; Crawford, R. J.; Wang, J.; Ivanova, E. P. Bacterial Retention on Superhydrophobic Titanium Surfaces Fabricated by Femtosecond Laser Ablation. *Langmuir* **2011**, *27* (6), 3012–3019.
- (21) Zhang, X.; Wang, L.; Levänen, E. Superhydrophobic Surfaces for the Reduction of Bacterial Adhesion. *RSC Adv.* **2013**, *3* (30), 12003.
- (22) Barthlott, W.; Neinhuis, C. Purity of the Sacred Lotus, or Escape from Contamination in Biological Surfaces. *Planta* **1997**, *202* (1), 1–8.
- (23) Bandara, C. D.; Singh, S.; Afara, I. O.; Tesfamichael, T.; Wolff, A.; Ostrikov, K. (Ken); Oloyede, A. Bactericidal Effects of Natural Nanotopography of Dragonfly Wing on Escherichia Coli. *ACS Appl. Mater. Interfaces* **2017**, *acsami.6b13666*.
- (24) Ma, J.; Sun, Y.; Gleichauf, K.; Lou, J.; Li, Q. Nanostructure on Taro Leaves Resists Fouling by Colloids and Bacteria under Submerged Conditions. *Langmuir* **2011**, *27* (16), 10035–10040.
- (25) Mahalakshmi, P. V.; Vanithakumari, S. C.; Gopal, J.; Mudali, U. K.; Raj, B. Enhancing Corrosion and Biofouling Resistance through Superhydrophobic Surface Modification. *Curr. Sci.* **2011**, *101* (10), 1328–1336.
- (26) Zhang, D.; Li, G.; Wang, H.; Chan, K. M.; Yu, J. C. Biocompatible Anatase Single-Crystal Photocatalysts with Tunable Percentage of Reactive Facets. *Cryst. Growth Des.* **2010**, *10* (3), 1130–1137.

- (27) Gottenbos, B.; Van Der Mei, H. C.; Busscher, H. J.; Grijpma, D. W.; Feijen, J. Initial Adhesion and Surface Growth of *Pseudomonas Aeruginosa* on Negatively and Positively Charged Poly(methacrylates). *J. Mater. Sci. Mater. Med.* **1999**, *10* (12), 853–855.
- (28) Jucker, B. a; Jucker, B. a; Harms, H.; Harms, H.; Zehnder, A. J. B.; Zehnder, A. J. B. Adhesion of the Positively Charged Bacterium. *Microbiology* **1996**, *178* (18), 5472–5479.
- (29) Nonckreman, C. J.; Fleith, S.; Rouxhet, P. G.; Dupont-Gillain, C. C. Competitive Adsorption of Fibrinogen and Albumin and Blood Platelet Adhesion on Surfaces Modified with Nanoparticles And/or PEO. *Colloids Surfaces B Biointerfaces* **2010**, *77* (2), 139–149.
- (30) Movafaghi, S.; Leszczak, V.; Wang, W.; Sorkin, J. A.; Dasi, L. P.; Popat, K. C.; Kota, A. K. Hemocompatibility of Superhemophobic Titania Surfaces. *Adv. Healthc. Mater.* **2016**, 1600717.
- (31) Smith, B. S.; Yoriya, S.; Grissom, L.; Grimes, C. A.; Popat, K. C. Hemocompatibility of Titania Nanotube Arrays. *J. Biomed. Mater. Res. - Part A* **2010**, *95 A* (2), 350–360.

## CHAPTER 5

### CONCLUSIONS AND FUTURE WORK

#### 5.1 Conclusion

Titania nanotube arrays have been investigated for a variety of biomedical uses. Previous work has investigated their ability to promote endothelialization and osseointegration, affect cell growth and differentiation, deliver drugs, promote implant acceptance and integration, or reduce the occurrence of bacterial infections. Previous research has also shown that titania nanotube arrays improve the hemocompatibility of titanium as a biomaterial. Thrombogenesis and bacterial adhesion remain pressing challenges for medical implants due to the complications they cause for patients, as no long-term solution has been found to prevent the attachment of cells or bacteria. Superhydrophobic and superhydrophilic surfaces have been investigated in other contexts due to their ability to affect the attachment of different particles to a surface. Superhydrophobic surfaces have been shown to reduce cell attachment and protein adsorption on surfaces tested. There has been little work, however, on the ability of superhydrophobic surfaces to repel blood and potentially act as superhemophobic surfaces. The ease of fabricating titania nanotube arrays and easily altered surface chemistry, along with their established biocompatibility, make them an ideal candidate for use in reducing the adhesion of bacteria and interactions between the titania and blood.

This research examines the effect of silanized titania nanotube arrays on the adhesion of platelets, whole human blood, and both gram-positive and gram-negative bacteria. The silanized titania nanotube arrays were compared to an unmodified titanium

control and uncoated titania nanotube arrays. The titania nanotube arrays used were uniformly vertically oriented and densely packed with a high aspect ratio. The titania nanotube arrays were fabricated using an electrochemical etching and oxidation technique followed by annealing to set the crystal structures. The silanes were bonded to the titania nanotube arrays by etching the arrays with atmospheric oxygen plasma, and then using chemical vapor deposition or liquid deposition depending on the silane. The characterization of the surface topographies was accomplished using SEM, XPS, GAXRD, and contact angle goniometry. The results confirm that the silanes bonded to the titania nanotube arrays and increased the diameters by approximately 10 nm on average, while making the surfaces superhydrophobic and superhydrophilic as expected based on the silane used. The underlying crystal structures of the nanotube arrays remained unchanged through the silanization process, indicating no significant change in the material properties of the nanotube arrays.

The hemocompatibility of titania nanotube arrays was investigated by measuring blood protein adhesion, cytotoxicity, platelet and leukocyte adhesion, platelet activation, and hemoglobin adsorption, along with the contact and roll-off angles of blood. The results showed reduced protein adsorption and hemoglobin adsorption on the superhydrophobic surfaces compared to the controls. The measurements of the contact and roll-off angle showed that the titania nanotube arrays with the fluorinated silane could be considered superhemophobic using the angle thresholds for superhydrophobicity – a contact angle above  $150^\circ$  and roll-off angle below  $10^\circ$ . The results for cell adhesion and activation were inconsistent however, potentially due to the variation in the number of platelets present in the human plasma depending. The results indicate that

superhemophobic surfaces have potential as method for improving hemocompatibility on blood-contacting surfaces. But more work needs to investigate further whether the superhydrophobic surfaces have significant differences in cell adhesion from titania nanotube arrays.

The bacterial adhesion on titania nanotube arrays was investigated using SEM and fluorescence imaging to determine the number of adhered bacteria and their morphology. Both gram-positive and gram-negative bacteria – *S. aureus* and *P. aeruginosa* – were chosen because of the differences in their cell walls. The results showed that fewer bacteria of both types adhered to the superhydrophobic surfaces compared to the other surfaces. The superhydrophilic surfaces did not significantly reduce the adhesion of bacteria compared to the uncoated titania nanotube arrays. There were not significant differences in the attachment of the gram-positive and gram-negative bacteria to any of the surfaces. No nanotube arrays showed significant biofilm formation, while the unmodified titanium did have biofilms of both bacteria. These results show that superhydrophobic titania nanotube arrays have potentially slow the adhesion of bacteria and formation of biofilms, but not eradicate the bacteria completely.

## **5.2 Future Work**

Superhydrophobic and superhemophobic titania nanotube arrays have shown promise in improving hemocompatibility and reducing bacteria adhesion over the short term. A big challenge for all biomedical implants is performance over long periods of time. Future studies can investigate the performance of these materials over longer periods of time – past 3 h for blood and blood proteins and beyond 24 h for bacteria. Additionally,

the experiments presented here were performed under static conditions. Future work can investigate the adhesion of cells and bacteria under dynamic flow conditions. The silanes used for the titania nanotube arrays came from three different classes of silane – alkane, fluorinated, and polyethylene-glycol based silanes. Each class of silanes encompasses many chemicals with varying alkane chain lengths and chemical compositions, so future studies could compare the effects of different silanes of similar compositions. Additionally, the effects of different components of human blood on the hemophobicity or hemophilicity of a surface are poorly known. The effects of blood and protein adsorption on the contact angles of the surfaces should be investigated further. The effect of different silanes on bacterial adhesion could be investigated in addition to their effects on blood. Other strains of bacteria, such as gram-indeterminate bacteria, should also be investigated along with other strains of gram-positive and gram-negative bacteria. The main challenge for all superhydrophobic and superhydrophilic surfaces is the ease with which their topographies can be damaged. Since the superhydrophobic surfaces reduce the adhesion of bacteria but do not completely eliminate them, research into ways superhydrophobic surfaces can be combined with other techniques, such as drug-eluting nanotubes, could further improve their performance and biocompatibility. Because damage to the topographies will negate the superhydrophobicity or superhydrophilicity of the surface, a strategy for improving the durability of these surfaces would greatly increase the applications of these surfaces. Further research into improving the durability of the titania nanotube arrays should be done along with these other studies.